NTNU – Norwegian University of Science and Technology
Department of Petroleum Engineering and Applied Geophysics

CO2 as Injection Gas for Enhanced Oil Recovery and Estimation of the Potential on the Norwegian Continental Shelf

by

Odd Magne Mathiassen
Chief Reservoir Engineer
Norwegian Petroleum Directorate

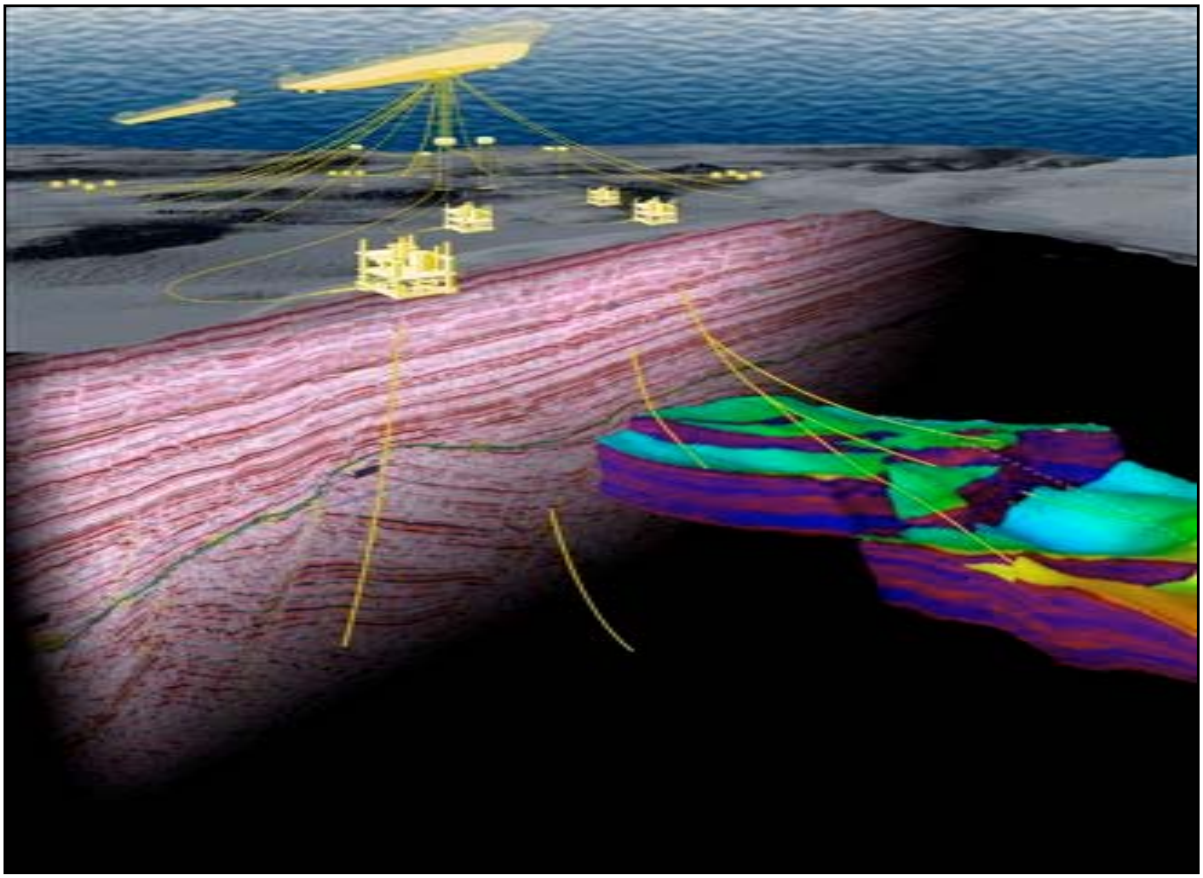

Trondheim / Stavanger, May 2003

Part I of II

ACKNOWLEDGEMENT

I would like to thank my supervisor Professor Ole Torsæter at the Norwegian University of Science and Technology for excellent guiding and help in my work with this thesis. I would also like to thank my employer, the Norwegian Petroleum Directorate, for giving me the opportunity and time to complete the thesis. My thanks also go to my colleagues Mr. Gunnar Einang, Mr. Søren Davidsen and Mr. Jan Bygdevoll for valuable discussions while working with this thesis. Finally, I would like to thank Dr. Eric Lindeberg and senior researcher Idar Akervoll at the Sintef Research for valuable information on CO_2 related issues.

SUMMARY

The main objective of this thesis is to investigate the possibility of using CO_2 as injection gas for enhanced oil recovery and estimate the potential of additional oil recovery from mature oil fields on the Norwegian Continental Shelf (NCS). Because of the lack of CO_2 data from offshore oil fields, a literature study on CO_2 flood experience worldwide was undertaken. In addition, the physical properties of CO_2 and CO_2 as a solvent have been studied.

The literature study makes it possible to conclude that CO_2 has been an excellent solvent for enhanced oil recovery from onshore oil fields, especially in the USA and Canada. Almost 30 years of experience and more than 80 CO_2 projects show that the additional recovery is in the region of 7 to 15 % of the oil initially in place.

The estimation is based on specific field data for all fields and reservoirs included in the thesis. CO_2 data are limited to studies and reservoir simulations from Forties, Ekofisk, Brage and Gullfaks. Since Forties is a UK oil field, most of the data used are from the three Norwegian oil fields.

This thesis includes all oilfields currently in production. Fields under development, fields with approved plan for development and operation (PDO), or discoveries under evaluation are not included. However, they may have potential for use of CO_2 in the future. The candidates are screened according to their capability of being CO_2 flooded, based on current industry experience and miscibility calculations. Then a model based on the most critical parameters is developed. Finally, risk analysis and Monte Carlo simulations are run to estimate the total potential. Applying the model developed and compensating for uncertainties, the additional recovery is estimated between 240 and 320 million Sm^3 of oil. This potential constitutes large increases in oil production from the Norwegian Continental Shelf if CO_2 can be made available at competitive prices. For some of the time critical fields, immediate action is called upon, but for the majority of the fields dealt with in this thesis, CO_2 injection can be postponed 5 years or more.

TABLE OF CONTENTS

ACKNOWLEDGEMENT 2
SUMMARY 2
TABLE OF CONTENTS 3
1. INTRODUCTION 5
2. THE PHYSICAL PROPERTIES OF CO_2 6
2.1 Phase transitions and phase diagram for CO_2 9
2.1.1 Phase equilibrium 9
2.1.2 The Clausius - Clapeyron equation 10
2.1.3 Solid - Liquid Equilibrium 10
2.1.4 Solid – Vapour Equilibrium 11
2.1.5 Liquid - Vapour Equilibrium 12
2.1.6 Phase diagram calculated from the derived equations 12
2.2 CO_2 - rock and fluid interactions 13
2.2.1 PVT conditions 13
2.2.2 CO_2 hydrates 13
2.2.3 Wettability 13
2.2.4 Scale 14
2.3 Injectivity abnormalities 14
2.3.1 Injectivity increases 14
2.3.2 Injectivity reduction 15
2.3.3 Entrapment 15
2.3.4 Relative permeability 15
2.3.5 Heterogeneity 16
2.3.6 Concluding remarks on injectivity abnormalities 16
2.4 Advantages and disadvantages by using CO_2 as a solvent in miscible floods 17
2.4.1 Advantages 17
2.4.2 Disadvantages 17
3. ENHANCED OIL RECOVERY 18
4. ENHANCED OIL RECOVERY BY MISCIBLE GAS/CO_2 FLOODING 20
4.1 Miscibility and drive mechanism 20
4.2 First contact miscible flooding 20
4.3 Multiple contact miscible flooding 21
4.3.1 Vaporizing gas drive 21
4.3.2 Condensing gas drive 22
4.3.3 Combined vaporizing and condensing mechanism 23
4.4 Minimum miscible pressure from slimtube miscibility apparatus 23
4.5 Some remarks on the MMP and the calculation of the MMP 25
5 SUMMARY OF CO_2 FLOOD PROJECTS WORLDWIDE 26
5.1 The Permian Basin 27
5.1.1 The SACROC Unit in the Permian Basin 28
5.1.2 SACROC CO_2 project, key parameters 30
5.2 The Weyburn Oil field in Canada 30
5.2.1 Weyburn oil field, key parameters 34
5.2.2 The Weyburn CO_2 Monitoring Project 34
5.3 EOR projects in the US and the role of CO_2 floods 35
5.4 CO_2 availability and prices in US and Canada 37
5.4.1 CO_2 sources 37

5.4.2 CO_2 pipelines 38
5.4.3 CO_2 prices 39
5.5 US and Canadian CO_2 screening criteria 40
5.6 Experience gained from CO_2 floods in US and Canada 41
5.7 Discussing 41
6. NORTH SEA CO_2 STUDIES 43
6.1 The Sleipner field 43
6.2 The Forties field 45
6.2.1 Forties CO_2 EOR project 46
6.3 The Ekofisk field 47
6.3.1 Ekofisk EOR screening 48
6.3.2 Ekofisk CO_2 WAG study 48
6.4. The Brage field 49
6.4.1 Brage Statfjord South CO_2 WAG injection study 50
6.5. The Gullfaks field 51
6.5.1 Gullfaks Brent CO_2 WAG study 51
6.6 Summary and discussion of the North Sea CO_2 studies 53
7. SCREENING OF CANDIDATES FOR TERTIARY CO_2 FLOODS 55
7.1 Screening method 59
7.2 Calculation of MMP 60
7.2.1 Minimum miscibility pressure calculations 61
7.2.2 Combined drive mechanism 61
8. ESTIMATION OF THE CO_2 EOR POTENTIAL 64
8.1 Method 64
8.2 Estimation 66
8.3 Conclusions 67
8.4 Spreadsheet model used for Monte Carlo simulations 67
9. ABBREVATIONS AND NOMECLATURE 72
10. REFERENCES 73
APPENDIX A 79
Results from the Monte Carlo simulation 80
APPENDIX B 96
Confidential enclosure 96

1. INTRODUCTION

With production from many mature oil fields on the Norwegian Continental Shelf declining and approaching tail production, the field owners have to consider enhanced oil recovery as a way of recovering more oil from the fields. Enhanced oil recovery through the injection of CO_2 as a tertiary recovery mechanism, preferably after water flooding, is one mechanism with which to recover more oil, extend the field life and increase the profitability of the fields.

Experience gained from CO_2 flooding worldwide indicates that enhanced oil recovery by using CO_2 as injection gas may result in additional oil ranging from 7 to 15 % of the oil initially in place. As regards oil fields on the Norwegian Continental Shelf, it is not granted that this additional recovery can be obtained, but field studies indicate that there is potential. With initially oil in place close to 8000 million Sm^3 in the oil fields currently in production, also small percentages represent large volume of extra oil. Few other tertiary recovery mechanisms seem to be able to compete with this, and albeit years of research have been invested in them, other methods are not considered to be economically viable. Miscible gas flooding by using hydrocarbon gas might be an alternative, but because of the high market price for gas, it is more profitable to sell the gas

An estimation of this potential is in great demand, both from the industry and the authorities. However, too little CO_2 data has been available from the Norwegian Continental Shelf to predict the overall potential of CO_2 flooding. The Norwegian Petroleum Directorate, in cooperation with the operators, has initiated reservoir studies to be performed by the operators of three representative fields in production, the Ekofisk, Gullfaks and Brage fields. Data from these studies will be made available for this thesis, in addition to available information from other studies, field experience and pilot projects worldwide. There are also several papers dealing with this subject.

This thesis generally uses available information, does calculations on critical field data and develops a method of estimating the enhanced oil recovery potential of CO_2 floods. Reservoir studies and simulations are not required for all fields, but nevertheless a significant amount of data will be used to establish a method of estimating the overall potential. In addition, an overview of industry experience worldwide and how CO_2 act as a solvent will be given and used as background material for the estimation.

CO_2 is a greenhouse gas, and Norway has entered into international agreements to reduce the emission of greenhouse gasses. This thesis will not look into the environmental impacts of reducing CO_2 emissions, but may contribute some useful material in that respect. By using CO_2 as injection gas, significant amounts of CO_2 can be stored in the reservoirs upon flooding and after the oil fields have been abandoned.

2. THE PHYSICAL PROPERTIES OF CO_2

Pure CO_2 is a colourless, odourless, inert, and non-combustible gas. The molecular weight at standard conditions is 44.010 g/mol, which is one and a half times higher than air. CO_2 is solid at low temperatures and pressures, but most dependent on temperature as shown in figure 2.1. But by increasing the pressure and temperature, the liquid phase appears for the first time and coexists with the solid and vapour phases at the triple point. The liquid and the vapour phase of CO_2 coexist from the triple point and up to the critical point on the curve.

Below the critical temperature CO_2 can be either liquid or gas over a wide range of pressures. Above the critical temperature CO_2 will exists as a gas regardless of the pressure. However, at increasingly higher supercritical pressures the vapour becomes and behaves more like a liquid.

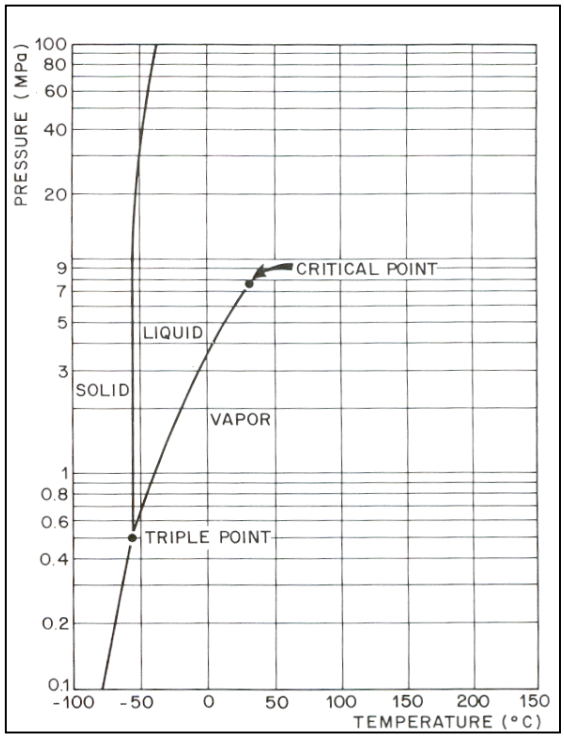

The properties under standard condition at 1.013 bar and 0 ^oC are:

- Mol. weight: 44.010 g/mol
- Sp. gravity to air: 1.529
- Density: 1.95 kg/m^3

Critical properties:

- Tc: 31,05 ^oC
- Pc: 73.9 bar
- Vc: 94 cm^3/mol

Triple point:

- Ttr: - 56,6 ^oC
- Ptr: 5.10 bar

Figure 2.1 - CO_2 phase diagram [1]

Figure 2.1 shows the phase diagram for CO_2. The phase behaviour, transition and boundaries will be described in more detail in chapter 2.1 where the equations involved will be used to calculate and construct the CO_2 phase diagram.

The next figures will give an expression of the behaviour of CO_2 with respect to:

- Density
- Compressibility
- Viscosity
- Solubility

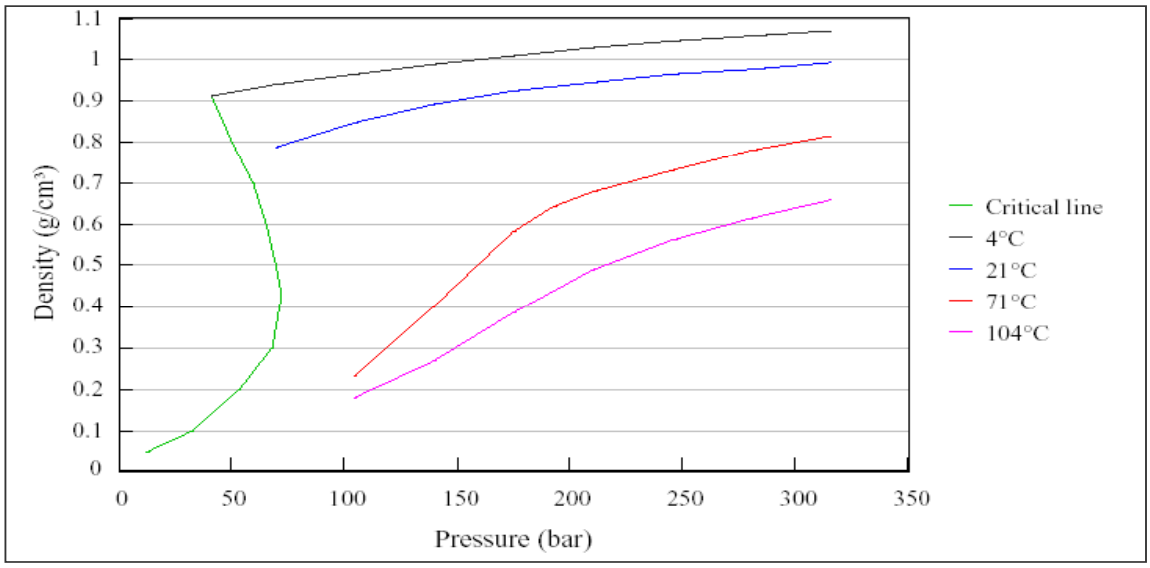

Figure 2.2 - CO_2 density as a function of pressure and temperature [2 and 3]

Figure 2.2 shows that the fluid density increases with pressures at temperatures above critical conditions, but abrupt discontinuities appear at temperatures below the critical region.

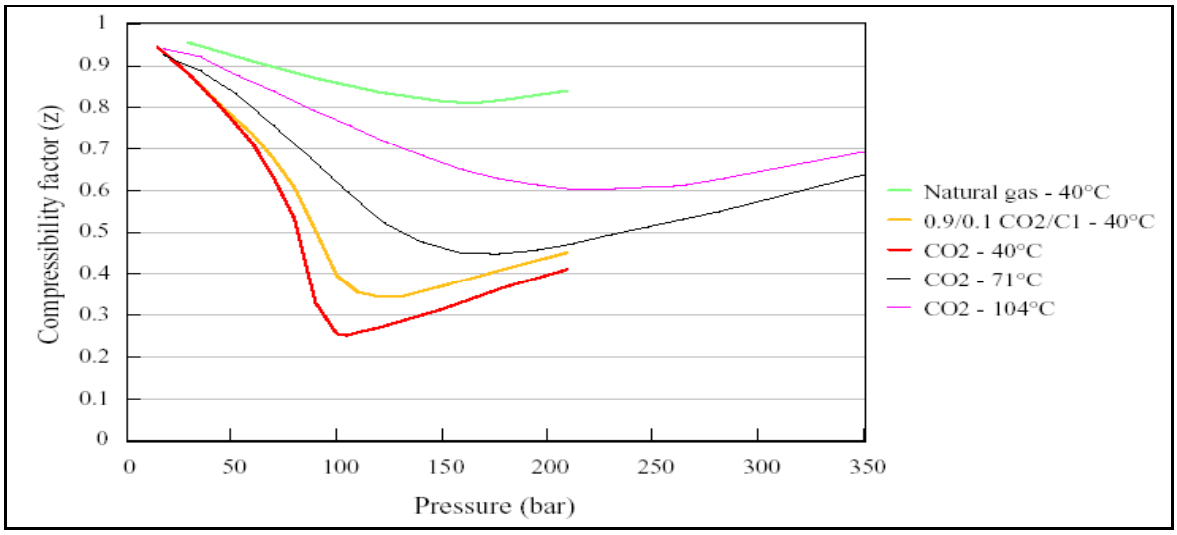

Figure 2.3 - Compressibility as a function of pressure and temperature [2, 4 and 5].

Figure 2.3 shows the compressibility of CO_2, natural gas and CO_2-methane mixture as a function of pressure at some different temperatures. As shown in the figure, the compressibility of CO_2 is considerably different than for the natural gas and CO_2-methane mixture. At 100 bar and 40 ^oC the compressibility varies respectively from 0,25 to 0,4 and 0,85 for the natural gas.

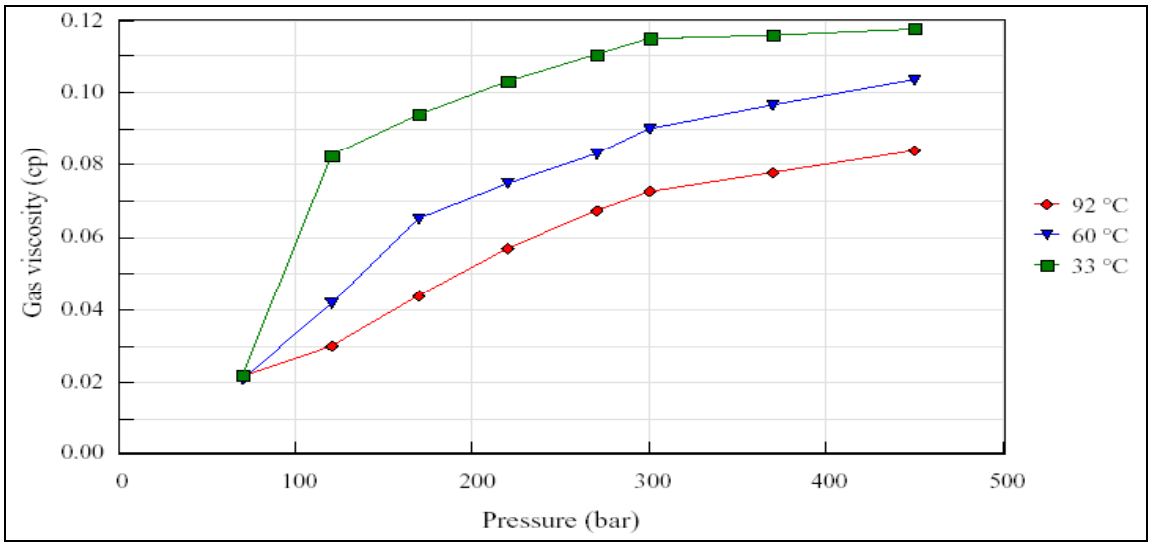

Figure 2.4 - CO_2 viscosity as a function of pressure and temperature [2].

Figure 2.4 shows that the CO_2 viscosity strongly depends on pressure and temperature, and the viscosity increases considerably when pressure increases for a given reservoir temperature. The viscosity for natural gas and formation water are in the range of 0,02 to 0,03 and 0,3 to 1,0 cp, respectively. As shown in the figure, the viscosity of CO_2 is somewhere in between the viscosity of natural gas and formation water for all relevant temperatures and pressures. By means of viscosity, the displacement of water with CO_2 is more effective than displacement with natural gas. Together with the CO_2 density shown in figure 2.2, the CO_2 will properly not override the water with the same degree as a HC gas.

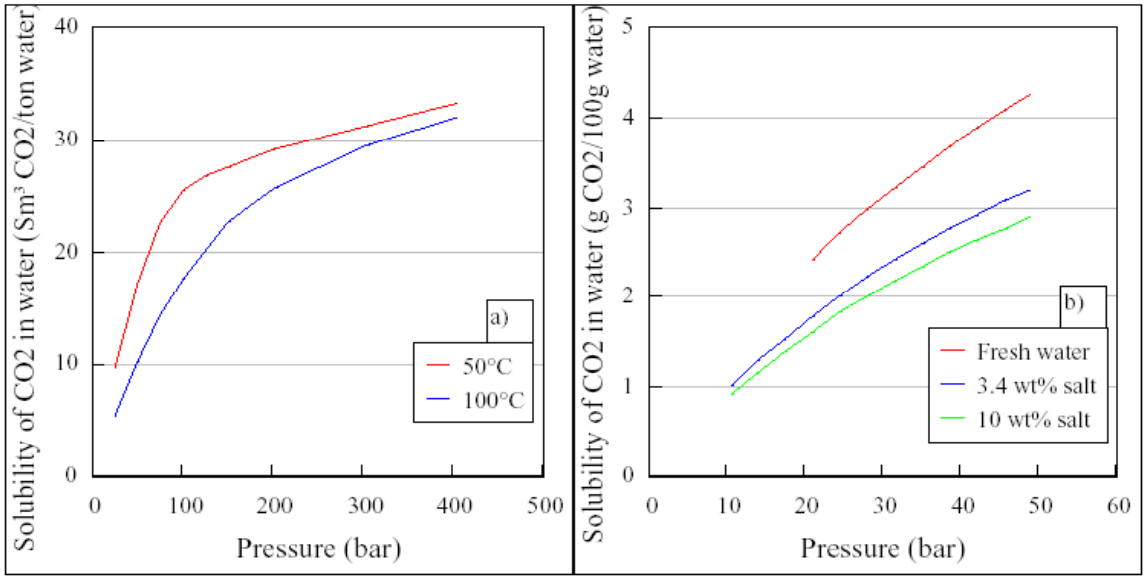

Figure 2.5 - Solubility of CO_2 in water as function of (a) pressure and temperature, and (b) pressure and salinity [2, 6 and 7].

The solubility of CO_2 in water as a function of pressure, temperature and salinities is shown in figure 2.5. CO_2 has an increasing solubility in water with increasing pressure. The opposite effect is seen with increased temperature and salinity.

2.1 Phase transitions and phase diagram for CO_2

The properties of CO_2, and the phase behaviour are important to understand when a CO_2 flood is considered. However, the most important behaviour is how CO_2 interfere with reservoir fluids and reservoir rock when it flows through the reservoir under different temperature and pressure conditions.

The simplest applications of thermodynamics are the phase transitions that a pure substance can undergo. The process involves a single substance that undergoes a physical change. A phase of a substance is a form of matter that is uniform throughout in chemical composition and physical state. A phase transition, the spontaneous conversion of one phase to another, occurs at a characteristic temperature for a given pressure. A phase diagram of a substance is a map of the ranges of pressure and temperature at which each phase of a substance is the most stable. The boundaries between regions, or the phase boundaries, show the values of P and T at which two phases coexist in equilibrium.

In the following, a method to construct the CO_2 phase diagram will be explained by separately considering the three types of equilibrium based on the criteria for phase equilibrium, the Gibbs free energy and the Clausius - Clapeyron equation.

2.1.1 Phase equilibrium

For two phases to be in equilibrium, the chemical potential of the substance in both phases must be equivalent.

$$\begin{aligned} \mu\alpha &= \mu\beta \\ \mu\alpha &= \mu\gamma \\ \mu\beta &= \mu\gamma \end{aligned} \qquad (2.1)$$

By assuming an infinitesimal change in temperature or pressure to two phases in equilibrium,

$$\begin{aligned} \mu(\alpha) + d\mu(\alpha) &= \mu(\beta) + d\mu(\beta) \\ \mu(\alpha) + d\mu(\alpha) &= \mu(\gamma) + d\mu(\gamma) \\ \mu(\beta) + d\mu(\beta) &= \mu(\beta\gamma) + d\mu(\gamma) \end{aligned} \qquad (2.2)$$

and apply the definition of the chemical potential,

$$\begin{aligned} d\mu(\alpha) &= -S(\alpha)dT + V(\alpha)dP \\ d\mu(\beta) &= -S(\beta)dT + V(\beta)dP \\ d\mu(\gamma) &= -S(\gamma)dT + V(\gamma)dP \end{aligned} \qquad (2.3)$$

and defining the transition,

$$\begin{aligned} \alpha &\Leftrightarrow \beta \\ \alpha &\Leftrightarrow \gamma \\ \beta &\Leftrightarrow \gamma \end{aligned} \qquad (2.4)$$

the slope of any phase boundary can be obtained from the Claperyron equation as shown schematically in figure 2.6.

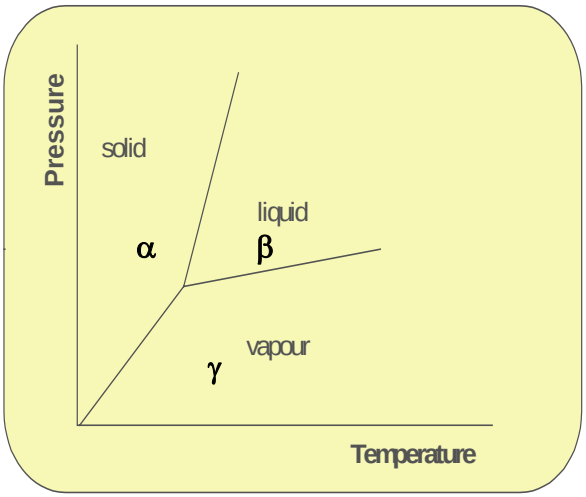

Figure 2.6 - Schematic phase diagram and phase transitions

2.1.2 The Clausius - Clapeyron equation

$$\left(\frac{\partial P}{\partial T}\right)_{\Delta G} = \frac{\Delta S}{\Delta V} \qquad (2.5)$$

Since the phases are in equilibrium with each other at any point on the line, the Gibbs free energy for the transition is zero everywhere on the phase line.

$$\Delta G = 0 \qquad (2.6)$$

For a process at constant temperature we will have,

$$\Delta G = \Delta H - T\Delta S \qquad (2.7)$$

which combined with equation 2.6 gives,

$$\Delta S = \frac{\Delta H}{T} \qquad (2.8)$$

Equation 2.5 can now be written as,

$$\left(\frac{\partial P}{\partial T}\right)_{\Delta G} = \frac{\Delta H}{T\Delta V} \qquad (2.9)$$

Equation 2.5 or 2.9 is useful if we want to integrate dP to find P as a function of T. Booth equations are exact, but to integrate them, we can make the approximation that either ΔS or ΔH is reasonably constant over the temperature range. Since the ΔH varies more slowly with temperature than ΔS, it is better to integrate equation 2.9.

2.1.3 Solid - Liquid Equilibrium

A solid is in equilibrium with its liquid when the rate of at which molecules leave the solid is the same as the rate at which they return. The process of melting of a solid is known as fusion. Note that the melting point is not a very strong function of temperature. For most compounds,

the melting temperature rises as the pressure increases. (For water the opposite is true). Hence, here we assume that both ΔH and ΔV are constant. That is because we consider the transition solid-to-solid or liquid to solid to be approximately constant. Equation 2.9 prepared for integration gives,

$$\int_{P_1}^{P_2} \partial P = \frac{\Delta H}{\Delta V} \int_{T_1}^{T_2} \frac{1}{T} \partial T \qquad (2.10)$$

and equation 2.10 integrated gives,

$$P_2 = P_1 + \left(\frac{\Delta H_{fus}}{\Delta V_{fus}} \right) \ln \left(\frac{T_2}{T_1} \right) \qquad (2.11)$$

P_2 is the equilibrium pressure of the substance at temperature T_2, and P_1 is the equilibrium pressure at temperature T_1. ΔH_{fus} and ΔV_{fus} are the changes in enthalpy and volume of the substance that accompany melting. Starting with a known point along the curve (for example the triple point) we can calculate the rest of the curve referenced to this point.

2.1.4 Solid – Vapour Equilibrium

A solid is in equilibrium with its vapour when the rate of at which molecules leave the solid is the same as the rate at which they return. The process of vaporization of a solid is known as sublimation. For a given temperature, the pressure at which the solid is in equilibrium with its vapour is called the vapour pressure. Vapour pressure increases as temperature rises.

Since ΔV is not close to be constant for the solid to vapour or liquid to vapour case, we have to do two more approximations. One;

$$\Delta V = V_{gas} - V_{liquid} \approx V_{gas}$$
$$\Delta V = V_{gas} - V_{solid} \approx V_{gas} \qquad (2.12)$$

and two; using the ideal gas equation,

$$V_{gas} \approx nRT / P \qquad (2.13)$$

Equation 2.9 together with 2.12 and 2.13 can now be written as,

$$\left(\frac{\partial P}{\partial T} \right)_{\Delta G} = \frac{\Delta H}{T \frac{nRT}{P}} = \frac{\Delta \bar{H}}{R} \frac{P}{T^2} \qquad (2.14)$$

and prepared for integration,

$$\int_{P_1}^{P_2} \frac{1}{P} \partial P = \frac{\Delta \bar{H}}{R} \int_{T_1}^{T_2} \frac{1}{T^2} \partial T \qquad (2.15)$$

Integration of equation 2.15 gives,

$$P_2 = P_1 \exp\left(-\left(\frac{\Delta H_{sub}}{R}\right)\left(\frac{1}{T_2}-\frac{1}{T_1}\right)\right) \qquad (2.16)$$

where P_2 is the vapour pressure of the substance at temperature T_2, and P_1 is the vapour pressure at temperature T_1. ΔH_{sub} is a constant and known as the enthalpy of sublimation and correspond to the heat that must be absorbed by one mole of the substance to sublime it. We can now describe the solid-vapour curve if we know the ΔH_{sub}.

2.1.5 Liquid - Vapour Equilibrium

$$P_2 = P_1 \exp\left(-\left(\frac{\Delta H_{vap}}{R}\right)\left(\frac{1}{T_2}-\frac{1}{T_1}\right)\right) \qquad (2.17)$$

where P_2 is the vapour pressure of the substance at temperature T_2, and P_1 is the vapour pressure at temperature T_1. ΔH_{vap} is a constant and known as the enthalpy of vaporizing. We can now describe the liquid-vapour curve if we know the ΔH_{vap}.

Equation 2.11, 2.16 and 2.17 can now be used to construct the entire phase diagram. If we know two points on the curve we can solve for ΔH. If we know one point on the curve and ΔH, we can solve any other point or even have the entire curve.

2.1.6 Phase diagram calculated from the derived equations

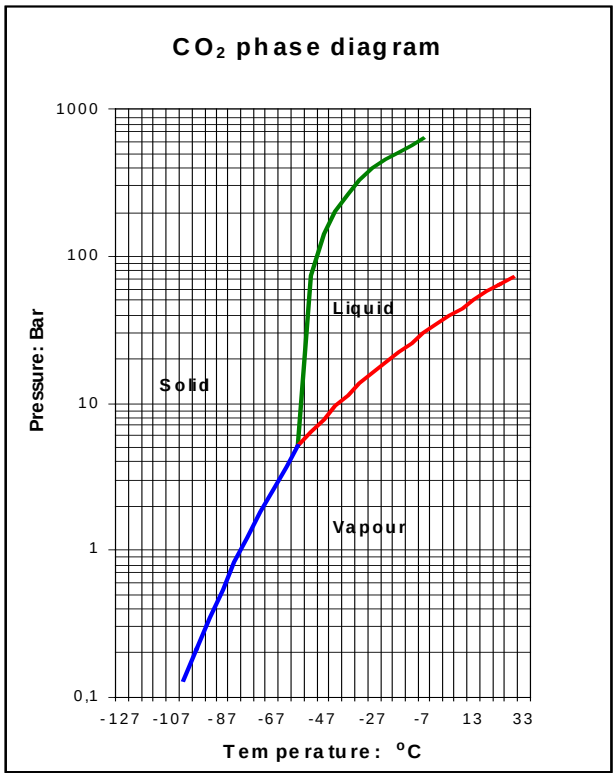

The calculation and construction of the phase diagram are based on equation 2.11, 2.16 and 2.17, and the following numbers:

Ptr	= 5.10 bar
Ttr	= -56.6 °C (304.2 °K)
Gas constant	= 8.314 J/mol °K
ΔHfus	= 8330 J/mol °K
ΔHsub	= 25230 J/mol °K
ΔHvap	= 16900 J/mol °K
ΔV	= 0.027 litre /mol

Figure 2.7 - Calculated phase diagram for pure CO_2

2.2 CO_2 - rock and fluid interactions

The effect of the interaction between CO_2, rocks and reservoir fluids varies with type of rock and fluids as well as pressure and temperature. In addition, CO_2 shows more complex phase behaviour with reservoir oil then most of the other solvents. In the following, some important issues are briefly described.

2.2.1 PVT conditions

The PVT conditions are more complex in a CO_2 flood then for instance in a HC flood, and the phase behaviour with reservoir oil is both difficult to predict and measure during the entire flood period. The relatively high solubility in water and the associated reduction in pH will affect the reservoir chemistry depending on the PVT conditions, reservoir fluid and rock composition. Grigg and Siagian [8] have investigated those phenomena for a four-phase flow in low temperature CO_2 floods. The main conclusion from this work is:

- Up to five phases, aqueous, liquid HC, liquid CO_2, gaseous CO_2 and solid asphaltene precipitate, can coexist in a CO_2 flood.
- The actual number of phases depends on pressure, temperature and composition.
- Gas who condensing into a second liquid phase can be significant at temperatures just above the critical CO_2 pressure, and near the saturation pressure for CO_2 at lover temperatures. It is assumed that this would only occur behind the temperature front for a typical offshore oil field.
- CO_2 displacement efficiency may increase as the pressure is decreased until the minimum miscibility pressure is reached.
- It is necessary to consider all this complex behaviour when predicting flood performance. Therefore, it is important to do detailed compositional simulations as a part of the planning of the CO_2 flood.

2.2.2 CO_2 hydrates

When water is present, CO_2 hydrate can form at appropriate temperatures and pressures. CO_2 hydrates can occur at temperatures as high as 10 ^oC if the pressure is greater than 45 bar. Hydrate formation can be a problem at chokes and valves where pressure is reduced suddenly and CO_2 cools because of expansion, Stalkup [7]. It is experienced that hydrate has occurred in projects where original reservoir temperature are as high as 27^oC. This has happened in the North Cross Devonian Unit [9], where it usually occurs in wells with high gas-oil ratio and high CO_2 cuts.

The possibility of forming CO_2 hydrates must be taken into account when CO_2 floods are considered in NCS reservoirs, where CO_2 hydrates will form at temperature of approximately 10 ^oC over the pressure range expected upstream of the separators [7].

2.2.3 Wettability

Wetting characteristic of the reservoir rock appear to be the most controlling factor of the operating strategy for an EOR process, but according to McDougal, Dixit and Sorbie [10], the precise taxonomy of wettability is still lacking. There are also indications that core floods and capillary tube visual cell tests can give inconsistent changes in wettability due to CO_2 miscible flooding. CO_2 reduces the brine pH, and there is some experimental evidence that this reduces the water-wetness in capillary cells. Experience from both laboratory tests and studies of field data supports that wetting characteristic is critical to CO_2 floods.

Rogers and Grigg [11] concludes that water-wet conditions suggest continuous gas injection, while oil-wet conditions suggest water alternating with gas (WAG) process with an optimum of equal or 1:1 velocity ratio. Jackson, Andrews and Clarigde [12] stated also that mixed-wet states indicate maximum recovery is a stronger function of slug size in secondary CO_2 recovery than in a tertiary flood. In addition, water-wet laboratory models indicate gravity forces dominate while in oil-wet tertiary floods where viscous fingering is a controlling factor.

2.2.4 Scale

Scaling problem is often seen in connection with water injection or where produced water is increasing. It is not a problem for the fluid flow in the reservoir, but it puts restriction on flow through the production wells and the injection wells. When CO_2 is injected it tends to exacerbate any $CaCO_3$ scaling problem because the bicarbonate concentration in the produced water increases. Since the scaling, and the problems related to scaling will not have any impact on the work on estimating the EOR potential from CO_2 floods, a closer look into the problem will not be done here. But Yuan, Mosley and Hyer [13] have looked into the problem in a study on mineral scaling control. Shuler, Freitas and Bowker [14] has also discussed the problem when selecting scale inhibitors for a CO_2 flood.

2.3 Injectivity abnormalities

Experience from CO_2 floods in US shows examples of both increasing and decreasing injectivity when implementing CO_2 injection or WAG. Based on the fluid flow properties of CO_2, one would intuitively expect that gas injectivity would be greater than the waterflood brine injectivity. However, in practice this behaviour is not always observed. In addition, water injectivity may be higher or lower than the waterflood brine injectivity. What is more perplexing is that some reservoirs may lose injectivity and others may increase injectivity after the first slug of CO_2 is injected. In addition, this phenomenon may occur on a local scale. Injection wells in the same field and reservoir may have significantly different behaviour.

2.3.1 Injectivity increases

Increased injectivity is seen in the SACROC Unit during the WAG process. This is further discussed by Langston, Hoadley and Young [15]. Yuan, Mosley and Hyer [13] reported that the water injectivity increased after injection of liquefied CO_2 in the Sharon Rigde Canyon Unit. It is a limestone reservoir, and the effect may be a result of increased permeability caused by dissolution of calcium from the limestone rock by carbonic acid. Jasek, Frank, Mathis and Smith [16] have reported that the same effect is seen from the Goldsmith San Andreas Unit CO_2 pilot. A number of CO_2 floods have also experienced higher gas injection relative to pre water flood injections. One example here is the North Ward Estes CO_2 flood, studied by Ring and Smith [17] and Prieditius, Wolle and Notz [18].

Roper [19] has seen that after the first CO_2 slug in a WAG process the brine injectivity tend to increase. It is assumed that this is attributed to combined effects of:

- High degree of heterogeneity
- Cross flow
- Oil viscosity reduction
- Penetration of CO_2 through high permeability zones
- Compressibility and redistribution of the reservoir pressure profile during shut-in periods prior to injection of brine
- Solubility of CO_2 in injected brine near wellbore

It's assumed that the injectivity increase will not be as great where vertical permeability is lower, pay section is thicker, or the injection well is stimulated and production well is not stimulated.

2.3.2 Injectivity reduction

Reduction of injectivity is problematic for a CO_2 flood. This could be seriously detrimental to a WAG project if it led to a shortfall in voidage replacement that reduces the reservoir pressure below the minimum miscibility pressure for the CO_2. A review of the WAG field experience is further discussed in a study done by Christensen, Stenby and Skauge [20]. They also indicate that reduced injectivity could be caused by wellbore heating that closes thermal fractures, or hydrate or asphaltene precipitation in the near wellbore region.

For some fields there is reported great loss in injectivity, Stein, Frey, Walker and Parlani [21] gives an example from the Slaughter Estate Unit, where the most mature patterns suffered a 40% loss of injectivity for CO_2, and 57% loss for water. This is a dolomite reservoir, and the injection was below the reservoir parting pressure.

2.3.3 Entrapment

Entrapment has been suggested as a cause of injectivity loss. Mechanisms found to affect trapping in miscible displacements at laboratory scale are solvent diffusion, oil swelling, water saturation and solvent contact time. In a CO_2 flooding process, the oil becomes increasingly heavy, suggesting that some oil is initially bypassed and later recovered by extraction.

Capillary entrapment is a phenomenon that could occur in a CO_2 tertiary flood since the solvent must displace water in order to mobilize and recover the oil. This entrapment occurs when the oil saturation becomes low, and the oil phase network loses its continuity. At this point, viscous and gravitational pressure gradients become insufficient to mobilize the remaining oil that is trapped against capillary barriers in the reservoir. Those phenomena are further discussed in a study done by van Lingen and Knight [22].

2.3.4 Relative permeability

Relative permeability, the permeability of one phase relative to another, determines the mobility ratio of the CO_2 flood displacement. Defined as the ratio of the displacing to the displaced mobility, the overall efficiency of miscible displacement may be lowered by the effect of an unfavorable mobility ratio. Relative permeability occurs because the rock porosity contains multiple phases including oil, water, and gas. Relative permeability affects the injectivity of CO_2 and, therefore, is an important factor in the rate at which CO_2 will be sequestered.

Relative permeability is an important input to any reservoir modelling and simulations, but it must be regarded as a lumping parameter that includes effects of wetting characteristics, heterogeneity of reservoir rock and fluid (interfacial tensions), fluid saturations and other micro and macro influences. It has been seen from laboratory studies that large differences in CO_2 and oil relative permeability's can generate large differences for predicted injectivity, Prieditis and Brugman [23]. Roper, Pope and Sepehrnoori [24], have shown in their analyses of tertiary injectivity of CO_2 that a sharp injectivity reduction at the start of the brine cycle can be associated with relative permeability reduction near the well and then gradually experience an increasing injectivity trend throughout the rest of the cycle. It is not a monitored case, but simulated, and the reason is suggested to be due to two-phase flow of gas

and brine initially near the well. While the cycle proceeds, the saturations and the relative permeabilities change.

In a literature analysis of the WAG injectivity abnormalities in the CO_2 process, Rogers, Reid and Grigg [11] have discussed the permeability effects in more detail. One observation is that CO_2 relative permeabilities in West Texas carbonates can be 0.01 times oil relative permeability end points, and therefore errors in CO_2 relative permeabilities can cause large errors in injectivity predictions. Errors in CO_2 relative permeabilities seem to affect gas production and injectivity more than it effects oil recovery.

2.3.5 Heterogeneity

Pizarro and Lake [25] have studied the effect of heterogeneity on injectivity through geo statistical analysis and autocorrelation of the reservoir permeability distribution. They found that injectivity in a heterogeneous reservoir is a function of 10 parameters:

$$I = f(k_x, k_z, \mu, P_L, L, h_1, h_2, H, W, q)$$

In this function, k_x and k_z are the permeability in x and z direction, μ is the viscosity, P_L is the pressure at well location x, L is the length of a rectangular reservoir, h_1 and h_2 represent the bottom and the top of the perforation interval, H is the reservoir thickness, W is the width of a rectangular reservoir and q is the flow rate.

WAG recovery is more sensitive to reservoir heterogeneity than oil recovery by water injection alone, and therefore this is an important issue to consider in a CO_2 flood where WAG is regarded as the optimum recovery mechanism.

Heterogeneity by means of stratification may strongly influence the water-gas displacement process. This is discussed in a study done by Surguchev, Korbrl and Krakstad [26]. Vertical conformance of WAG displacement is strongly influenced by conformance between zones. In a none communicating layered system, vertical distribution of CO_2 is dominated by permeability contracts, Gorrell [27]. The ratio of viscous to gravity forces is the prime variable for determining the efficiency of WAG injection and controls the vertical conformance and displacement efficiency of the flood. Roper, Pope and Sepehrnoori [24] indicate that cross flow or convective mixing can substantially increase injectivity even in the presence of low vertical to horizontal permeability ratios.

2.3.6 Concluding remarks on injectivity abnormalities

A literature analysis of the WAG injectivity abnormalities in the CO_2 process is done by Rogers and Grigg [11], and the conclusions on factors effecting injectivity drawn from the literature are: Hence, the bullet points below shows only the headlines.

- Lower injectivity is not necessarily a near-wellbore effect.
- Oil banks.
- Salinity and pH may change the reservoir wettability.
- Wettability.
- There is considerable disagreement as to whether dissolution, precipitation and particle invasion/migration occurs during injection of CO_2 and/or the WAG process.
- Fluid trapping or bypassing.
- Relative permeability effects.

- Directional permeability effects.
- Phase behaviour.

2.4 Advantages and disadvantages by using CO_2 as a solvent in miscible floods

CO_2 is regarded to be an excellent solvent for miscible CO_2 floods. But still there are both advantages and disadvantages to take into consideration when considering an EOR project.

2.4.1 Advantages

The greatest difference compared to other gases is that CO_2 can extract heavier components up to C_{30}. The solubility of CO_2 in hydrocarbon oil causes the oil to swell. CO_2 expands oil to a greater extent than methane does. The swelling depends on the amount of methane in the oil. Because the CO_2 does not displace all of the methane when it contacts a reservoir fluid, the more methane there is in the oil, the less is the swelling of oil. CO_2 has the following characteristics in a flood process:

- It promotes swelling
- It reduces oil viscosity
- It increases oil density
- It is soluble in water
- It can vaporize and extract portions of the oil
- It achieves miscibility at pressures of only 100 to 300 bar
- It reduces water density
- It reduces the difference between oil and water density, and then reduce the change for gravity segregation
- It reduces the surface tension of oil and water, and result in a more effective displacement

2.4.2 Disadvantages

One of the main problems in achieving profitable CO_2 flooding has been the high mobility of the CO_2. The relative low density and viscosity of CO_2 compared to reservoir oil are responsible for gravity tonguing and viscous fingering. The effect of CO_2 is more severe than those problem are in a water flood. In order to avoid those negative effects, several attempts have been don to improve the sweep efficiency. Those can be:

- Installation of well packers and perforating techniques
- Shutting in production wells to regulate flow
- Alternating CO_2 and water injection (WAG)
- Addition of foaming solutions together with CO_2

The volumetric sweep efficiency can be significantly improved by implement the WAG process. The gas mobility in the reservoir will be reduced, and becomes close to the mobility of the water. However, the complete evaluation of the process must take into account the possible effect of hysteresis on relative permeability's in drainage and imbibitions, and it is important to find an optimal water/CO_2 ratio. Another option to reduce the mobility of CO_2 is to implement foaming solution combined with CO_2 injection. This can either be done to improve the sweeping conditions or blocking the CO_2 in more permeable layers. Foam is further discussed by Chang, Owusu, French and Kovarik [28].

3. ENHANCED OIL RECOVERY

Enhanced Oil Recovery (EOR) is a term applied to methods used for recovering oil from a petroleum reservoir beyond that recoverable by primary and secondary methods.

The main objective of all methods of EOR is to increase the volumetric (macroscopic) sweep efficiency and to enhance the displacement (microscopic) efficiency, as compared to an ordinary water flooding. One mechanism is to increase the volumetric sweep by reducing the mobility ratio between the displacing and displaced fluids. The other mechanism is targeted to the reduction of the amount of oil trapped due to capillary forces. By reducing the interfacial tension between the displacing and displaced fluids the effect of trapping is lowered.

In general, EOR technologies fall into four groups of the following categories:

- Gas miscible recovery
- Chemical flooding
- Thermal recovery
- Microbial flooding

This thesis will focus on the CO_2 miscible process, and therefore, examples of EOR technologies are just briefly described here.

Gas miscible recovery:

The injection fluid (solvent) is normally natural gas, enriched natural gas, flue gas, nitrogen or CO_2. These fluids are not first contact miscible with reservoir oils, but with sufficiently high reservoir pressure they achieve dynamic miscibility with many reservoir oils. Miscibility and drive mechanisms are further described and discussed in chapter 4. CO_2 flooding has proven to be among the most promising EOR methods, especially in the US because it takes advantage of available, naturally occurring CO_2 reservoirs. Injection of CO_2 in mature oil fields on the Norwegian Continental Shelf is presently also under evaluation. This is further described in chapter 6. US experience is described in chapter 5.

Chemical recovery:

Polymer flooding
In this enhanced water flooding method, high molecular weight water-soluble polymers are added to the injection water to improve its mobility ratio, reducing oil "bypassing" and raising yields. Permeability profile modification treatments with polymer solutions are becoming increasingly common.

Surfactant flooding
Also known as micellar-polymer flooding, low-tension water flooding, and micro-emulsion flooding, this method typically involves injecting a small slug of surfactant solution into the reservoir, followed by polymer thickened water, and then brine. Despite its very high displacement efficiency, miscellar-polymer flooding is hampered by the high cost of chemicals and excessive chemical losses within the reservoir.

Thermal recovery:

Steam injection
Steam injection and flooding are very effective in recovering heavy viscous crudes. Thermal recovery is applicable for individual well stimulation or field-wide flooding.

In-situ combustion
This process attempts to recover oil by burning a portion of in-place crude. Air or oxygen is injected to facilitate burning. The process is very complex involving multiphase flow of flue gases, volatile hydrocarbons, steam, hot water, and oil. Its performance in general has been insufficient to make it economically attractive to producers.

Microbial recovery:

This method takes advantage of microbial byproducts in the reservoir, such as CO_2, methane, polymer, alcohol, acetone, and other compounds. These, in turn, can change oil properties in a positive direction, and thereby facilitate additional oil recovery.

4. ENHANCED OIL RECOVERY BY MISCIBLE GAS/CO_2 FLOODING

After a field is flooded by water there are large volumes of oil remaining in the reservoir because of capillary forces and surface forces acting in the fluid-rock system. This residual oil is the target for tertiary CO_2 flooding which will be further described in this thesis. The estimated recovery from oilfields on the NCS varies from about 15 to 65 % of STOIIP, averaging on 44%, which means that the EOR potential is large.

4.1 Miscibility and drive mechanism

To explain the different processes in miscible flooding, ternary diagrams are widely used. In the following, ternary diagrams will be shown for the different flooding conditions. Figure 4.1 summarizes the different processes.

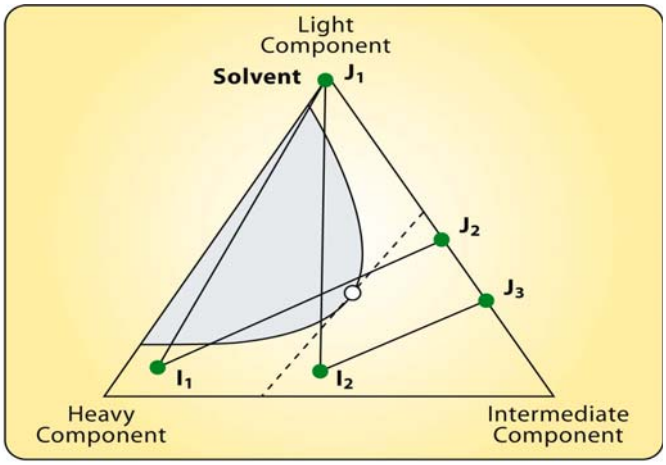

I_1 - J_1: Immiscible drive
I_2 – J_3: First contact miscible
I_2 – J_1: Vaporizing gas drive
I_1 - J_2: Condensing gas drive

Figure 4.1 - Conditions for different types of oil displacement by solvents [29].

Since the dilution path (I_2-J_3) in figure 4.1 does not pass through the two-phase region or cross the critical tie line, it forms first contact miscible displacement. The path (I_1-J_1), which entirely lies on the two-phase region, forms immiscible displacement. When the initial and injected compositions are on the opposite side of the critical tie line, the displacement is either a vaporizing gas drive ((I_2-J_1) or a condensing gas drive (I_1-J_2).

4.2 First contact miscible flooding

The most direct method to achieve miscible displacement is by injecting a solvent that mixes with the oil completely, such that all mixtures are in single phase. To reach the first-contact miscibility between solvent and oil, the pressure must be over the cricondenbar since all solvent-oil mixtures above this pressure are single phases. If she solvent, for instance a propane-butane mixture is liquid at reservoir pressure and temperature, the saturation pressure for the mixture of oil and solvent will vary between the bobble-point pressure for the oil and the bobble-point pressure for the solvent. In this case the cricondenbar is higher than the two bobble-point pressures. If the solvent is gas at reservoir pressure and temperature, the phase behaviour is more complicated. In this case, the cricondenbar may occur at mixtures intermediate between pure oil and pure solvent.

If natural gas or CO_2 is chosen as a solvent to sweep the reservoir, a miscible slug must be created ahead of the injected gas in order to reach a miscible displacement process. The slug may be of propane or liquefied petroleum gas, and the slug must be completely miscible with the reservoir oil at its leading edge and also completely miscible with the injected gas at its

tailing edge. The volume of the injected slug material must be sufficient to last for the entire sweep process. The first contact flooding will not continue if the slug is bypassed. The first contact minimum miscible pressure (FCMMP) is the lowest pressure at which the reservoir oil and injection gas are miscible in all rations.

4.3 Multiple contact miscible flooding

The degree of miscibility between a reservoir oil and injection gas is often expressed in terms of the minimum miscibility pressure (MMP). The multiple contact miscibility pressure (MCMMP or just MMP) is the lowest pressure at which the oil and gas phases resulting from a multi-contact process, vaporizing or condensing, between reservoir oil and an injection gas are miscible in all rations.

Multiple contact miscible injection fluid is normally natural gas at high pressure, enriched natural gas, flue gas, nitrogen or CO_2. These fluids are not first-contact miscible and forms two-phase regions when they mix directly with the reservoir fluids. The miscibility is achieved by mass transfer of components witch results from multiple and repeated contact between the oil and the injected fluid through the reservoir. There are two main processes where dynamic miscible displacement can be achieved. Those are the vaporizing and the condensing gas drive.

The following descriptions explain the mechanisms for gas drives in general, but the difference between CO_2 and natural gas is that the dynamic miscibility with CO_2 does not require the presence of intermediate molecular weight hydrocarbons in the reservoir fluid. The extraction of a broad range of hydrocarbons from the reservoir oil often causes dynamic miscibility to occur at attainable pressures, which are lower than the miscibility pressure for a dry hydrocarbon gas.

4.3.1 Vaporizing gas drive

Vaporizing gas drive is a particular case of a multiple contact miscibility process. It is based on vaporization of the intermediate components from the reservoir oil. A miscible transition zone is created, and C_2 to C_6 (CO_2can extract up to C_{30}) is extracted due to the high injection pressure. A vaporizing gas miscible process can displace nearly all the oil in the area that has been contacted. However, the fraction of the reservoir contacted may be low due to flow conditions and reservoir heterogeneities. The process requires high pressure at the oil-gas interface, and the reservoir oil must contain a high concentration of C_2 to C_6, particularly if HC gas is used.

The pressure required for achieving dynamic miscibility with CO_2 is usually significantly lower than the pressure required for other gases as natural gas, flue gas or nitrogen. By using CO_2, also higher molecular weight hydrocarbons can be extracted. The lower pressure and the extraction of higher hydrocarbon fractions are a major advantage of the CO_2 miscible process.

Figure 4.2 shows a ternary diagram for this process. The displacement is not first contact miscible because the dilution path passes through the two-phase region. To explain the process in the figure, one has to image that there are a series of mixed cells that represent the permeable medium in a one-dimensional displacement. The first cell initially contains crude oil to which one adds an amount of solvent so that the overall composition is given by the mixture. The first mixture (the point on the tie line L_1-G_1 where it crosses the solvent – crude line) will split into two phases, gas G_1 and liquid L_1, determined by the equilibrium lines. The gas G_1 will have a much higher mobility than the liquid L_1, and moves into a second mixing

cell to form the next mixture. The liquid L_1 remains behind to mix with more pure solvent. In the second cell the mixture splits into G_2 and L_2 and so on. Behind the second cell as it is shown in this figure the gas phase will no longer form two phases on mixing with the crude. From this point all compositions in the displacement will be a straight dilution path between the crude and a point tangent to the bimodal curve. The displacement will be first contact miscible with a solvent composition given by the point of tangency. Now the process has developed miscibility since the solvent has been enriched in intermediate components to be miscible with the crude. The vaporizing gas drive occurs at the front of the solvent slug. The process is called a vaporizing gas drive since the intermediate components have vaporized from the crude.

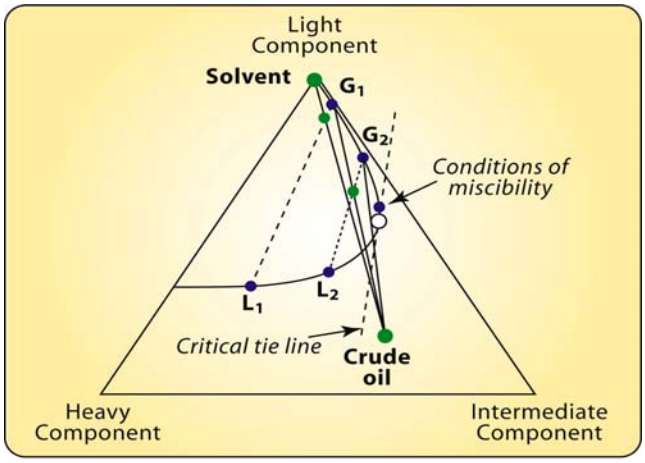

Figure 4.2 - Multiple contact vaporising gas drive [29].

4.3.2 Condensing gas drive

When a rich gas is injected into oil, oil and gas are initially immiscible. Multiple contacts condensing drive will occur when the reservoir oil in a particular cell meets new portions of fresh solvents. A miscible bank forms through condensation of the intermediate components from gas into oil. Then a process similar to the vaporizing drive will be developed, and the oil behind the front becomes progressively lighter. The successive oil compositions formed behind the front will occupy a greater volume in the pores than the original oil because of swelling. This will then lead to form a mobile oil bank behind the zone of gas stripped of intermediate components. The process continues unless developed miscibility conditions are met.

The process is shown schematically in figure 4.3 where the first mixing cell splits into liquid L_1 and gas G_1. Gas G_1 moves on to the next mixing cell and liquid L_1 mixes with fresh solvent to form the next mixture. Liquid L_2 mixes with fresh solvent, and so on. The mixing process will ultimately result in a single-phase mixture. Since the gas phase has already passed through the first cell, the miscibility now develops at the rear of the solvent-crude mixing zone as a consequence of the enrichment of the liquid phase from the intermediate components. The front of the mixing zone is a region of immiscible flow owing to the continual contacting to the gas phases G_1, G_2, and so on. Since the intermediate component condenses into the liquid phase, the process is called a condensing gas drive.

CO_2 cannot form miscibility alone, but through a vaporizing drive were injected CO_2 vaporizes some of the light components in the oil. These are subsequently re-condensed at the

displacement front creating an enriched zone with favourable mobility characteristics, referred to as a combined vaporizing and condensing drive.

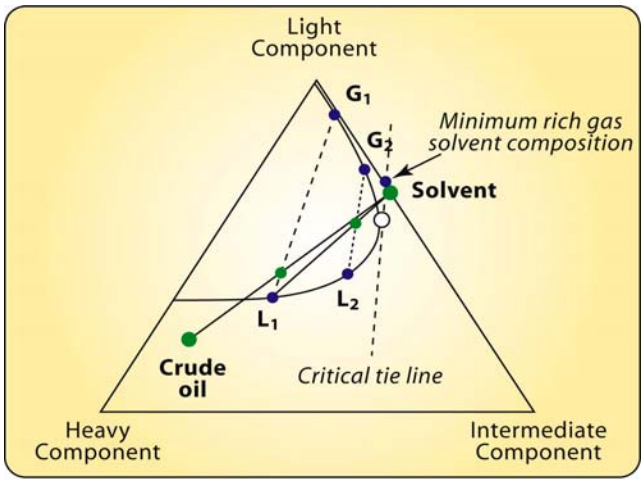

Figure 4.3 - Multiple contacts condensing gas drive [29].

4.3.3 Combined vaporizing and condensing mechanism

Experimental observations and calculations with equation of state have shown that miscible displacement by rich gas injection seems to be due to a combined vaporizing and condensing mechanism. Zick [30], Novosad and Costain [31]. The main conclusions from those articles are:

- A combined vaporizing and condensing gas drive mechanism is more likely than a pure condensing gas drive when rich gas is injected into reservoir oil.
- A pseudo miscible zone develops quite similar to that in a condensing gas drive.
- Some residual oil remains trapped behind the displacement as in a vaporizing gas drive.

For the CO_2 case, a combined drive can be developed under the right circumstances. MMP calculations done with PVT-Sim (se chapter 8.2) results in consequently lover MMP for the combined drive than for the vaporizing drive for a wide range of fluid compositions.

4.4 Minimum miscible pressure from slimtube miscibility apparatus

The minimum miscibility pressure can also be measured by using a slim tube miscibility apparatus. There exist various types of slimtube apparatus based on the chosen operation conditions.

The apparatus is usually constructed to measure miscibility conditions at reservoir pressure and temperature, and in general terms it works the way that the gas to be tested is injected at a desired pressure through the slim tube previously cleaned and saturated in oil by means of a high-pressure pump. A backpressure regulator maintains a constant pressure inside the system. The effluents can be observed through a capillary sight glass tube. They are then exposed to atmospheric pressure and temperature through a backpressure regulator. The volume of liquid effluents is then monitored continuously using a digital volume-measuring detector. The produced gas can be measured with a wet gas meter. A set of recovery curves can be plotted by using the raw data obtained from the different miscible displacement experiment. MMP for the fluid flooded by gas or CO_2 can be constructed as shown in figure

4.5. Density meter and gas chromatograph may be installed to extend the capabilities of the instrument. Figure 4.4 shows a schematic view for a slim tube apparatus.

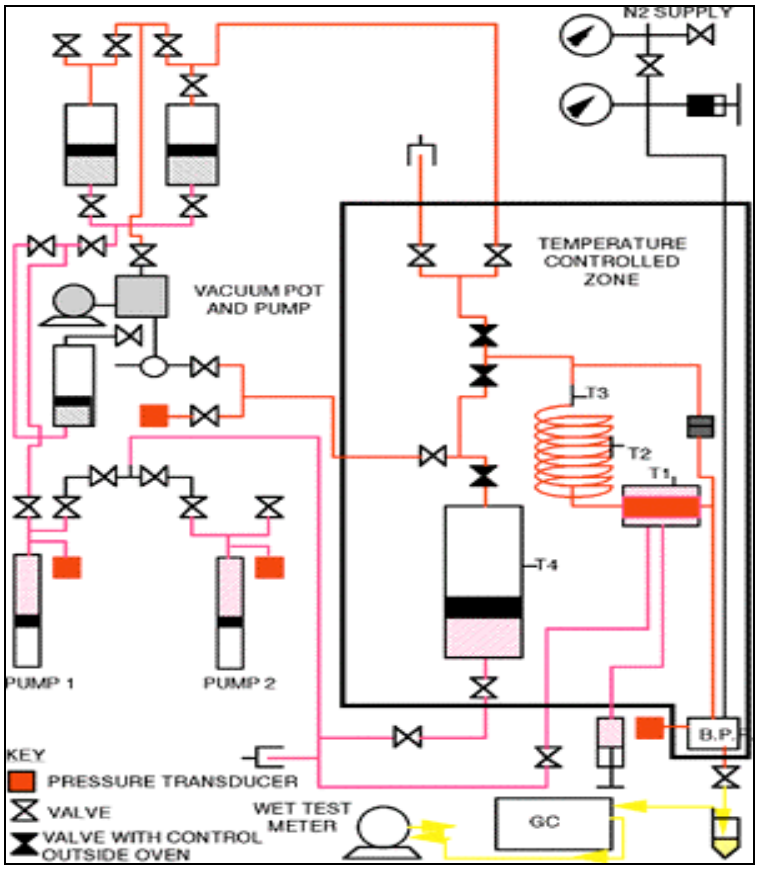

Figure 4.4 - Schematic view of a slim tube apparatus [32].

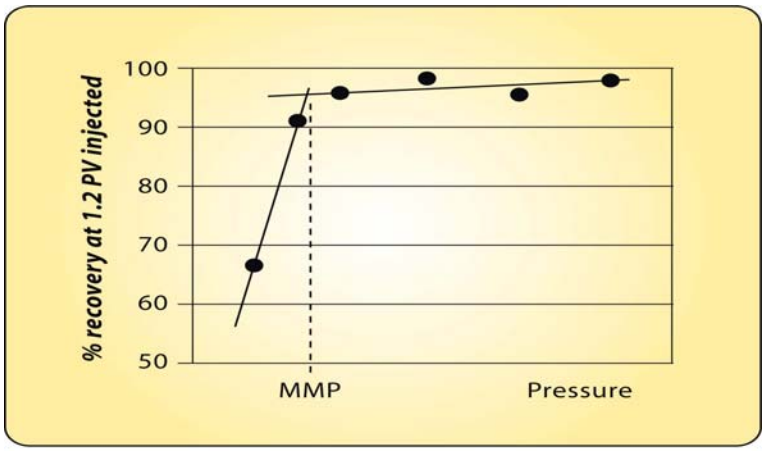

Slim tube MMP:
The MMP is defined [1] as the pressure for which the oil recovery is at least 90 % after 1.2 PV of solvent is injected.

Figure 4.5 – MMP estimation by recovery curves at different pressures.

A slimtube miscible measurement is often of high quality. However, a reliable slimtube test is strongly dependent on the packed grain sizes. This is attributable to difference in the pore throat sizes and associated pore invasion pressure due to capillarity. This is further discussed in a paper presented by F.B Thomas, T. Okazawa, P. Hodgins, X. Zhou, A. Erlian and D.B. Bennion. [33].

Slimtube experiments and interpreted slimtube simulations can provide a reliable determination of MMP for a system. But one of the major problems with this type of miscibility tests is the severe case-dependent dispersion, physical or numerical. Those effects have to be taken into account in order to avoid an overestimation of the MMP. Stalkup [34] and Lars Høier, Curtis H. Whitson [35] have investigated those effects.

4.5 Some remarks on the MMP and the calculation of the MMP

Miscibility pressure is one of the most important parameters for a CO_2 miscible flood. The different factors effecting the MMP, correlations and reliability is investigated by varies author. Stalkup [34] have summarised some of the experience gained up to 1983:

- Dynamic miscibility occurs when the CO_2 density is sufficiently great that the dense gas CO_2 or liquid CO_2 solubilizes the C_5 through C_{30} hydrocarbons contained in the reservoir oil.
- Reservoir temperature is an important variable, and higher temperature results in higher MMP requirement.
- MMP is inversely related to the total amount of C_5 to C_{30} present in the reservoir oil. The more of these, the lover is the MMP.
- MMP is affected by the molecular weight distribution of the individual C_5 to C_{30}. Low molecular weight results in lower MMP.
- MMP is affected of the types of hydrocarbons, but too much lesser degree than the fractions. For example, aromatics result in lower MMP.
- Properties of heavy fractions, > C_{30} also affect the MMP, but not as much as the total quantity of C_{30}^+.
- MMP does not require the presence of C_2 to C_4.
- The presence of methane in the reservoir does not change the MMP appreciably.

Høier and Whitson [35] have investigated miscibility variation in compositionally grading reservoirs (paper from 1998). They have gone through the various mechanisms. One important conclusion from this work regarding EOR is that the MMP in oil reservoirs always increases with depth, both for vaporizing and condensing/vaporizing mechanisms. Vaporizing MMP is always greater than or equal to the bobble-point pressure, while the condensing/vaporizing MMP can be greater than or less than the bubble point pressure.

Resent work by various authors seems to conclude that analytical approach and new developments of analytical equations gives good results in determining the MMP and MME (minimum miscibility enrichment). Hua Yuan and Russell T. Johns from the University of Texas at Austin have recently developed a simplified method for calculation of the MMP and MME [36 and 37]. They have focused on method robustness. This new method differs from other published methods by significantly reducing the number of equations and unknown parameters. It is a fast and robust method for calculation, and it can avoid trivial and false solutions.

5 SUMMARY OF CO_2 FLOOD PROJECTS WORLDWIDE

CO_2 as injection gas for oil recovery has been mentioned as early as 1916 in the literature, but it was dismissed as a laboratory curiosity due to the absence of large and economically prised supplies. But in the early 1950s the industry started to look more seriously into miscible flooding. It began with looking at first contact miscible floods projects by using propane, LPG and natural gas. But these solvents were soon regarded to be too expensive and unsuitable at that time because of their low viscosity and density, which could result in low volumetric sweep efficiency. As a result of rejecting those solvents, CO_2 was again on the agenda. The first project, the Ritchie field, started CO_2 injection in 1964.This was a small project, and first in 1972 the bigger CO_2 project, SACROC Unit in Scurry County in the Permian Basin, started to inject CO_2 as an immiscible secondary recovery mechanism. After that, CO_2 floods have been used successfully throughout several areas in the US, especially in the Permian Basin. Outside the US, CO_2 floods have been implemented in Canada, Hungary, Turkey, Trinidad and Brazil.

Except from US, there are not many CO_2 floods worldwide. The main reason for this has most probably to doe with the availability of CO_2. Huge volumes are required, and there are lack of both infrastructure and sources in most of the oil producing regions world wide, except from US, especially in the Permian Basin. Today there are about 78 CO_2 floods in operation world wide, 67 in US, 2 in Canada, 2 in Turkey, 5 in Trinidad and 1 in Brazil [38]. But all together there have been more than 100 EOR projects with CO_2 flooding since the first flood took place [39 and 40].

Operations History:

- USA: 85 projects
- Canada: 8 projects
- Hungary: 3 projects
- Turkey: 2 projects
- Trinidad: 5 projects
- Brazil: 1 project, onshore oil field [38]

United States:

- 67 floods (66 miscible and 1 immiscible)
- The first large project SACROC started in January 1972
- Average life of producing properties is about 12 years
- 21 companies are operating floods in 2001 (1 to 16 projects)
- There are over 6,400 producing wells and 4,200 injection wells
- Depths varies from 820 to 3280 m

Canada:

- Retlaw Mannville: Nov. 1983 (Immiscible CO_2, Terminated)
- Joffre Viking Pool: Jan. 1984 (Miscible CO_2, Operating)
- Abandoned field: (produced about 16% OOIP in mature area)
- Midale Midale Beds: July 1986 (Miscible CO_2, Suspended)
- Harmattan East Rundle: 1988 (Miscible CO_2, Terminated)
- Zama Keg River: 1995 (Miscible acid gas, Terminated)
- Elswick Midale Beds: Apr. 2000 (Miscible CO_2, Suspended)
- Weyburn Midale Beds: Oct. 2000 (Miscible CO_2, Operating)

Other countries:

- Hungary: 3 projects 1971 – 1996 (Immiscible CO_2, Terminated)
- Turkey: 2 projects 1986 (Immiscible CO_2, Operating)
- Trinidad: 5 projects 1974 (Immiscible CO_2, Operating)
- Brazil: 1 project[32] - (Aracas field, miscible operating)

5.1 The Permian Basin

The Permian Basin is one of the most prolific petroleum provinces of North America. It is in a mature stage of both exploration and development. Almost half of the CO_2 floods around the world are located in this area. The CO_2 floods in the Permian Basin uses more than 28.3 million Sm^3 of CO_2 per day and produce more than 20 % of the areas total oil production, more than 22000 Sm^3/day. Oil and gas have been found in rocks ranging from Cambrian to Cretaceous age, but most of the hydrocarbons are found in rocks of Paleozoic age. It is one of the largest structural basins in North America. It encompasses a surface area in excess of 220000 km^2 and includes all or parts of 52 counties located in West Texas and southeast New Mexico. The area is shown in figure 5.1. The name of the basin derives from the fact that the area was down warped before being covered by the Permian sea and the subsidence continued through much of the Permian period. Consequently, it contains one of the thickest deposits of Permian rocks found anywhere.

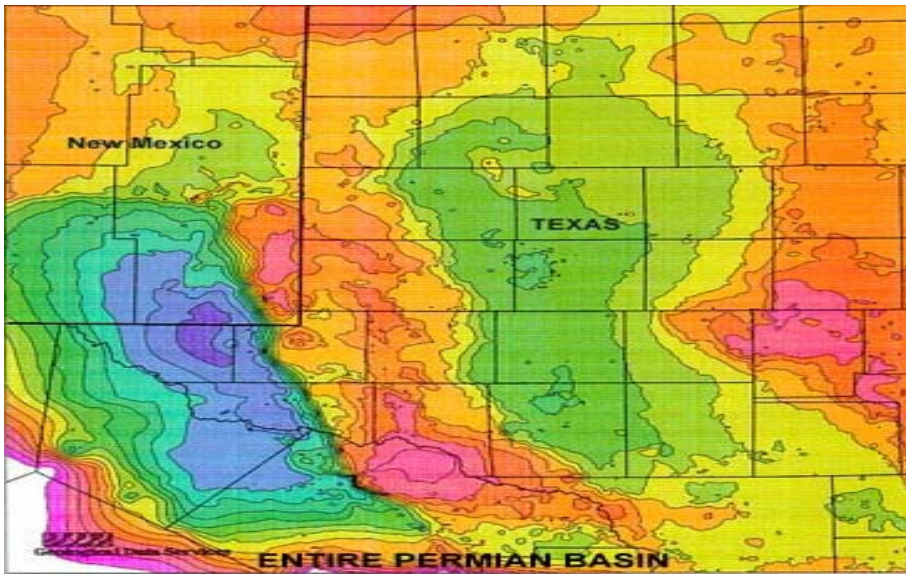

Figure 5.1 - The Permian Basin [41].

Structurally, the Permian Basin is bounded on the south by the Marathon Ouachita Fold Belt, on the west by the Diablo Platform and Pedernal Uplift, on the north by the Matador Arch, and on the east by the Eastern Shelf of the Permian (Midland) Basin and west flank of the Bend Arch. The basin is separated into eastern and western halves by a north-south trending Central Basin Platform. In a cross section, the basin is an asymmetrical feature. The western half contains a thicker and more structurally deformed sequence of sedimentary rock as shown in figure 5.2.

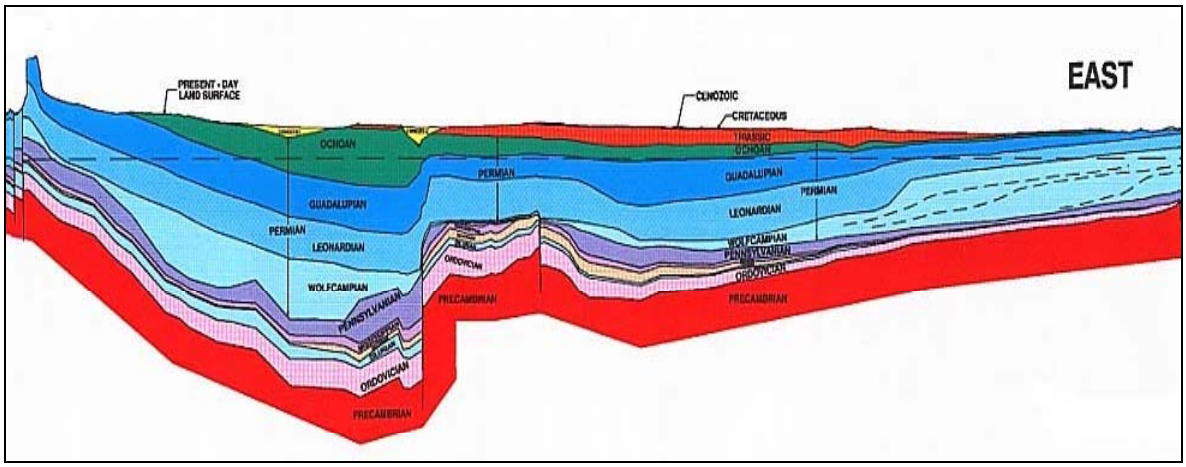

Figure 5.2 - West to East Cross-section of the Permian Basin [42].

Figure 5.2 shows a West to East cross-section of the basin. By combining the contoured map in figure 5.1 with the cross section in figure 5.2, one can observe the Central Basin Platform high in the middle with the deep Delaware Basin to the left and shallower Midland Basin to the right.

The Permian Basin has been characterized as a large structural depression formed as a result of down warp in the Precambrian basement surface. The basin was filled with Paleozoic and, to a much lesser extent, younger sediments. It acquired its present structural form by Early Permian time. The overall basin is divisible into several distinct structural and tectonic elements.

As mentioned, the basin is mature, but already in the early 1970s many oil reservoirs were maturing and the owners started to lock into tertiary recovery methods to increase the oil recovery. Because of the large quantities of CO_2 saturated natural gas near the oil fields, relatively low priced CO_2 was available at that time. Large quantities of CO_2 were being extracted from natural gas and emitted to the atmosphere. A Chevron affiliate conceived and developed the first CO_2 flood in the area, and a 354 km long CO_2 pipeline from four CO_2 extraction plants (OXY - Terrell, Valero - Grey Ranch, Northern - Mitchell, and Warren - Puckett) were built to supply CO_2 to the Sacroc Unit. This was the beginning of the successful history of CO_2 floods in the Permian Basin.

5.1.1 The SACROC Unit in the Permian Basin

The SACROC (Scurry Area Canyon Reef Operators Committee) Unit in the Permian Basin was the first large scale CO_2 flood in the world. The SACROC operation covers an area of 205 km^2 within the depleted Kelly Snyder oil field in the eastern part of the Permian Basin in West Texas.

The oil is mainly produced from limestone reservoirs of the Canyon Reef Formation of late Pennsylvanian age. The field is internally complex, and tight shale zones vertically segregate the oil reservoir into numerous stacked compartments. The zones are not in pressure communication and the fluid flow is essentially horizontal. The reservoir is large and holds approximately 336 million Sm^3 originally oil in place.

Primary oil production started in 1948. To maintain the oil production, secondary oil recovery method with water injection was implemented in 1954. A CO_2 immiscible flood was

implemented in 1972, and 21 year later a tertiary CO_2 miscible flood was implemented, and it is still ongoing.

During the period from 1972 to 1975 the CO_2 came from nearby natural gas processing plants about 270 km away from the oilfield. The CO_2 was naturally occurring in the gas, and had to be separated before further transportation. The CO_2 was a by-product that otherwise would be emitted to the atmosphere. In 1996 they had to change the source of CO_2 supply when the old CO_2 pipeline converted to transport natural gas. The SACROC and the nearby North and South Cross fields converted then to natural CO_2 supplied from Shell CO_2 Company. From 1998 SACROC was supplied with CO_2 from the Val Verde gas treatment plant.

In the early stages of the CO_2 flood the injection rate was about 5.1 million Sm^3/day, but declined to 1.7 million Sm^3/day in 1995. The cumulative gross total CO_2 injected was then about 30 billion Sm^3 and had contributed to 11 million Sm^3 of EOR oil.
EOR performance could have been considerably better within certain portions of the SACROC Unit in area where water flooding had been mature by the time CO_2 injection started. In one area, 2.4 km^2 and 24 wells, injection during the first 5 years led to an incremental recovery of 10 % of the STOIIP. Results over a 7 years period over a larger area, 10.9 km^2 and 100 wells gave incremental oil recovery of 7.5 % of the STOIIP. The previous operator, Pennzoil, has estimated the CO_2 miscible flooding to recover an additional 8 % of the STOIIP. The present operator, Kinder Morgan CO_2 has more than 80 % ownership stake in the SACROC, and are focusing on increasing the CO_2 injection in order to produce more EOR oil. The oil production rate has increased by approximately 50 % since Kinder Morgan acquired interest in SACROC and assumed operations in June 2000. To increase the EOR oil, new CO_2 infrastructure is needed. The building of additional infrastructure will increase CO_2 deliveries to the project from 3.5 million Sm^3/day to well over 5.7 million Sm^3/day when the expansion comes online in late 2003. The unit has produced more than 191 million Sm^3 of oil since its discovery in 1948 and it still has significant additional oil reserves recoverable by CO_2 injection operations.

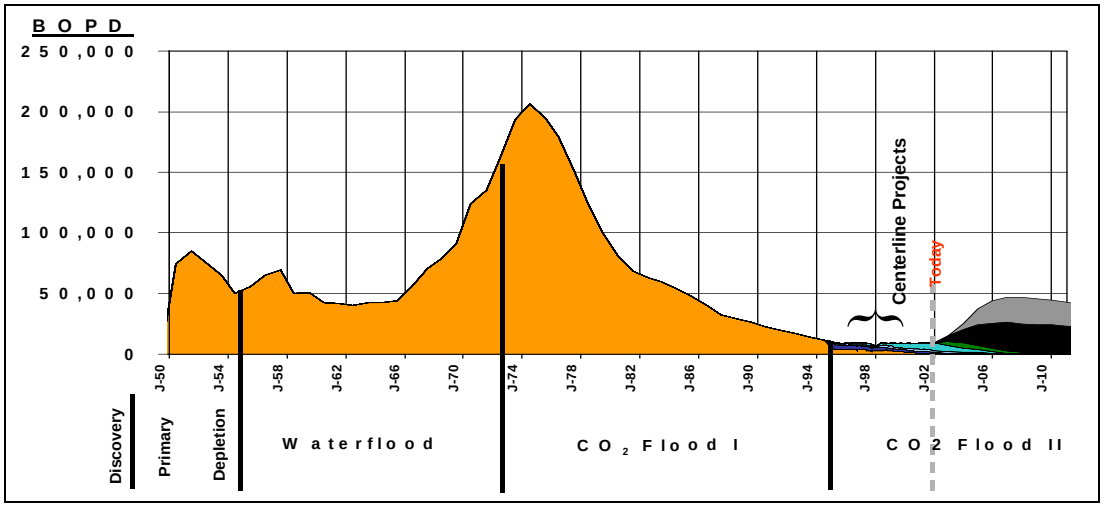

Figure 5.3 - SACROC Unit development history and prognoses up to 2010 [43].

From figure 5.3 one can see that the field has gone through all stages of the general features of an oilfields life periods with a peek production above 31800 Sm^3/day 19 years after the waterflood was implemented. Immiscible CO_2 flood was implemented in 1972 just before the peek production, but after that, the production decreased rapidly. In 1995 the second CO_2

flood was implemented, a tertiary miscible CO_2 flood. At this point the production was down to 1900 Sm^3/day. With the expansion, oil production is expected to grow from approximately 1900 Sm^3/day currently to more than 3180 Sm^3/day by late 2003, with substantial continued growth thereafter, [43 and 44].

5.1.2 SACROC CO_2 project, key parameters

Reservoir:	Limestone, Canyon Reef Formation
Production wells:	325
CO_2 injectors:	57
Original oil in place:	336 million Sm^3
Current EOR area:	200 km2
Estimated EOR prod:	26.8 million Sm^3 (8% of OOIP)
Initial reservoir pressure (-1311 m):	216 bar
Bubble point pressure:	128 bar
Reservoir temperature (-1311 m):	54.4 ^oC
Average porosity:	7,6 %
Average permeability:	19,4 md
Average initial water saturation:	21.9%
Oil viscosity:	0.35 cp
Oil gravity:	0.82
Oil volume factor:	1.5 res m^3/Sm^3
Solution GOR:	178 m^3/m^3
Water-oil mobility ratio:	0.3
CO_2-oil mobility ratio:	8.0

5.2 The Weyburn Oil field in Canada

The Weyburn CO_2 flood is the largest horizontal injection program in the world, involving a 30 m thick fractured carbonate reservoir at 1400 m depth. Approximately 1000 wells, including 137 horizontal wells with 284 lateral legs, have been used to recover 24 % of the oil originally in place. Pan Canadian, the operator, converted 19 patterns of horizontal wells to CO_2 injection. Injection of 85000 to 198000 Sm^3/day per well has occurred since early October 2000. The goal of the CO_2 flood is to increase the production by at least 15 % incremental oil.

The field covers 210 km^2 southeast of Weyburn, just north of the North Dakota border. Production consists primarily of medium gravity crude oil with a low gas to oil ratio. Central Del Rio Oils Limited, a predecessor company that became part of PanCanadian in 1971, discovered the field in December 1954. The actual Weyburn Unit was established in 1962. The 50 companies and individuals then producing from the field pooled their interests into one unit and initiated a water flood project to increase the reservoir pressure. PanCanadian holds now the largest share of the current 37 partners in the field and is operator of the oil field.

Pan Canadian announced in 1997 that they would develop an EOR project to extend the lifetime of the Weyburn field by more than 25 years. The project will involve a CO_2 miscible flood, which is anticipated to extract an additional 19.4 million Sm^3 or more from the field. The CO_2 for the project will come from the Great Plains Synfuels plant in Beulah, North Dakota, operated by the Dakota Gasification Company (DGC). The route of the pipeline is shown in figure 5.4.

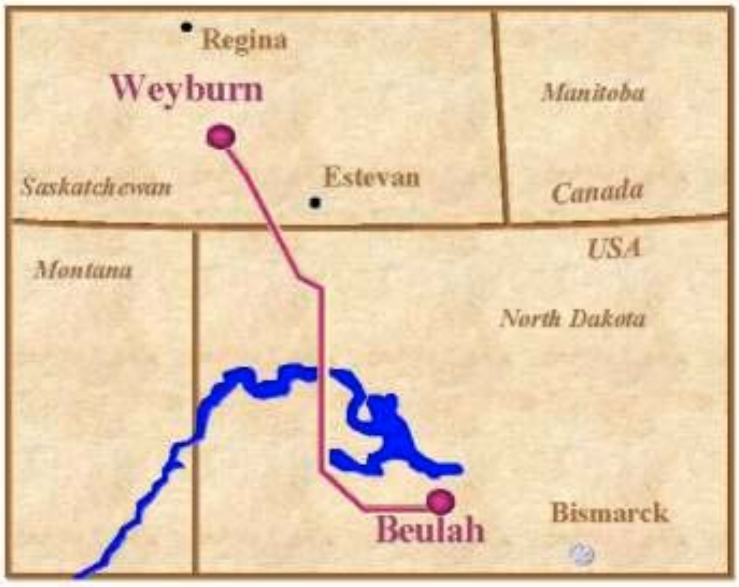

Figure 5.4 - Route of CO_2 Pipeline from North Dakota to Weyburn oilfield [45].

There are two huge compressors pushing the CO_2 through the pipeline. Each compressor is driven by a15 megawatt electric motor. Should additional demand for CO_2 arise, more compressors and a booster station would be required. During normal operations CO_2 will be carried in the pipeline as a gas, but in a supercritical condition and acts much like a liquid. During the pipe filling process, the CO_2 is in a gaseous state. As the pipeline fills and its pressure increases, CO_2 does become liquid. Then as the pressure continues to increase, the CO_2 returns to the gas phase and enters the supercritical state.

Weyburn CO_2 project represents another new by-product for the Synfuels Plant. With CO_2 the Synfuels Plant now has eight by-products on its production list, along with about 3.8 million Sm^3 of synthetic natural gas per day, which is the primary product. PanCanadian will use up to 2.7 million Sm^3 of CO_2 daily, about 40 % of the Synfuels Plant's capacity. At the plant, CO_2 is produced from the Rectisol unit in the gas cleanup train. The pipeline project is a result of the CO_2 sales contract signed in July 1997 between DGC and PanCanadian.

Few of the existing projects use CO_2 from anthropogenic, and the sequestration of CO_2 in this field will make a direct contribution to reducing anthropogenic emissions of CO_2 and will provide an example for future sequestration projects of the potential available from use of this technique.

On September 14, 2000, CO_2 began flowing. The first additional oil from the Weyburn CO_2 flood started to flow in 2001.

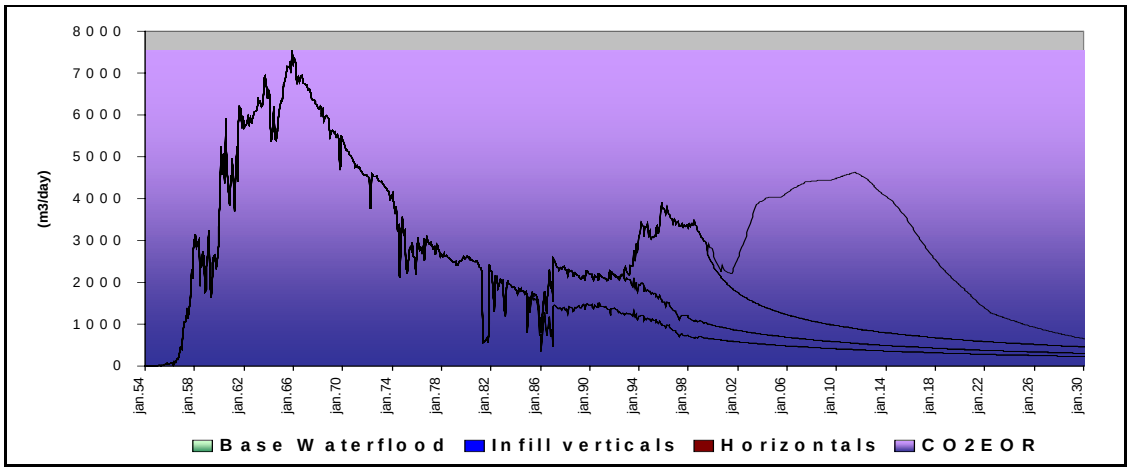

Figure 5.5 - Weyburn production, history and prognoses (1954 – 2030) [45].

Figure 5.5 shows the expected incremental oil production from the miscible CO_2 injection. The production profile is a good example of the feature of an oil field, showing the base case, increased production from infill wells followed by a tertiary EOR technique. A rapid increase in oil production is observed after the CO_2 started to flow into the reservoir. The present aim is to reach a recovery at 40 % of the originally oil in place. It has been estimated that up to half of the injected CO_2 can be stored in the immobile oil that remains in place in the oilfield at the end of production. Pan Canadian will inject 5000 tonnes of CO_2 per day into the Weyburn field as part of its CO_2 EOR operations. Over the 20 years of predicted lifetime it is expected that 20 million tonne of CO_2 will be stored in the Weyburn oil field. In production terms the project will store about 535 m^3 of CO_2 per Sm^3 of oil produced.

The Weyburn field produces from the Mississippian Midale Beds of the Charles Formation, figure 5.6. The reservoir is made up of two parts, the uppermost Marly dolomite and the lowermost Vuggy limestone. The reservoir is overlain by an anhydrite unit that forms the top and up dip lateral seal to the reservoir. The combination of the overlying anhydrite and the porous upper part of the reservoir provides an acoustic impedance contrast and a seismic reflector coincident with the reservoir interval. The reservoir zone generally averages 30 m in thickness, has a temperature of 63 °C, and a pressure of approximately 207 bar.

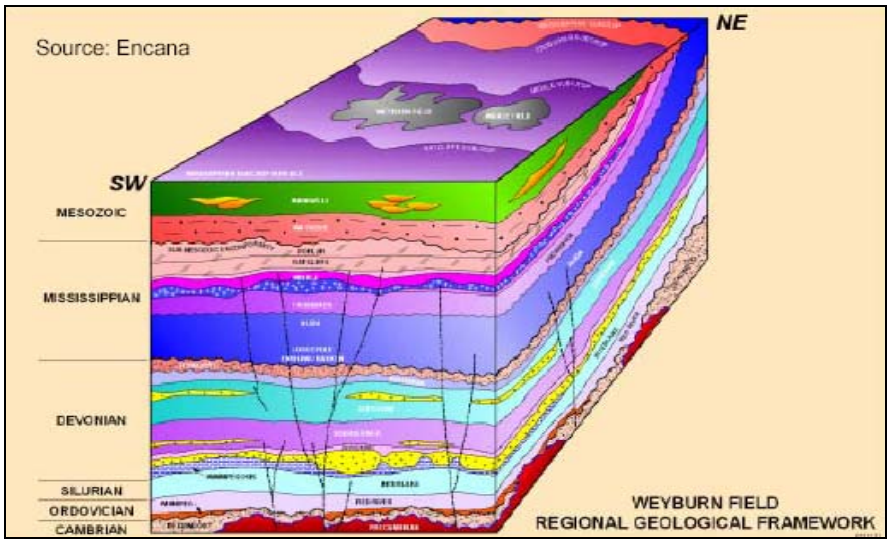

Figure 5.6 – Weyburn regional geological framework [46].

The most porous unit is the Marly, averaging 26 % porosity. Permeability of this zone is low, averaging 10 md. Horizontal wells drilled since 1991 in Weyburn Field have targeted the Marly as a zone of bypassed pay. These wells have substantiated the belief that the Marly unit was not as effectively swept as its underlying counterpart, the Vuggy. The Vuggy averages 11 % porosity and 15 md permeability. The flow capacity of the formation is the product of permeability and net thickness. The Marly has a relatively low flow capacity relative to the Vuggy and correspondingly low sweep efficiency. The potential for bypassed oil in the Marly is greater with CO_2 flooding than it is with water flooding because of the comparatively high mobility of CO_2. Figure 5.6 illustrates the Weyburn field regional geological framework.

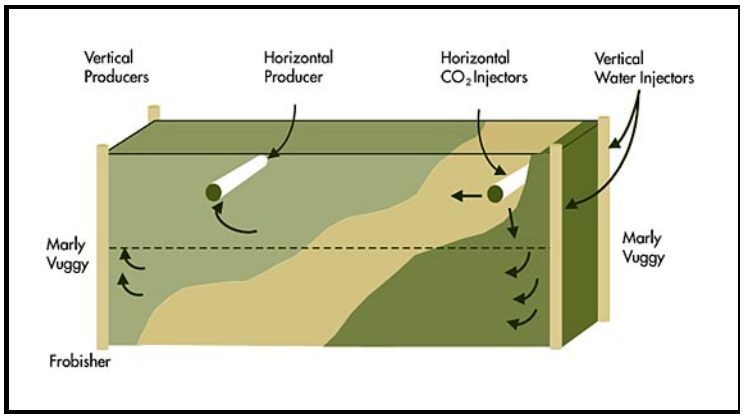

Figure 5.7 – Sketch of Weyburn well configuration [47].

Figure 5.7 illustrates schematically the reservoirs and the horizontal wells, both injectors and producers. Injected CO_2 is flowing both vertically and horizontally away from the horizontal injectors. The geologic model obtained from the history match includes a zone of relatively large vertical permeability in the vicinity of the injection well that allows fluid flow between the upper Marly and lower Vuggy layers. The greatest fracture density occurs in proximity to the faults. The open fracture systems are conduits for fluid movement vertically and laterally in the reservoir. Permeability is the biggest uncertainty in the reservoir modelling thus far. Table 5.1 gives an overview of the reservoir parameters.

Reservoir Zone	Lithology & Textures	Porosity (avg.%, Type)	Matrix Permeability (avg.,md)	Heterogeneity	Fracture Density
Marly (M1, M3)	Dolostone mudstone, wackestone	20-37 (26) intercrystalline moldic	<0.1 - 100 (10)	Low bioturbation dolomitization	Low - Moderate (2-4m spacing) >25% Ø~unfract.
Upper Vuggy (V1)	Limestone packstone, wackestone	2-15 (10) interparticle intraparticle	<0.01 - 20 (1)	Medium thick bedded, bioturbation	High (<1m spacing)
Lower Vuggy (V2-V6)	Limestone mudstone to grainstone	5-20 (15) fenestral vuggy	<1 - 500 (50)	High well bedded, high order cyclicity, complex diagenesis	Moderate - High (<1-2m spacing) microfractured

Table 5.1 – Weyburn reservoir parameters [48].

5.2.1 Weyburn oil field, key parameters

Discovered:	1954
Started water flood:	1964
Started CO_2 flood:	2001
Vertical wells:	490 OP, 181 WI, 16 WAG injectors
Horizontal wells:	184 OP, 1 WI, 13 CO_2I
Originally oil in place:	228 million Sm^3
Cum. Produced (09/01):	56.6 million Sm^3
Total recovery to date:	25,4%
Expected recovery:	40.0% (with additional 8.6% contribution from the CO_2 flood)
Current oil rate:	3300 m^3/d
Area:	180 km^2
Dept:	1450 m
Average res. thickness:	30 m
Res. temperature:	63 ^{0}C
Res. pressure:	207 bar
Sour Crude:	0.9 to 0.86
Geology:	Mississippian Midale Beds/Charles Formation
Vuggy (Limestone):	11% porosity and 15 md permeability
Marly (Dolomite):	26% porosity and 11md permeability

5.2.2 The Weyburn CO_2 Monitoring Project

An intensive research program closely follows the Weyburn field, and the information and experience gained will contribute to a better understanding of the CO_2 effect both to EOR, sequestration and capture. The program is organised by the International Energy Agency (IEA). The project has government and industrial sponsors, and there are a range of research partners from Canada, USA and Europe. The project is described in more detail in the project proposal for funding prepared by the Petroleum Technology Research Centre Regina, Saskatchewan January 26, 2000 [49], and [46]. The main project objectives and some milestones are listed below:

Specific project objectives:

- Develop expertise in CO_2 EOR and sequestration
- Prove the ability of oil reservoirs to securely store CO_2
- Identify the risk associated with geological storage and propose mitigation measures
- Develop CO_2 mobility control methods
- Develop technology to monitor CO_2 movement
- Develop an economic model

Project history:

- The project began with a workshop on Sequestration in Regina fall 1999
- A research consortium, comprised of public and private sector research from Canada, USA and Europe was established in 2000
- Funding requested from various Governments and Industry
- Baseline data gathered in 2000
- Major funding in place in 2001
- Full scope of project launched fall 2001

5.3 EOR projects in the US and the role of CO_2 floods

Since the peak production in the late 1980s, US have seen a gradually declining in domestic oil production, and thereby more dependent on oil import. This may be one of the reasons that US is the leading producer of EOR oil world wide, and in particular with respect to CO_2 floods. The initial force behind many of the current CO_2 floods in US can also be traced to incentives contained in the Crude Oil Windfall Profit Tax Act of 1980 [50]. The legislation referentially taxed some EOR projects profits at 30 %, compared with a conventional crude oil profit tax of 70 % [51], but this incentive ceased with the collapse of oil prices in early 1986.

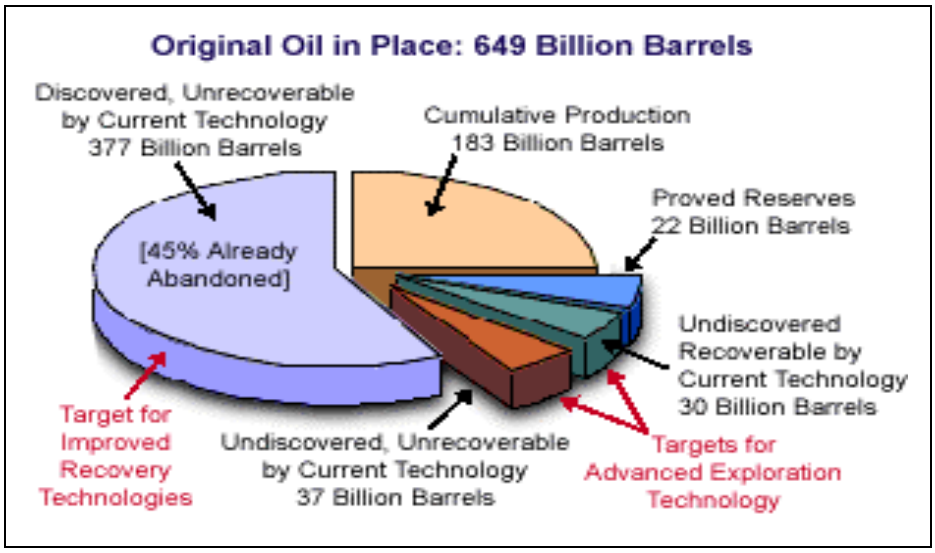

Figure 5.8 - US oil resources and target for improved oil recovery [52].

Average oil recovery from US reservoirs is only about 32 %. Although it is physically impossible to recover all of the oil that is discovered, but the potential for improvement with the use CO_2 projects and new technology in general is regarded as large. As mentioned above, the US leads the world in EOR technology, and already more than 12 % of the US oil production comes from EOR applications, and that fraction is growing steadily. In comparison, the world's EOR production is about 3 % and also growing. Figure 5.8 gives an impression of US oil resources and target for improved oil recovery.

From figure 5.9 and 5.10 one can see that the CO_2 floods is the EOR technique that have contributed the most to field growth in the US. Thermal EOR is still the largest contributor, but with a decreasing trend. It is also important to note that despite the decline in number of EOR projects, and the low oil prise during 1998 and 1999, the EOR production still was a significant portion of the US, about 12 % of the total oil production.

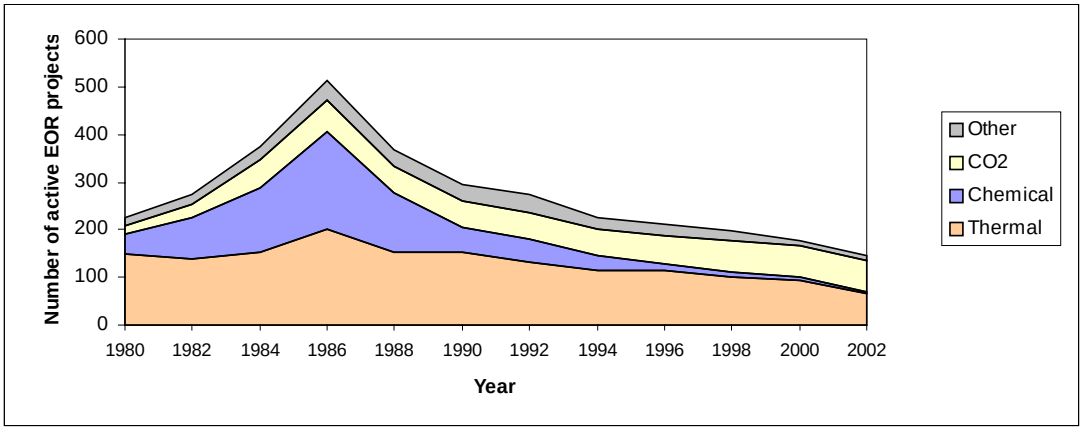

Figure 5.9 - Number of active EOR projects in US [53].

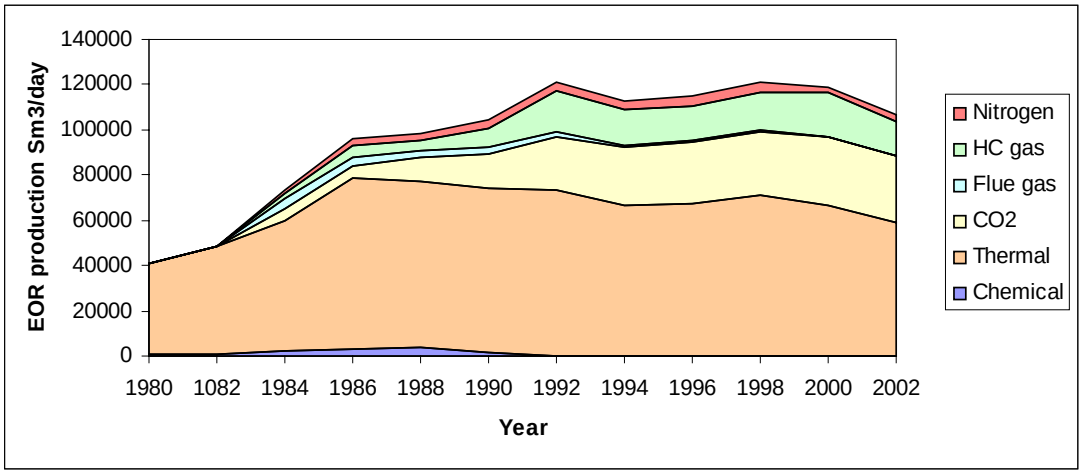

Figure 5.10 – EOR production from US projects [53].

In 2002 the CO_2 floods accounts for about 28 % of US total EOR production, which represents about 3.3 % of the total US crude oil production. As mentioned in the introduction, a typical CO_2 flood can, under the right conditions, yield an additional 7 to 15 % of the original oil in place, and extending the life time of a producing field by as much as 15 to 30 year [51]. The current injection of CO_2 in mature US oil field is about 32 million ton per year, and together with the benefits of oil recovery it also capture CO_2 in the reservoirs and thereby reduces the emission of greenhouse gasses to the atmosphere.

Prospects for further growth and expansion of CO_2 floods look promising, and analyst estimates for the Permian Basin alone indicates that more than 50 additional prospects seems to have economic to be implemented in the near future. This could add another 80 million to 160 billion Sm^3 of oil [54]. However, the economic for the different projects are variable and dependent on pieces and available technology. One of the operators in the Permian Basin is planning to initiate 4 to 5 new projects over a five years period, and in addition about 10 expansions of existing projects. It's not unlikely that other operators have similar planes.

Future areas for CO_2 floods in the US will most probably be in Wyoming, Kansas and California. The planed CO_2 miscible flood demonstration project in Kansas will be the first CO_2 flood project in Kansas [54 and 55]. The goal is to demonstrate the technical feasibility of the process in a major Kansas reservoir, the Hall Gurney Field, one of several CO_2 flood

candidate fields in central Kansas.This is a project where an electrical co-generation, ethanol fuel production will provide CO_2 to the EOR demonstration project. Waste heat from a 15-megawatt gas turbine generator provides heat inputs for to the ethanol plant, and the CO_2, a fermentation process by product of ethanol production, will be utilized in the CO_2 miscible flood demonstration project. Efficiencies gained in by product utilization and energy use by linking traditional and alternative energy systems enhance the economics of each while creating environmental benefits through geologic sequestration of CO_2. Many experts believe that California will be the next large area for CO_2 floods, but the distance to present CO_2 sources is long, and infrastructure still misses. California is the fourth largest oil producing state in the US.

5.4 CO_2 availability and prices in US and Canada

With the success of the SACROC flood, high oil prices and many old oil fields to be flooded, the demand for CO_2 was so high that major oil companies built three long CO_2 pipelines into the Permian Basin in the early to mid 1980s. Distribution pipelines were built in the area to feed the oil fields with CO_2. Most of these pipelines were built on the strength of ten year take or pay CO_2 purchase contracts, which began expiring in the mid 1990s. At that time oil prices had been relatively low for many years, new floods where postponed, and existing floods were not being expanded. At the present time activity is increasing and many projects are under consideration. In 1998 the Val Verde pipeline started to deliver CO_2 into the Canyon Reef Carriers CO_2 pipeline, and in 2000 the pipeline from Dakota to Canada started to deliver CO_2 to the Weyburn field. Figure 5.11 shows the major CO_2 sources and pipelines in US.

Figure 5.11 – CO_2 sources and pipelines in US [51].

To give an impression of the existing CO_2 sources, the main sources and delivery pipelines is listed below [56 and 57]. It is not the intention to describe the sources and pipelines in detail, but it is important to know that the availability of CO_2 and infrastructures for delivering CO_2 in this area is quite different from most of the other oil provinces where CO_2 floods are considered as an alternative EOR technique.

5.4.1 CO_2 sources

The major part of the CO_2 sources used in EOR projects in US comes from natural domes and natural gas processing plants, but some volumes is also captured form power plant flue gas.

The McElmo Dome
This is one of the world's largest known accumulations of nearly pure CO_2. The dome produces from the Leadville formation at 2440 m depth with 44 wells that produce at individual rates up to 2.8 million Sm^3/day. Due to increasing demand, both the McElmo Dome and its pipelines have recently been expanded. At present, more than 28.2 million Sm^3/day can be delivered to the Permian Basin and an additional 1.7 million Sm^3 to Utah. Additional expansions are under consideration.

The Sheep Mountain Field
This is the smallest CO_2 source field serving the Permian Basin, with published initial reserve estimates of 57 to 85 billion Sm^3 CO_2 and produces from 1830 m in the Dakota and Entrada formations in Huerfano County, Colorado

Bravo Dome
It is located in northeastern New Mexico and covers an area of more than 3600 km^2 with initially reserves about 226 billions Sm^3 of CO_2. The dome currently produces more than 11.3 million Sm^3/day from more than 350 wells. Production comes from Tubb Sandstone at 701 m depth. Recent developments include more than 40 new wells, as well as an upgrade to the compression plant.

Val Verde Associated:
The CO_2 comes from four gas treating plants in West Texas and deliver CO_2 into the Canyon Reef Carriers pipeline for further transportation to projects in the Permian Basin. SACROC is one of them.

Synfules Plant
The Synfules gasification plant, outside of Beulah in North Dakota deliver CO_2 to the Weyburn field in Canada. CO_2 is one of eight by products from the plant. The Weyburn field will take up to 2.7 million Sm^3/day.

5.4.2 CO_2 pipelines

The Canyon Reef Carriers pipeline
The pipeline was constructed in 1972, and it's the oldest CO_2 pipeline in West Texas and extends 225 km from McCamey, Texas, to the SACROC field. The diameter is 0.41 m and it has a capacity of 6.8 million Sm^3/day.

The Estes Pipeline
It is a 192 km long pipeline with a capacity of 7 million Sm^3/day at Denver City and 4.2 million Sm^3/day at the Salt Creek terminus.

The Central Basin Pipeline
The line varies in diameter from 0.66 m at Denver City down to 0.41 m near McCamey, Texas. The present capacity of the line is 17 million Sm^3/day, but if power were added, the capacity could be increased to 34 million Sm^3/day.

The Sheep Mountain pipeline
The pipeline runs 296 km southeast to the Rosebud connection with the Bravo Dome source field. The diameter is 0.51 m and the line has a capacity of 9.3 million Sm^3/day. A separate line with a diameter on 0.61 m has a capacity of 13.6 million Sm^3/day and runs 360 km south to the Denver City Hub and onward to the Seminole San Andres Unit.

The Bravo Pipeline
The pipeline has a diameter on 0.51 m and runs 351 km to the Denver City Hub and has a capacity of 10.8 million Sm^3/day, delivering CO_2 at 125-130 bars. Major delivery points along the line include the Slaughter field in Cochran and Hockley counties, Texas, and the Wasson field in Yoakum County, Texas.

The Val Verde Pipeline
It is a 132 km pipeline in West Texas connecting four gas-treating plants to the Canyon Reef Carriers CO_2 pipeline.

Synfules Plant pipeline
This is a 325 km long pipeline from the Synfules Plant to Canada where the Weyburn field gets its CO_2.

West Texas Pipeline and the Llano lateral
The West Texas Pipeline extends from the Denver City Hub 204 km south to Reeves County, Texas. The Llano lateral runs 585 km off the Cortez main line. Both pipelines vary from 0.2 to 0.3 m in diameter and have capacities of approximately 2.8 million Sm^3/day.

Cortez Pipeline
The diameter is 0.76 m, and the pipeline runs 808 km from the McElmo Dome and carries CO2 to the Denver City Hub in West Texas. Cortez has a capacity of 28 to 113 mill Sm^3/day with currently 98 % pure CO_2.

McElmo Creek Pipeline
It is a small pipeline with a diameter on 0.2 m and it runs 64 km from the McElmo Dome to Utah. The capacity is approximately 1.7 million Sm^3/day.

5.4.3 CO_2 prices

On onshore fields in US and Canada CO_2 flood costs have dropped dramatically since the 1980s. The range of the drop are from more than $1 million per pattern, to less than half of that. CO_2 prices have also fallen by 40 %. However, flood costs vary depending on field size, pattern spacing, location and existing facilities, but in general, total operating expenses exclusive of CO_2 cost ranges from $12.6 to $18.9 pr m^3. Compared to a water flood, this represents about 10 % more than an average water flood operating expenses.

An optimal candidate to be CO_2 flooded is a mature water flooded oilfield. The field should be on decline, and located in the neighboured of existing CO_2 infrastructure. If so, and with the other criteria's fulfilled (as mentioned in chapter 5.5), the possibility should be good to extend the field's lifetime and increase the value form the field. Estimated costs for a new CO_2 flood, based on a price of $113 per Sm^3 (18 $/bbl) show a profit potential of more than $48 per Sm^3. Figure 5.12 shows cost split for an average Permian Basin field with reservoir properties within the criteria required for a miscible CO_2 flood.

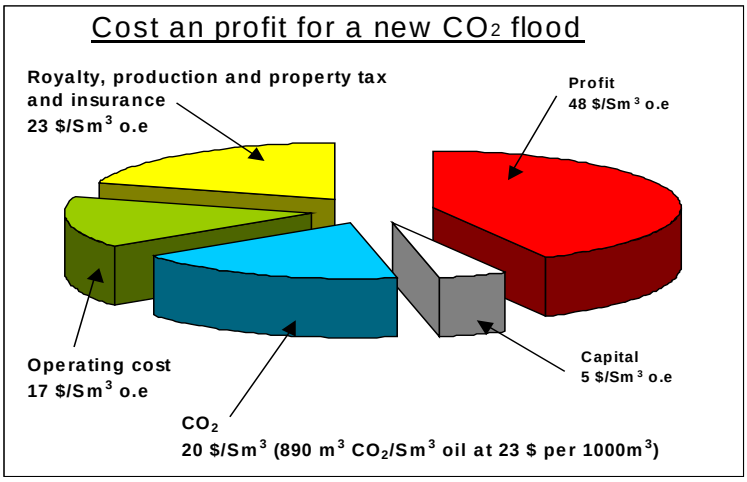

Figure 5.12 – Cost and profit for a new CO_2 flood based on a price of 113 $/Sm^3 [58].

From figure 5.12 one can see that the CO_2 price plays an important role in the total project economy, and a nearby source of CO_2 is a key factor. At the present time [54], the delivery cost for CO_2 varies from 23 $ per thousand Sm^3 from natural domes, 35 $ per thousand Sm^3 from natural gas processing to 106 $ per thousand Sm^3 when it is captured from power plants flue gas.

5.5 US and Canadian CO_2 screening criteria

Since CO_2 injection became economical in US in the early 1970s there are published several of methods to screen CO_2 flood candidates. It is not the intention to go through all those, but table 5.2 gives an overview of criteria's given by various authors.

Reservoir Parameters	Geffen (1973)	Lewin and Associates (1976)	NPC (1976)	McRee (1977)	Iyoho (1978)	OTA (1978)	Caroana (1982)	Tarber and Martin (1983)
Visc. (cp) at res. cond	<3	<12	=<10	<5	<10	=<12	<2	<15
Gravity (^{o}API)	>30	>30	>=27	>35	30-45	27-30	>40	>26
Sor_w	>0,25	>0,25	-	>0,25	>0,25	-	>30	>30
Depth (ft)	-	>3000	>2300	>2000	>2500	2500-7200	<9800 (1)	>2000
Temp (^{0}F)	-	NC (2)	<250	-	-	-	<195	NC
Reservoir pres. (pisa)	>1100	>1500	-	-	-	-	>1200	-
Perm. (md)	-	NC	-	>5	>10	-	>1	NC

(1): Due to temperature constraint, (2): NC: Not a critical factor

Table 5.2 – US CO_2 flood screening criteria's [59].

Methods to screen and carry forwards new candidates have matured over time, and new and updated criteria's are developed. Below is an example of a set of criteria's that may be regarded as an industry standard in US [60].

- Oil gravity, light oil with density <900 kg/m^3
- Oil saturation, S_o >25%,
- Reservoir pressure >76 bar and ideally 14 bar higher than the MMP at the time of CO_2 injection starts
- Porosity >15%
- Permeability >1 md

The screening criteria's mentioned here are meant to be used as a first order of screening, and more detailed studies has to be undertaken before a decision to implement new CO_2 flood projects can be taken.

5.6 Experience gained from CO_2 floods in US and Canada

Experience from a large number of CO_2 flood projects in the Permian Basin, Canada and other regions in US summarizes that there are some major factors that have been important in order to implement profitable CO_2 floods and further growths in existing and new floods:

- CO_2 sources. (When the first CO_2 project started, large quantities of CO_2 was available)
- Fiscal regime. (In US there are tax reduction for EOR projects, but different rules from state to state)
- Infrastructure (New pipelines was rapidly developed to feed CO_2 into areas with mature oil fields)
- Low CO_2 and transportation costs. (The cost for delivered CO_2 costs has dropped approximately 40 % since the 1980s)
- Screening methods to reduce risks. (CO_2 Companies has developed proven tools to help to select the best CO_2 flood candidates)
- Flood design. (New technology helps to get the most production from the least CO_2, while preventing breakthrough and other reservoir problems)
- Less expensive equipment. (Experience shows that the same equipment used for water flooding can generally be used for CO_2 flooding)
- New areas with mature oil fields for CO_2 EOR keeps focus on improvement.
- Large quantities of CO_2 sources still available from natural domes and gas processing plants.

5.7 Discussing

US followed by Canada and to some degree also Turkey, Trinidad, Hungary and Brazil has demonstrated that enhanced oil recovery from CO_2 floods is proven technology, and that most of the mature oil fields facing the end of production can extend their lifetime and increase their values by implementing tertiary CO_2 floods. US are the leading country in CO_2 EOR, and it is expected that new floods in Wyoming, Kansas and California will increase the EOR production tremendously. Great focus on emission of greenhouse gases and demand for energy seems to be the driving force in accelerating the implementation of new CO_2 floods in these areas.

The success from US and Canadian CO_2 floods and the growing focus on environment issues can be the releasing factor for investigating and implementing CO_2 floods on mature oil fields

on the Norwegian Continental Shelf. However, it is not straightforward to extrapolate the experience gained from existing CO_2 floods world wide to North Sea conditions.

North Sea oil fields will most likely be exposed to different technical challenges and operating costs than current CO_2 floods, but beside of this, the mature North Sea oil fields should easily pas the criteria's used for US and Canadian projects. In many cases North Sea oil fields will fit those criteria's more favourable than many, or most, of the US and Canadian onshore oil fields. Looking at the disadvantages, availability of CO_2 at an acceptable price seams to be one of the major obstacles. Another area of concern is the huge and complex offshore installations and the investments needed to upgrade the installations in response to production of the injected CO_2 and the corrosive environment this creates.

To conclude, experiences gained in existing CO_2 floods in US and Canada are not directly comparable to EOR projects on mature North Sea oil fields. But it indicates that there is a large EOR potential, and technology is available to be used careless of types of reservoirs. The main question is how much more oil can be extracted, and what are the main success criteria's and the most important reservoir parameters to be used in a brooder estimation of the total technologic EOR potential. A closer look into the studies done on North Sea oil fields will hopefully give a better answer to this.

6. NORTH SEA CO_2 STUDIES

Together with the MMP calculations and the CO_2 candidates' field data and critical reservoir parameters, the results from the studies below are crucial inputs to the estimation of the total CO_2 EOR potential from NCS oilfields. The studies include Sleipner (CO_2 injection experience, but not EOR data), Forties, Ekofisk, Brage and Gullfaks. It was also the intention to include the Draugen field, but the operator chose to do a hydrocarbon miscible gas injection study instead of a CO_2 study.

6.1 The Sleipner field

Sleipner is the first and only offshore field that inject CO_2 into the ground in large volumes. The objective was not EOR related, but to reduce the content of CO_2 from the produced gas. Sleipner gas has a content of 9 % of CO_2, which has to be removed in order to comply with the sales gas specifications. Over time, this represents large volume of CO_2, and releasing it into the atmosphere was not an alternative. Since the Utsira formation, a large saline aquifer reservoir was located just between the gas reservoir and the sea floor, it was decided to inject the CO_2 into this formation. Utsira is a high porous (35 %) and high permeable (2-5 Darcy) formation with about 250 m of thickness located 1000 m under the seafloor, and it covers an area nearly 100000 km^2. It was not straightforward to start the injection, and injectivity, storage effects and other matters of concerns was investigated. The injection of CO_2 started in October 1996 with around 1 million ton CO_2/year.

Figure 6.1 shows a regional seismic line through the Utsira geotechnical system, and figure 6.2 shows schematically the installation, reservoirs and the Utsira formation where CO_2 is injected.

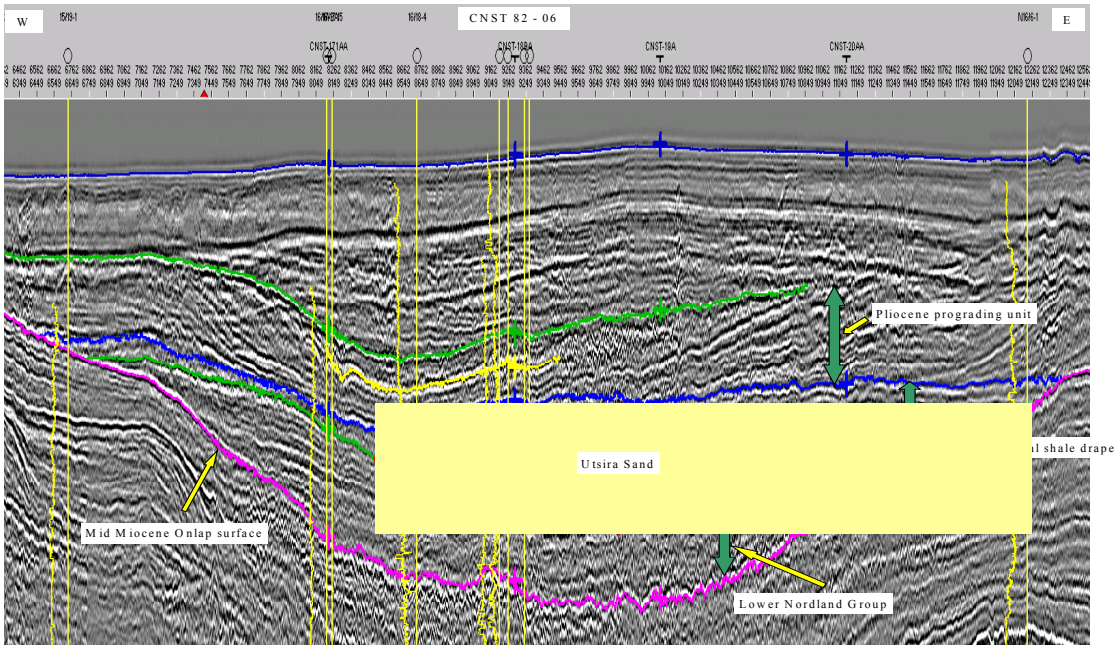

Figure 6.1 - Regional seismic line through the Utsira geotechnical system [61].

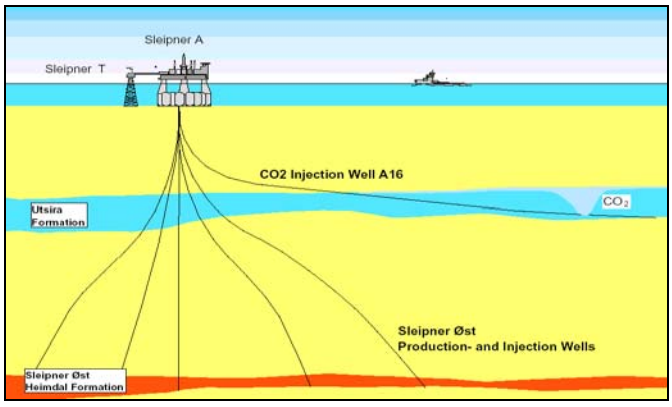

Figure 6.2 – Schematically overview of the Sleipner CO_2 injection [62].

The Saline Aquifer CO_2 storage Project (SACS Project) [63] was initiated in 1998, and data collection and interpretations is still ongoing. It is a multidisciplinary project involving reservoir mapping, rock and fluid agrochemical evaluation, reservoir water flow and CO_2 brine mixing implication. The EU THERMIE programme together with a wide spectre of participating companies and institutions are funding the project.

The SACS Final Technical Report, February 2000 [61] gives a short summary of the work carried out during the first project period. One important message from the SACS Project is that the measured behaviour of CO_2 compares to the simulated behaviour. Figure 6.2 gives an impression of the movement of CO_2 over time from a seismic interpreted picture. According to Lindeberg, Zweigel, Bergmo, Ghaderi and Lothe [64] the measured data has a relatively good match to the simulations. The first survey was completed in September 1999 when the CO_2 bubble around the injection well was large enough, and in such concentrations, that it was possible to monitor it by a 4D "time laps" seismic survey.

Another issue of concern was the injectivity of CO_2 and handling of equipment as compressors, pumps, and separation units were hydrate problems could occur. But after some problems in the beginning, it seems to be under control. A production shut down on Sleipner will have great impact on the field economy because of the high daily delivery of sale gas.

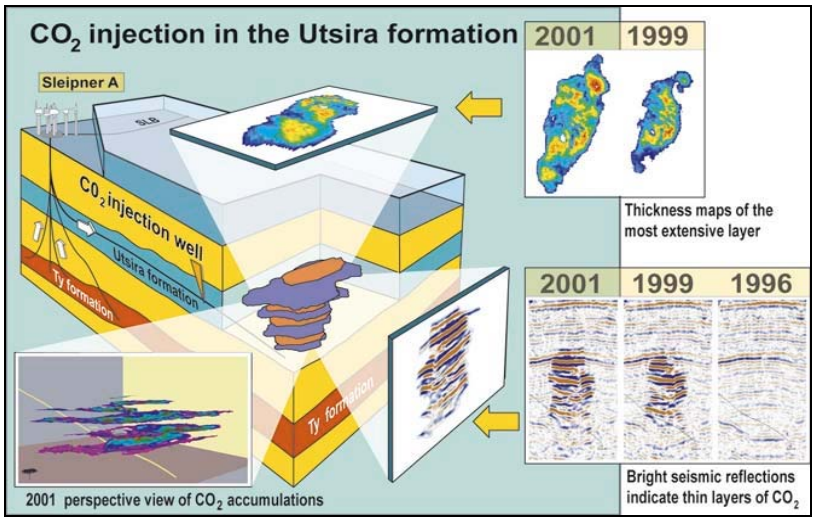

Figures 6.2 - Movement of CO_2 over time from a seismic interpreted data [65].

The missing link in this project with respect to EOR is the compositional effects between CO_2 and hydrocarbons and gravity segregation. Gravity segregation of CO_2 when it flows trough the reservoir is an important factor with respect to sweep efficiency and oil recovery. The Utsira formation is not an oil-bearing reservoir, and does not give any information about these effects in that respect.

6.2 The Forties field

The Forties field is mentioned in this thesis because it is one of few mature offshore oilfields in the North Sea were CO_2 injection has been studied as an EOR alternative [66]. When this is written, BP, the major owner of the field is planning to sell its 96.14 % stake in the field to a US independent oil and gas company, Apache, for 1.3 billion US dollar. How this change in ownership will affect the CO_2 EOR project is not known.

The Forties field is a giant offshore oil field in the UK sector of the North Sea, located in the South Viking Graben. The field was discovered in 1970, and has been in production since November 1975. The field reached its peak production in 1978, approximately 79500 Sm^3/day. At the present time the production is 7950 Sm^3/day with water cut approaching 90 %. The oil is transported onshore to Cruden Bay through a 91 cm pipeline. There is no gas export system, and associated gas has to be flared or used to power generation. Today the entire gas production is utilised for power generation.

The producing reservoir is a turbudite sandstone sequence from Upper Paleocene. Average depth is approximately 2130 metres subsea. The reservoir consists of four main channel sand complexes, Alpha, Bravo, Echo and Charlie. The Charlie sand is isolated from the other channels. The Main Sand reservoir is composed mostly of sandy sediment deposited as a submarine fan, while much of the separate Charlie Sand accumulated within feeder channels of sand flowing across the sea floor. Paleocene turbidite sandstones are not widespread on the NCS, but exist in the Frigg and Heimdal area, Cod, Balder, Sleipner and Grane oil and gas fields.

Seawater injection is used for pressure support and sweep. STOIIP at discovery was 670 million Sm^3. Cumulative production to date has been about 59 % of STOIIP. Remaining reserves are currently about 19 million Sm^3, giving an expected ultimate recovery factor of approximately 62 %.

The bulk of the reservoir has been well swept by water and the remaining oil exists at low saturation (15 – 30 %) with low mobility. In addition pockets of bypassed high saturation oil exist where the formation has been shielded by shale’s or in pockets at the top of the formation.

Figure 6.3 shows the tree different EOR targets where oil is not properly swept by water. The targets are attic oil, remaining oil under shale and intermediate saturations.

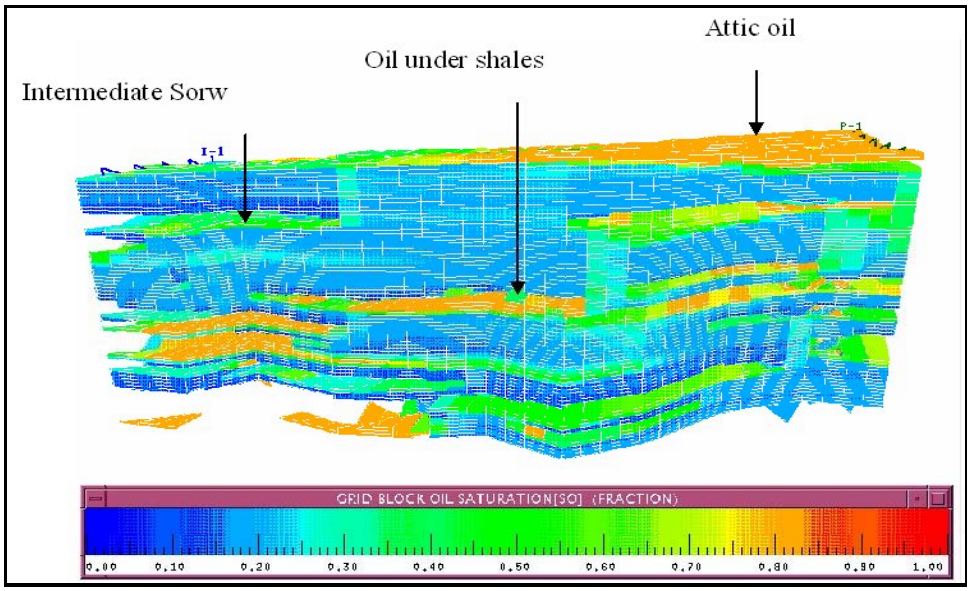

Figure 6.3 – Cross section of the reservoir and oil saturation [67].

Forties field data:

Area:	91 km2
Water depth:	128 m
STOIIP:	670 million Sm^3
Reservoir depth:	213 m subsea (average)
Reservoir thickness:	170 m (average)
Reservoir pressure:	194 bar (current pressure)
Reservoir temperature:	96 ^oC
Oil density:	840 kg/m^3.
GOR:	53 Sm^3/m^3
Sorw:	0.15 – 0.30

6.2.1 Forties CO_2 EOR project

With resources of 250 million Sm^3 remaining in the reservoir after current production plans, great efforts has been done to lock at potential EOR projects. A screening resulted with a potential to improve the recovery factor up to 10 % with EOR contributing half of the total potential. To evaluate the EOR potential, studies were performed in four areas:

- Miscibility and fluid properties
- Small-scale displacement efficiency
- Reservoir sweep
- Implications for surface facilities

After an evaluation of hydrocarbon gas, CO_2 and air as possible injection gases, CO_2 was chosen as the optimal EOR method. Hydrocarbon gas had to be enriched with NGL to achieve miscibility, and was rejected because of the high cost. The key requirement for modelling the large changes in fluid compositions and hence fluid properties in such a process is to be able to model the near critical region of the thermodynamic diagram. An Equation of State was developed for this purpose. To constrain the EOS, swelling tests and multiple contact tests were performed. Basic data from a swelling test provide liquid saturations as a function of pressure for a range of injected gas mole fractions. Cross plotting the data as lines of constant liquid quality shows convergence at the critical point at a CO_2 mole fraction just over 0.7.

A set of slim tube displacements was performed to validate the EOS. The MMP for pure CO_2 was 187 bar, approximately 21 bar below current reservoir pressure.

Core scale displacement:
To perform the test, a composite core was constructed by butting together core plugs (7.5 cm long by 3.8 cm diameter) cut from Forties core samples. The core was filled with representative reservoir oil and swept by injected CO_2 under reservoir conditions in order to verify the displacement efficiency. An injection gas comprising 90% CO_2 and 10% methane was used to mimic performance after breakthrough of CO_2 when produced gas including hydrocarbons was blended into the injection stream. An initial waterflood was performed to create the initial saturation and distribution of oil found in well swept parts of the reservoir. This was followed by a simulated WAG flood co-injecting water and the CO_2 /methane mixture in a 1: 1 ratio. At the end of the initial waterflood the average oil saturation in the core was 0.27, and in consistent with the range of field values observed. After injection of 19 PV of CO_2/methane, the average oil saturation had been reduced to less than 10 % confirming that the displacement mechanism was effective at the core scale.

Reservoir simulations:
The simulation was based on a full field model scaled up from a single area model. The upscale methodology used here was adopted from a model developed by Arco. The same model has previous been successfully used on Prudhoe Bay and Kuparuk oilfields in Alaska. To deal with the uncertainties due to scaling up from a relatively small model to a large full field model several recovery curves was generated corresponding to different areas of the reservoir. These curves were then used in the scaling up tool in order to limit the uncertainties. An extensive review of uncertainties in the model inputs was undertaken to enable optimisation of the displacement. Predicted incremental reserves ranged from 16 million Sm^3 for an injection rate of 2 million tonnes CO2/year rising to 32 million Sm^3 for an injection rate of 4 million tonnes/year.

Conclusions:
- CO_2 EOR is considered to be the best option due to high additional oil recovery.
- CO_2 EOR can give up to 4,7 % of STOIIP by inject 4 million tonnes CO2/year.
- Miscibility and core flood studies indicates that up to 15 % methane can be tolerated in the injected stream before recovery is adversely affected.
- 40 – 80 million tonnes of CO_2 can be stored in the subsurface over a twenty-year period.
- Some significant obstacles to implementation were identified:
    - Lack of low cost CO_2
    - Surface facilities has to be modified
    - Fiscal regime (lower marginal tax rate)

6.3 The Ekofisk field

Ekofisk was the first producing oilfield on the NCS. The production started in 1971 and according to current prognoses, the field will produce at least until 2028, which is the date when the license period expires. The field was produced with primary depletion and to some degree gas injection (produced gas in excess of contract quantities) until 1987 when water injection started. The good response from the water injection resulted in a field wide expansion of water injection. Today the injection capacity is above 130000 m^3/day. Reservoir compaction and seabed subsidence required new installations due to safety concerns, and new process and transportation facilities were commissioned in 1998. Average oil production

today is 77000 Sm3/day. According to the current production plan the recovery is expected to be about 45 % of STOIIP. That means that there is large volume of remaining oil left in the reservoir to be produced by tertiary EOR methods.

Ekofisk is the largest oilfield in production on the NCS with respect to oil in place. Today there are 87 oil wells and 37 injecting wells in operation. Figure 6.4 gives an impression of the field size, and shows the top structure map for the Ekofisk field.

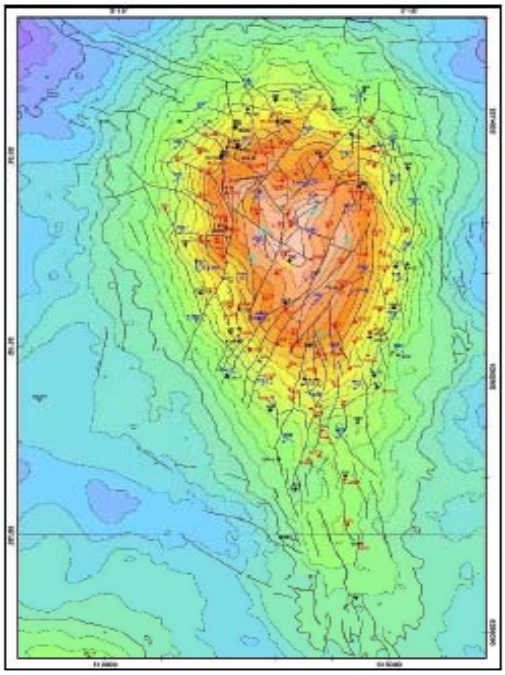

Ekofisk key data:

Recourses:	1049 million Sm^3 oil in place
Reserves:	468 million Sm^3 oil (preset estimate)
Recovery:	45 % of STOIIP (present estimate)
Reservoir:	Chalk, Ekofisk and Tor formations of Danian/Maastrichtian age
Height:	300 m +/-
Oil density:	0,840 kg/Sm^3
Oil viscosity:	0,35 cp
Bo:	1.78 Sm^3/m^3
Porosity:	30 % +/-
Permeability:	1-100 md
Pressure:	497 bar (initial)
Temperature:	131 ^oC

Figure 6.4 - Top structure map for Ekofisk field [68].

6.3.1 Ekofisk EOR screening

Since the Ekofisk oil field has a large STOIIP, 1049 million Sm^3, and in the same time a relatively low oil recovery, the field operator has high focus on how to increase the recovery. In order to meet those challenges, the operator has done a screening study where five different EOR methods were investigated [68].

6.3.2 Ekofisk CO_2 WAG study

The CO_2 WAG was estimated to be the second best alternative among the five alternatives, but currently rejected because of expected price and availability of CO_2 [69]. The calculated potential of 5.6 % of STOIIP represents almost 60 million Sm^3 of additional oil from the field. However, even if CO_2 could be available at a reasonable prise there are still some uncertainties that have to be investigated. The most precarious concerns are dissolution and compaction of the chalk, and the uncertainties about how the injected CO_2 will be able to contact residual oil in the chalk matrix. CO_2-oil PVT data from the field are limited, and has to be further investigated. Another matter of concern is possible forming of hydrates in the cold water flooded area. A single well WAG pilot test in 1996 resulted in a rapidly drop of gas injectivity (to zero after a few hours). This was in a well that had injected a total of 7 millions m^3 water over a 5 years period at that time. The reason for this was most probable

hydrate formation. Crestal gas injection has been ongoing since 1975 without any major problems.

Modelling:

A compositional simulator was used to model CO_2 injection phase behaviour and the ability of the injection gas to mobilize and recover incremental oil. To generate the EOR forecast a representative sector model from the central water flood area was selected to simulate the CO_2 EOR process. The model was build up of a 7x7x14 five-spot configuration and included representative reservoir layers, reservoir properties, well spacing and representative (available) fluid data. Residual oil saturation under water/oil displacement was 0.30 and 0.25 under the gas/oil displacement. The simulation model was based on a single porosity model with effective properties and viscous displacement characteristics tuned to match the history matched full field model.

The main result is based on a full field model, scaled of forecasts from the sector model. This was done for all the EOR alternatives, and without optimisation performed for the individual processes. Further, the WAG cycles and operating schedules were adjusted to existing facilities capacity limits. The CO_2 WAG was premised to start early 2004 and last for 13 years, followed by a blow down period from 2017 to 2028. All 30 current water injection wells were converted to WAG services:

- 10 wells for CO_2 injection at a 6 month schedule
- Injection capacity, 9.9 million Sm^3 CO_2 per day at 410 bar wellhead pressure
- 20 wells for water injection
- Water injection capacity, 130000 m^3/day

One of the key issues to estimate the oil recovery from a CO_2 flood is the ability of CO_2 to contact and mobilize water flooded residual oil in the fractured chalk. One of the premises in this process performance is that injected gas will be able to move into the chalk matrix to contact and viscously displace water flooded residual oil. This modelling premise is based on performance of the imbibitions/viscous displacement of oil by water under current water flood operations as represented in the current full-field Ekofisk model.

Outstanding issues:

There are some major issues that have to be investigated before further work or field pilot tests can be done.

- CO_2-oil PVT data
- The impact of CO_2 on compaction, sea bed subsidence and well failure
- Reaction of CO_2-rich injection water with calcium carbonate in the rock matrix (may consume fractions of the CO_2 injected, and then reduce the effect of the CO_2 slug)
- Slimtube MMP estimations

6.4. The Brage field

The Brage oil field is located in the Oseberg area in the northern part of the North Sea. The field was discovered in 1980 and oil production started in 1993. The field produces from reservoirs in the lower part of the Brent group, the Dunlin group (Intra Dunlin Sand) and the Statfjord formation. Production from the Statfjord formation started in 1997. The Statfjord formation has a gas cap and a higher content of associated gas than the other reservoirs. The production strategy for the Brent group and the Dunlin group is to maintain the reservoir

pressure by help of water injection. Brage has a STOIIP of 140 million Sm^3, with the biggest contribution from the Fensfjord reservoir. A field map is shown in figure 6.5.

The Statfjord formation:
Statfjord is a solid sandstone reservoir with some nodular calcite and siltstone. The permeability varies from 500 md to 2 D. The reservoir consists of two isolated units, Statfjord South and Statfjord North. The current production strategy is based on voidage replacement.

The Fensfjord formation:
Fensfjord is a sand-, siltstone reservoir with some calcite cemented layers and high permeable stringers. The permeability varies from 10 md to 6 D. Most of the time the drive mechanism has been WAG injection. Currently the pressure maintenance comes from water and gas injection, but not as a WAG schedule. In addition, solution gas drive provides some additional recovery mechanisms.

The Sognefjord formation:
Sognefjord is a layered sandstone-, siltstone reservoir of Kimmeridgian and Oxfordian age with a 16-17 m oil column. The permeability varies from 20 md to 2 D. The reservoir is produced by pressure depletion from a single horizontal well with high water cut and high gas oil ratio.

Since the production started in 1993 the field has produced 41 million Sm^3 of oil (referees to end of 2002). The estimated reserves to be produced are in the order of 45 million Sm^3, and the field is in the tail end production phase. Some additional resources are proven to increase the STOIIP from 140 to 150 million Sm^3, but the recovery from the additional resources is estimated to be low. All together, the current production plan will give a total recovery of just above 30 %. Therefore, the operator and owners are looking at alternatives to increase the oil production. CO_2 injection as a tertiary drive mechanism is under evaluation.

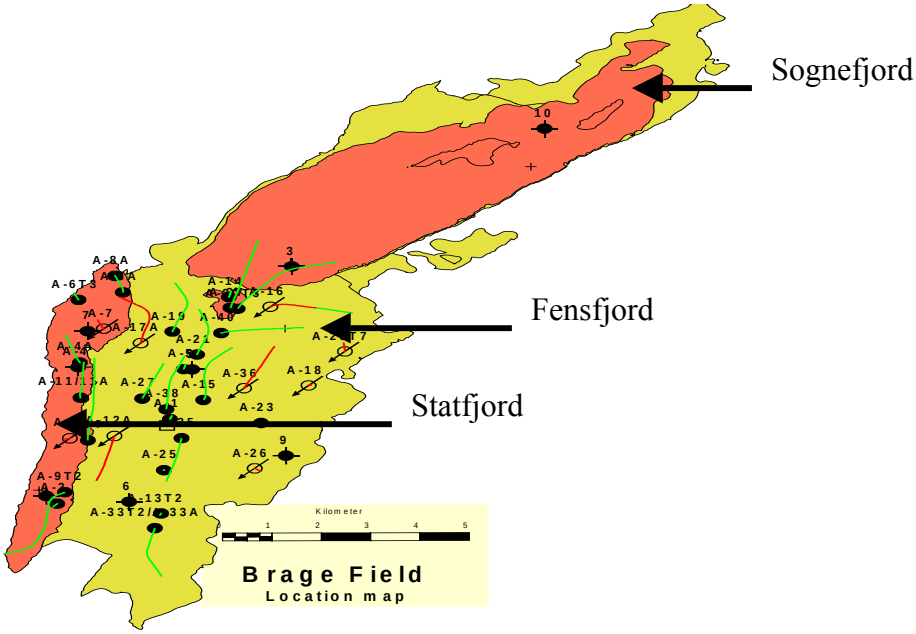

Figure 6.5 – Brage map [70].

6.4.1 Brage Statfjord South CO_2 WAG injection study

This is an update of a study done by the operator in 2000, where additional recovery from CO_2 injection was estimated to give about 3 millions Sm^3 extra oil from the Statfjord reservoir, about 6 % of the reference STOIIP. In 2002 two new studies were done, but now just on one the southern part of the Statfjord reservoir. The first study was a screening type where the Stone Steady State model was used. The additional oil recovery was estimated to 4.4 % of the STOIIP involved. This was more pessimistic than the results from the 2000 study, and a compositional simulation study was performed. The result from this study gave respectively 3.3 and 5.1 % of the STOIIP with a WAG ratio of 1:1 and 3:1. Scaling up the result from the simulation study to include the whole Statfjord reservoir and the Fensfjord reservoir, one can have an additional oil recovery in range of 6 million Sm^3 from the Brage field. The Sognefjord reservoir is not regarded as a candidate to be CO_2 flooded because of lack of pressure support. The result of the study was presented at the SPE Drilling, Completion and Reservoir Management Seminar in Bergen 1 April 2003 [70].

6.5. The Gullfaks field

Gullfaks is located in the Tampen area in the northern part of the North Sea. The field was developed with three Condep concrete gravity base structures. In addition to processing its own oil and gas, production from adjacent fields are tied in and processed. The field was discovered in 1978, and production started in 1986. The STOIIP is about 588 millions Sm^3 with an estimated recovery at 335 million Sm^3, which gives an average recovery of 57 %. Today, nearly 90 % of the reserves are produced, and the operator has focus on incremental production from the field. Different EOR methods are investigated, and CO_2 injection (CO_2 WAG) seems to be the most promising.

Gullfaks produces from Brent, Cook, Lunde and Statfjord formations. The main reservoir is Brent. The reservoir is relatively shallow at a depth of 1800 to 2200 m and is made up of several angled fault blocks. The field is complicated to produce due to the many faults. The main drive mechanism is primarily pressure maintenance from water injection, but there is also some gas injection (and WAG). Some fault segments are produced with pressure depletion because they are to small to make it profitable to drill injection wells.

6.5.1 Gullfaks Brent CO_2 WAG study

Current studies indicate that additional recovery from CO_2 injection can give from 17 to 34 million Sm^3 of oil dependent of number of injection wells. This represents 3.9 to 7.7 % of the STOIIP involved. Even higher recovery is possible. The studies done so far is limited to the Brent reservoir, but both Cook and Statfjord are regarded to have better reservoir conditions to CO_2 flooding than the Brent reservoir. That means that additional recovery from the Gullfaks field can be in excess of 8 % of the STIOIIP from those reservoirs.

Among the CO_2 studies done on North Sea oil fields, the Gullfaks study may be regarded as the most mature, and different research institutions and consultants are used for quality assurance and to assist in modelling and simulations. The reservoir simulation is to some degree similar to the methods used on the Forties study, and based on experiences from Prudhoe of Bay. Full field models on E100 (black oil) and sector models E300 (compositional) are transformed into a streamline model, FrontSim, and simulator-running time are reduced to minutes or hours. By doing this, a wider range of scenarios can be investigated. Figure 6.6 shows schematically how a traditional reservoir model is transformed to the streamline model, FrontSim, and how to present the saturation. It is expected that a decision to go further with the CO_2 WAG project will be taken later this year. Figure 6.7 shows schematically a model of the EOR simulation approach. The result of the study done so

far was presented at the SPE Drilling, Completion and Reservoir Management Seminar in Bergen 1 April 2003 [71].

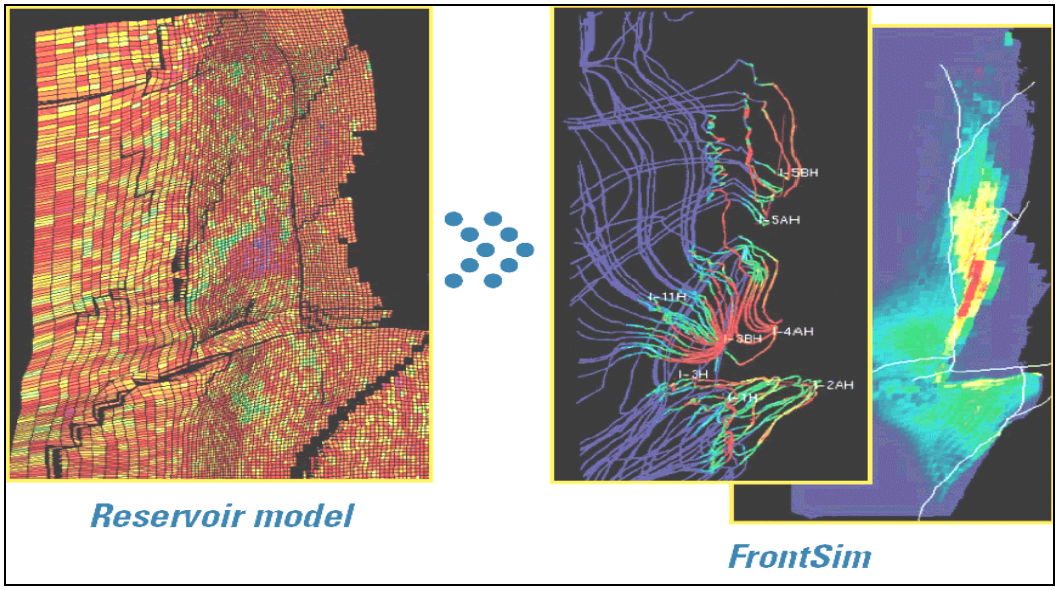

Figure 6.6 – FrontSim output [72].

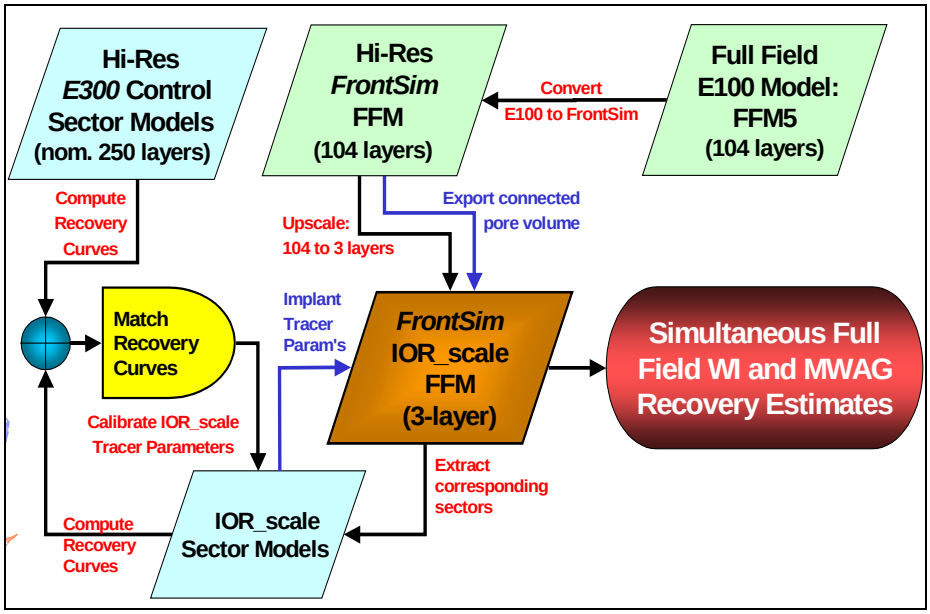

Figure 6.7 – Gullfaks EOR model [71].

6.6 Summary and discussion of the North Sea CO_2 studies

Main results:

Gullfaks:	3,9 – 7,7 % of STOIIP	(dependent on number of wells)
Brage:	3,1 – 5,1 % of STOIIP	(dependent on WAG ratio)
Forties:	4,7 % of STOIIP	(based on 4 million tonnes CO_2/year)
Ekofisk:	5.6 % of STOIIP	(based on 30 wells, 10 WAG and 20 WI)

Sleipner:
Sleipner is not a candidate to CO_2 EOR, but it is the only offshore field with experience in injection of CO_2. The CO_2 is injected into the Utsira formation, a large saline aquifer reservoir. There is minor production from the reservoir (some water production for injection purposes), and dynamic flow information through the reservoir is difficult to predict, likewise information on oil mobilization due to the lack of reservoir oil. However, valuable experience is gained from an operational point of view. Simulations on movement of CO_2 shows good match to the observation from seismic interpretations.

Forties:
The study indicates that CO_2 EOR can be up to 4.7 % of STOIIP depending on the amount of CO_2 injected. Compared to the low residual oil saturation and low oil mobility, this is a promising result with respect to similar EOR project on NCS oil fields. Forties produce from turbudite sandstones from Paelocene age, witch is not common on NCS oil fields except the few mentioned in chapter 6.2. However, the reservoir quality for the Forties field should not be very different form an average NCS sandstones reservoirs. Forties is a UK oilfield, and thereby it is difficult to get access to sensitive field data, but together with results and data from Ekofisk, Gullfaks and Brage it contributes with valuable data in order to establish a method to estimate the NCS CO_2 EOR potential.

Ekofisk:
There is some lack of CO_2-oil PVT data, and industry experience is to some extent used in the computational reservoir simulation. Those are the most critical parameters from a simulation point of view, and have to be further investigated. However, worldwide experience from CO_2 floods and studies indicates that recovery is possible over a wide range of fluid properties. In addition there is a major lack of knowledge in how CO_2 reacts with the chalk under reservoir conditions, and thereby limits the extraction of hydrocarbons over flooded portions of the reservoir. Subsidence is also a major concern and has to be properly investigated before full scale CO_2 injection can be implemented. The current estimated CO_2 EOR from Ekofisk is about 5.6 % of STOIIP. The study gives no clear indication of critical factors that can be used in a comparison with other similar reservoirs in Eldfisk, Hod, Tor and Valhall. However, by combining the data available it should give an indication on possible additional recovery from the other chalk fields.

Brage:
The study done by using the Stone Steady State model resulted in 4.4 % additional oil recovery of the reference volume involved. This was far less than the 2000 study showed, and a compositional study was performed. This study gave a result up to 5.1 % recovery. By scaling up the latest result from the compositional simulation, an increased recovery of 6

million Sm^3 of oil is estimated by including the Statfjord and Fensfjord reservoirs. The study is premature, and slim tube experiments, as well as full field simulations has to be further investigated. However, the results give a good indication that Brage is a candidate to CO_2 injection. Brage is one of few fields where injection should start as soon as possible.

Gullfaks:

The method used is to some degree similar to the Forties simulation study. The study is matured to the point where both compositional simulations and slim tube experiments have been carried out. Detailed studies are still ongoing both on reservoir, facilities, transport and CO_2 sources. The goal is to reach a level where the decision to go further with the CO_2 project can be taken. So far, the reservoir study is limited to the Brent reservoir, which is the main oil-producing reservoir on Gullfaks. The simulated recovery is about 7.7 % of the Brent STOIIP. This is the maximum case so far, and requires high well density. The Statfjord and Cook reservoirs are regarded to be candidates for CO_2 WAG flooding as well as the Brent, and from these reservoirs even higher recovery is possible.

Conclusions:

From CO_2 EOR studies done on North Sea oilfields so far it should be possible to give an answer on the range of additional recovery one can expect from CO_2 floods. The span from roughly 4 to 8 % of STOIIP is however below the industry experience from US CO_2 projects, which stands for the majority of worldwide CO_2 projects. Compared to the number of fields and reservoirs that are regarded as possible candidates to CO_2 injection, the results from these 4 studies does not give enough information itself, but all together they give a reasonable basis for further use in the estimation of the total CO_2 EOR potential. However, further studies and experiments are required. The Gullfaks study is regarded as the most mature among the studies done so far, and that will also be reflected in the results from the estimation and method used in this thesis.

7. SCREENING OF CANDIDATES FOR TERTIARY CO_2 FLOODS

Current candidates are mature oil fields that have reached a stage in their production life where CO_2 would be a natural choice as the reservoirs ideally should be at an advanced stage of water flooding. The main reason for this is that most of the mobile oil has been produced, and the remaining volume of oil is residual oil that cannot be produced without implementing EOR techniques.

The main objective is to estimate the total EOR volume from CO_2 floods in oil fields currently in production on the Norwegian Continental Shelf. It could have been possible, however, to give estimations by comprising candidates for secondary CO_2 floods, but as long as water injection or re-injection of produced gas is an alternative, its not likely that CO_2 will be used as secondary drive mechanisms.

The oil fields on the NCS vary in maturity from fields that recently started production to fields approaching the end of their lifetime. Most of the oil production, however, still comes from mature giants as Stratford, Gullfaks and Ekofisk. A plot of each field, showing production history and prognoses, is shown in the enclosure. Since oil prognoses on field level are confidential company data, said enclosure is not available to the public.

Figure 7.1 gives an overview of the candidates and shows the produced reserves, remaining reserves and the remaining resources left behind after current production plans (the EOR target). These fields have about 8000 millions Sm^3 of STOIIP. The recovery factor varies from 15 to 65 %, averaging at 44. The goal of the authorities is to recover 50 % of the oil in place, on average. This goal may be too optimistic, and in later years the recovery factor has seemed to flatten out. Not even 44 % of recovery can be reached without new initiatives from the field owners. Implementation of CO_2 injection is an option worth considering in this respect.

Table 7.1 summarizes the oil fields and reservoirs dealt with in this thesis. It shows the volumes in place and the recovery mechanisms for each oilfield. The volumes are oil, NGL, associated gas and gas cap (initially free gas).

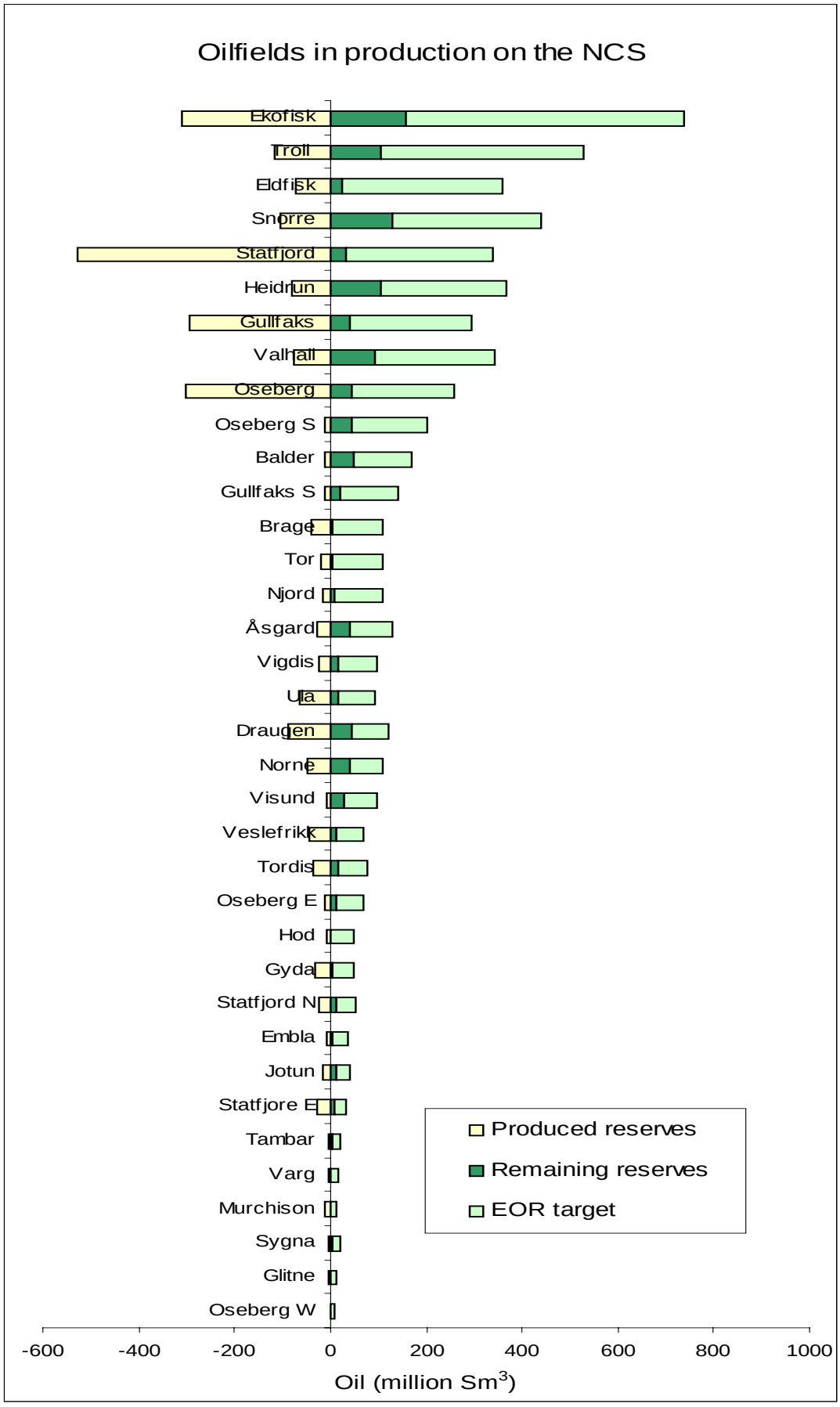

Figure 7.1 – Illustration of the EOR target for oilfields currently in production on the NCS

Oilfields	Reservoirs	Volume in place				Drive-Mechanisms			
		Oil	NGL	Gas	G. cap				
		10^6 Sm^3	10^6 Sm^3	10^9 Sm^3	10^9 Sm^3	WI	GI	WAG	PD
BALDER	Balder	76.8	0.0	0.0	0.0	x			
	Balder E4	13.8	0.0	0.0	0.0	x			
	Balder E5	12.9	0.0	0.0	0.0	x			
	Forseti	25.4	0.0	0.0	0.0	x			
	Ringhorn Jurassic	33.9	0.0	0.0	0.0	x			
	Ringhorn "prospecter"	19.9	0.0	0.0	0.0	x			
BRAGE	Fensfjord	79.2	4.0	7.4	0.0	x		x	
	Sognefjord	18.3	3.1	2.2	3.5				x
	Statfjord	45.3	1.5	2.7	0.0	x			
DRAUGEN	Garn	31.7	0.0	1.8	0.0	x			
	Rogn	178.2	0.0	9.9	0.0	x			
EKOFISK	Ekofisk og Tor	1049.0	0.0	277.9	0.0	x	x		
ELDFISK	Ekofisk og Tor	428.6	0.0	107.4	0.0	x			
EMBLA	Dev. og Perm.	43.4	0.0	15.1	0.0				x
GLITNE	Glitne, Heimdal Fm.	14.6	0.0	0.8	0.0	x			
GULLFAKS	Brent u/GFVest	441.0	0.0	42.7	0.0	x	x	x	
	Cook	45.0	0.0	4.5	0.0	x		x	
	Gullfaks Vest inkl. Shetland	6.9	0.0	0.8	0.0	x			
	Lunde	3.1	0.0	0.5	0.0				x
	Statfjord inkl. Krans, ++	92.0	0.0	13.4	0.0	x	x		
GULLFAKS SØR	GF Sør Brent	39.9	20.8	8.8	75.5		x		
	GF Sør Statfjord	35.7	2.7	6.6	9.7				x
	Gullveig Brent	7.0	2.4	1.9	2.1				x
	Rimfaks Brent	23.9	14.1	7.8	15.5		x		
	Rimfaks Statfjord	10.8	2.9	2.9	3.9		x		
GYDA	Gyda Jurassic	63.9	3.4	12.5	0.0	x			
	Gyda South	14.0	1.4	7.5	0.0	x			
HEIDRUN	HEIDRUN (gas total)		9.6	37.3	56.1				
	Fangst	155.0			yes	x	x		
	Tilje	123.0			yes	x			
	Åre	162.0			yes	x			
	Heidrun Nord	8.0	0.2	0.5	1.0	x			
HOD	Hod	14.5	0.0	2.4	0.0				x
	Tor/Ekofisk	39.8	0.0	5.8	0.0				x
JOTUN	Elli	34.8	0.0	1.2	0.0	x			
	Elli South	4.1	0.0	0.2	0.0	x			
	Tau	18.6	0.0	1.7	0.4	x			
NJORD	Ile East/Central	7.5	0.7	2.4	4.4		x		
	Ile North	4.0	0.0	1.7	1.9				x
	Tilje East/Central	81.8	0.0	16.4	4.0		x		
	Tilje North	30.7	0.0	6.9	0.0				x
NORNE	Norne	157.0	1.8	18.3	11.5	x	x		
OSEBERG	Ness	95.9	0.0	13.3	16.8		x		
	ORELN2	376.8	0.0	53.2	51.1	x	x		
	Tarbert	87.9	0.0	12.1	5.9	x	x		
OSEBERG SØR	C	25.1	0.0	3.3	0.0	x			
	G Øst	23.1	0.0	4.3	2.3	x			
	K Vest	13.2	0.0	2.8	0.1	x			

	K Øst	3.3	0.0	0.7	0.0	x			
	Omega Nord	64.0	0.0	9.0	2.2	x	x		
	Omega Sør	48.0	0.0	6.7	0.5	x			
OSEBERG VEST	Gamma Nord	10.7	0.0	1.6	9.4				x
OSEBERG ØST	Beta Sadel Nord Ness	1.3	0.0	0.1	0.0				x
	Beta Sadel Nord Ore	2.0	0.0	0.2	0.0				x
	Beta Sadel Nord Tarb.+Heather	0.4	0.0	0.0	0.0		x		
	Beta Sadel LOSST	0.2	0.0	0.0	0.0		x		
	Beta Sadel Ness	10.0	0.0	0.9	0.0		x		
	Beta Sadel ORE	25.7	0.0	2.2	0.0	x	x		
	Beta Sadel Tarbert+Heather	2.7	0.0	0.2	0.0				
	Beta Sør LOSST	0.3	0.0	0.0	0.0				
	Beta Sør Ness	13.3	0.0	1.1	0.0	x			
	Beta Sør ORE	18.5	0.0	1.6	0.0	x			
	Beta Sør Tarbert+Heather	5.4	0.0	0.5	0.0				
SNORRE	Snorre Syd, Statfjord/Lunde	399.0	0.0	43.1	0.0	x		x	
	Snorre B, Statfjord/Lunde	143.0	0.0	18.3	0.0			x	
STATFJORD	Brent	665.0	0.0	121.8	0.0	x	x		
	Dunlin	18.4	0.0	2.7	0.0	x			
	Statfjord	179.2	0.0	28.0	0.0	x	x		
STATFJORD NORD	Brent og Munin	77.1	0.0	5.8	0.0	x			
STATFJORD ØST	Brent	59.7	0.0	8.5	0.0	x			
SYGNA	Brent	24.1	0.0	1.5	0.0	x			
TAMBAR	Gyda Jurassic	21.9	1.1	5.1	0.0				x
TOR	Ekofisk og Tor	129.9	0.0	34.4	0.0	x			
TORDIS	Tordis	68.5	0.0	7.1	0.0	x			
	Tordis Sør Øst (STUJ)	5.1	0.0	0.5	0.0	x			
	Tordis Øst	14.8	0.0	1.5	0.0	x			
	Borg	27.7	0.0	3.8	0.0	x			
TROLL II	Gassprovinsen	444.0	0.0	0.0	0.0				x
	Mellomområdet	19.0	0.0	0.0	0.0				x
	Oljeprovinsen	155.0	0.0	0.0	0.0				x
	Troll Vest Fensfjord	26.5	0.0	0.0	0.0				x
ULA	Ula Jurassic	155.0	0.0	17.0	0.0	x			
VALHALL	Hod	114.0	0.0	29.7	0.0				x
	Tor	302.0	0.0	56.2	0.0				x
VARG	Varg	20.4	0.0	2.5	0.0		x		
VESLEFRIKK	VESLEFRIKK (gas total)		1.1	16.3	1.1				
	Brent/IDS	106.9			no	x		x	
	Statfjord	5.7			yes		x		
VIGDIS	Vigdis, Brent	63.3	0.0	4.4	0.0	x			
VISUND	Brent NI	15.0		4.4	no		x	x	
	Brent NII	32.7		44.1	yes		x		
	Statfjord/Amund SI	22.7		9.6	no		x		
	Brent SI	10.3		26.1	yes		x		
ÅSGARD	Smørbukk	35.5	136.2	12.1	162.7		x		
	Smørbukk Sør	99.7	29.2	35.7	25.8		x		
Sum total:		7984.0	236.0	1283.6	467.4				

Table 7.1 – Overview of volume in place and recovery mechanisms

7.1 Screening method

It is considered satisfactory to use the screening criteria in chapter 5.5. Originally, they were prepared for US and Canadian onshore oil fields, but they may be used to begin with when screening North Sea candidates. The most critical parameter with respect to miscible CO_2 flooding is the MMP. Preferably, the MMP at the start of a CO_2 flood should be at least 14 bar above the MMP to achieve miscibility of CO_2 and reservoir oil. This means that the ratio between reservoir pressure and minimum miscible pressure (P/MMP) normally should be greater than 1, but CO_2 flood EOR is still possible for P/MMP greater than 0.9. Because of the uncertainties of both calculation of MMP (see chapter 7.2) and measured pressure data, reservoirs with P/MMP greater than 0.9 are regarded as suitable for CO_2 floods by this screening if the reservoir pressure is lower than the original reservoir pressure at the start of CO_2 injection.

Reservoirs suitable for EOR by implementing CO_2 floods have various degrees of suitability depending on the intrinsic reservoir and oil properties. The range of reservoir characteristics and fluid properties suitable for CO_2 miscible injection is quite broad, and ideal reservoirs should have:

1. Oil gravity < 900 kg/m^3
2. Oil saturation >25 %,
3. Reservoir pressure > 0.9 MMP
4. Porosity >15 %
5. Permeability >1 md
6. Acceptable heterogeneity

In addition:

7. Does the oil field (reservoirs) have a major gas cap or large amounts of stored gas (after injection) for further sales?
8. Is the oil field mature?
9. Are the reservoirs flooded with water, gas or WAG?

Parameters as density, permeability, porosity and oil saturation are not regarded as critical to oilfields on the NCS because almost all of these fields will meet the criteria mentioned above. One could pay more attention to the residual oil saturation after water, gas or WAG flooding, but as long as the prognosis after depleting the various oil fields is in the range of 15 to 65 % of the STOIIP, a further approach to the criteria is not required.

Reservoir heterogeneity is also an important screening parameter, and it affects early CO_2 breakthrough and thus volume of CO_2 recycled. CO_2-WAG recovery is one aspect sensitive to reservoir heterogeneity (for more details, see chapter 2). All oil field on the NCS have varying degrees of heterogeneities, but they are all regarded as acceptable. Hence no oil field in this screening is rejected because of heterogeneity.

Criterion 7 is difficult to comply with, but it is used to reject candidates where postponed gas sales will result in reduced profitability compared to additional EOR oil from CO_2 injection. In addition, the criterion will reject reservoirs that will see reduced profitability if the processing cost of processing gas infiltrated with CO_2 before reaching sales gas specifications is higher than the profits made from the EOR oil. It is difficult to be exact about the last

criterion, but only a few fields will be affected by it as this is a question of costs, and new separation technology may change the outlook.

In addition, small isolated accumulations and small oil fields operated from stand-alone installations at a relatively great distance from existing infrastructure will not be considered to have CO_2 EOR potential. The Murchison oil field is also rejected because of the small Norwegian ownership in the field (22 %). The flow chart in figure 7.2 illustrates the screening process.

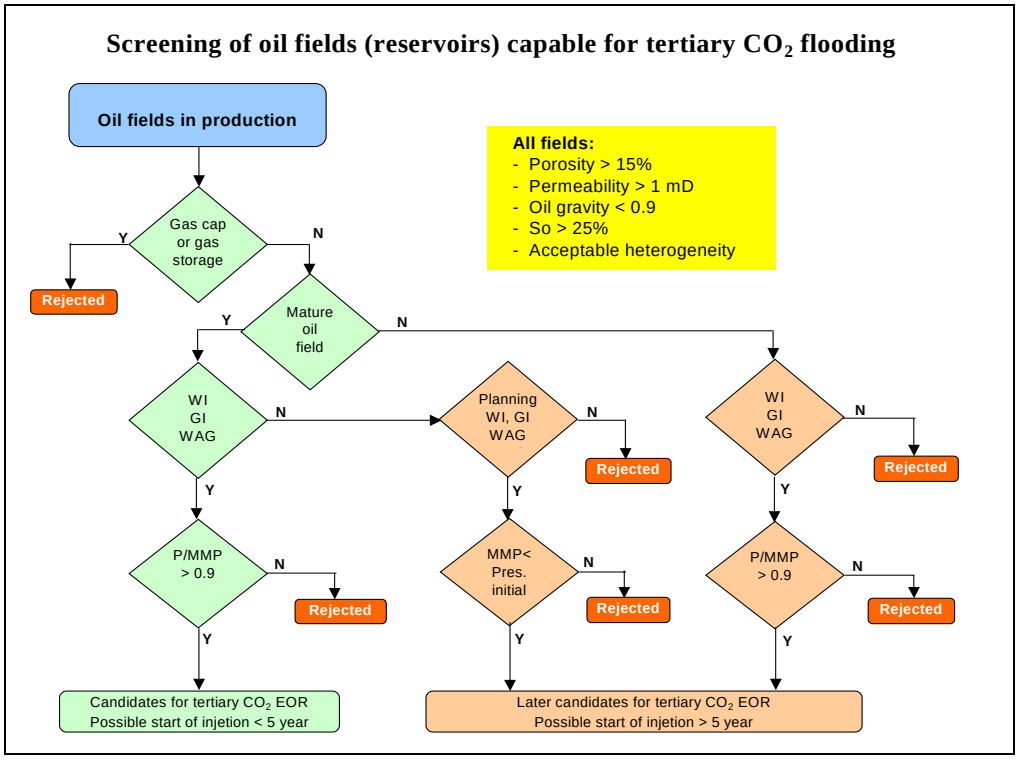

Figure 7.2 – Flow chart for screening of candidates for tertiary CO_2 floods

Candidates that have passed the screening criteria for CO_2 EOR are listed in the spreadsheet, table 8.4, for further risk analysis, calculation and simulation. The candidates are grouped in geographical areas and divided into candidates that can start CO_2 injection within five years, and candidates that can start injection in five years or later.

7.2 Calculation of MMP

To calculate the minimum miscibility pressure, the MMP module of the simulation tool PVTsim, version 12 is used. Input data is taken from files and databases in the Norwegian Petroleum Directorate.

There are indications that EOS calculations by using PVTsim may be to conservative. For some calculation, the data are compared to calculations done by Sintef (senior researcher Idar Akrevoll). The comparison of EOS against Glasø and Alison correlations done by Sintef supports that EOS calculations are conservative. For some fields those correlations are closer to slim tube results than the EOS method. However, in this thesis PVTsim MMP will be used.

7.2.1 Minimum miscibility pressure calculations

The MMP module of PVTsim permits calculation of the first contact minimum miscibility pressure (FCMMP) as well as the multiple contact minimum miscibility pressure (MCMMP), normally referred to as the MMP.

The FCMMP may be calculated by tracking the saturation pressure as a function of oil/gas mixing ratio. The highest saturation point pressure located during the tracking procedure equals FCMMP. Two different procedures are used in PVTsim for calculating vaporizing and condensing MCMMP. One is based on an extension of the procedures behind a ternary diagram to multi-component mixtures and the second is based on simulation. When simulating a condensing gas drive, the cell initially contains reservoir oil. Injection gas is added and any formed gas is removed. A set of differential mass balances and algebraic equilibrium relations of the following form describe the vaporizing drive,

$$dv_i = \left(f_i - o_i\right)dt; \quad i = 1, 2, ..., N \tag{7.1}$$

$$\frac{o_i}{O}\phi_i^v = \frac{v_i}{V}\phi_i^v; \quad i = 1, 2....., N \tag{7.2}$$

$$O = \sum_{i=1}^{N} o_i; V = \sum_{i=1}^{N} v_i \tag{7.3}$$

where f_i and o_i are respectively the rates of addition to and removal of component i from the cell in moles/time and v_i is the number of moles of component i in the cell.

Since the feed rate and feed composition are constant, integration over an arbitrary time step Δt gives

$$v_i\left(t + \Delta t\right) = v_i(t) + f_i\Delta t - \int_t^{t+\Delta t} o_i dt; \quad i = 1, 2, .., N \tag{7.4}$$

Using the trapezoidal rule for evaluation of the integral one gets

$$v_i(t + \Delta t) = v(t) + f_i\Delta t - \frac{o_i(t) + o_i(t + \Delta t)}{2}\Delta t; \quad i = 1, 2, ..., N \tag{7.5}$$

The compositions of the first equilibrium phases (t = 0) are known from the calculation of FCMMP. Adding $d\beta$ moles of reservoir oil to a gas at equilibrium causes $d\gamma$ moles of oil to be formed, and the initial relative flow rate of oil, $d\gamma/d\beta$, can be determined manipulating the equilibrium relations. Successive solution with a chosen time step Δt simulates the miscibility process. If an additional time step at some point does not result in a two-phase solution, miscibility has been established. If on the other hand the end result is constant compositions, miscibility cannot be obtained at the specified conditions. Simulations at different pressures determine MCMMP as the lowest pressure at which miscibility is obtained.

7.2.2 Combined drive mechanism

While the above mentioned method for determination of the MCMMP describes the situation where miscibility develops at the flood front or at the injection point, a more sophisticated approach is required to properly account for the situation where miscibility develops between the flood front and the injection point. In this case a key tie-line approach is applied. Tie lines are lines that connect points in composition space, for instance between an oil composition

and the composition of the gas that contacts it. When a tie line becomes a point, the two phases are miscible (they have the same composition). Ignoring dispersion, it can be shown that there exists a series of key tie lines, which control the development of miscibility. These represent the path which the composition changes in the system theoretically will follow. In order to locate the MMP the algorithm tracks this path at increasing pressures until one of the key tie lines reduce to a point.

Key tie lines are either connected by continuous variations or by shocks. The shocks represent the situations where oil is contacted by gas that it is not in equilibrium, causing an abrupt change in composition. In a fully self-sharpening system all key tie lines are connected by shocks (In a fully self sharpening system the gas moves faster than the contacted oil anywhere in the displacement process). Even when the system is not fully self-sharpening, the present method is considered to give a very good estimate of the true solution. It has been shown by Wang and Orr [73] that neighbouring key tie lines are coplanar and hence have a point of intersection. This information is used to locate the next key tie line in the series.

In order to determine co-planarity, the method developed by Jensen, Michelsen and Stenby [74] is applied. In this approach, the co-planarity criterion constrains the values of α and β to lie in the interval of [0; 1]. This makes the algorithm quite robust.

$$z^* = \alpha \underline{y}^{(1)} + (1+\alpha)\underline{x}^{(2)} = \beta \underline{y}^{(2)} + (1-\beta)\underline{x}^{(1)} \qquad (7.6)$$

The succession of N-1 intersecting key tie lines can then be written as

$$x_i^{j+1}(1-\alpha_j) + y_i^j \alpha_j - x_i^j(1-\beta_j) - y_i^{j+1}\beta_j = 0 \qquad (7.7)$$
$$i = 1,...,N-1$$
$$j = 1,...,N-2$$

where i are the component number and j the tie line number.

The first and last tie lines in the sequence are specified by the tie lines through the original oil and the injection gas respectively. Following the above nomenclature, these two compositions are specified as follows:

$$z_i^{oil} = x_i^{j=1}(1-\beta_{oil}) + y_i^{j=1}\beta_{oil} \qquad (7.8)$$
$$z_i^{inj} = x_i^{j=nc-1}(1-\beta_{inj}) + y_i^{j=N-1}\beta_{inj} \qquad (7.9)$$
$$i = 1,...,N-1$$

The equations above are solved subject to the usual phase equilibrium and mass balance constraints

$$x_i^j \varphi_i^L - y_i^j \varphi_i^V = 0 \qquad (7.10)$$
$$\sum_{i=1}^{N} x_i^j - y_i^j = 0 \qquad (7.11)$$
$$i = 1,...,N$$
$$j = 1,...,N-1$$

All of this may be rearranged to a set of non-linear equations to be solved for the co-planarity parameters (α, β) and the phase compositions.

The calculated MMP pressures are listed in table 7.2 together with the corresponding reservoir pressures and temperatures. In the screening process, the MMP for the combined method is used.

Oil field	**MMP**		**Reservoir pressure**		**Res.temp**
	Vaporizing Bar	Combined Bar	Current Bar	Originally Bar	Originally °C
Balder	383	339	165 +/-	172	77
Ringhorn	196	-	180 ?/-	188	78
Brage *Statfjord*	302	187	200 +/-	219	84
Draugen	164	117	155 +/-	165	71
Ekofisk	172 (1)– 275 (2) [75]		350 +/-	497	131
Eldfisk	369	212	200 +/-	472	122
Embla	321	205	-		159
Glitne	254	156	-	218	80
Gullfaks *Brent*	355	266	280 +/-	310	72
Statfjord	280	176	280 +/-	330	86
Gullfaks Sør *Brent*	551	277	370-420	460	125
Gyda	276	195	480 +/-	593	152
Heidrun *Fangst*	343	221	240 +/-	252	84
	299	189	230 +/-	251	85
Tilje	399	393	220 +/-	251	85
Åre					
Hod	330	145	150 +/-	467	98
Jotun	236	-	150 +/-	199	82
Njord	341	211	170-380	395	120
Norne *Tofte*	355	255	250 +	275	98
Oseberg	325	204	220 +/-	284	102
Oseberg Øst	253	162	220-250	325	124
Oseberg Sør	323	195	240 +/-	299	107
Oseberg Vest	363	260	-	321	107
Snorre *Lunde*	247	142	300 -	383	93
	257	151	280 +/-	383	93
Snorre B *Lunde*					
Statfjord *Brent*	281	175	320 +/-	383	89
Statfjord	269	158	330 +/-	404	100
Statfjord Nord	240	161	320 +/-	398	98
Statfjord Øst	300	169	320 +/-	378	91
Sygna	239	169	380 +/-	395	95
Tambar	299	195	-	538	165
Tor	319	195	140 +/-	497	127
Tordis *Tordis*	259	159	295	340	84
	237	-	310	337	84
Tordis Øst	289	169	330	334	91
Borg					
Troll	339	-	150 +/-	158	68
Ula	274	183	440 +/-	491	143
Valhall *Tor*	336	157	240 +/-	447	90
	309	158	240 +/-	449	89

	Ekofisk					
Varg		346	222	-	347	120
Veslefrik	*Oseberg*	285	188	300 +/-	321	125
		407	207	300 +	355	133
	Statfjord					
Vigdis	*Rannoch*	253	165	280 +	368	91
Visund	*Tarbert/Ness*	368	232	400 +/-	434	115
Åsgard	*Garn*	392	210	300 +/-	405	141

(1) MMP at 82 ^oC, (2) MMP at 131 ^oC

Table 7.2 – Reservoir temperature, -pressure and calculated MMP

8. ESTIMATION OF THE CO_2 EOR POTENTIAL

The screening of candidates and estimation of the EOR potential is based on available reservoir parameters and field data. Most of the data is taken from files and databases in NPD, which includes annual field reports and reservoir management plans for all fields dealt with in this thesis. A great part of the data is confidential, and therefore not included here. Some data, central to the calculations and methods used are enclosed as a confidential supplement to the thesis.

Although a large and specified amount of data are used, the result very much depends on the studies done by Statoil, Phillips Petroleum, Norsk Hydro and BP, on the potential for increased recovery from CO_2 (chapter 6) injection. All CO_2 flood experience today comes from onshore oil fields, but to some degree, methods and simulation techniques from successful simulations done on other projects, have been adopted, for example from the Prudhoe of Bay oil field in Canada (see chapter 6.5). Prudhoe of Bay has miscible gas flooding with a large quantity of CO_2 in the injecting gas.

Main results from the studies

Gullfaks:	3.9 – 7.7 % of STOIIP	(dependent on number of wells)
Brage:	3.1 – 5.1 % of STOIIP	(dependent on WAG ratio)
Forties:	4.7 % of STOIIP	(based on 4 million tonnes CO_2/year)
Ekofisk:	5.6 % of STOIIP	(based on 30 wells, 10 WAG and 20 WI)

The Gullfaks Brent study is regarded as the most mature of these. By including the Statfjord and Cock reservoirs, the CO_2 EOR from Gullfaks may exceed 8 % of the STOIIP of these reservoirs.

8.1 Method

The @RISK analysis and simulation tool has been used to do Monte Carlo simulations on the most critical variable parameter, the CO_2 EOR recovery factor. In addition, three other variables have been chosen to best describe the uncertainties involved. Figure 8.1 and table 8.1 show the method used. The three parameters, heterogeneity, recovery and residual oil saturation are given a low and high possibility instead of low, medium and high, as 27 and not 8 different adjustment factors would have had to be dealt with then, which is too much within this scope of work. One could also have used a set of distribution curves for each of the parameters and performed a risk analysis, but it is considered more correct to establish a set of fixed correlation factors.

The heterogeneity parameter is defined as high if the reservoir is faulted or layered. Also reservoirs with abnormal high well density are defined to have high heterogeneity. Homogeneous reservoirs or partly faulted reservoirs are defined to have low heterogeneity. The recovery factor is defined as the recovery (% of STOIIP) before EOR initiatives. This is a characteristic that says something about the reservoirs' productivity, and high recovery should indicate that CO_2 solvents should have good possibilities of contacting large volumes of residual oil during the flow through the reservoir. The third factor is the residual oil saturation. The factor is not only restricted to residual oil saturation after water or gas flooding, but includes bypassed oil and attic oil (see figure 6.3). The reservoirs are therefore described according to what kind of drive mechanism they have, water injection, gas injection, WAG or pure pressure depletion (see table 7.1). One may assume that reservoirs that have been water flooded have more residual oil left than reservoirs that have been gas or WAG flooded. This may not always be true, but usually, reservoirs suitable for secondary gas injection have lower Sorg then Sorw for a water flooded reservoir. All in all, the combination of these three parameters with fluid, temperature and pressure data should give a good indication of the reservoir properties and impact on CO_2 EOR.

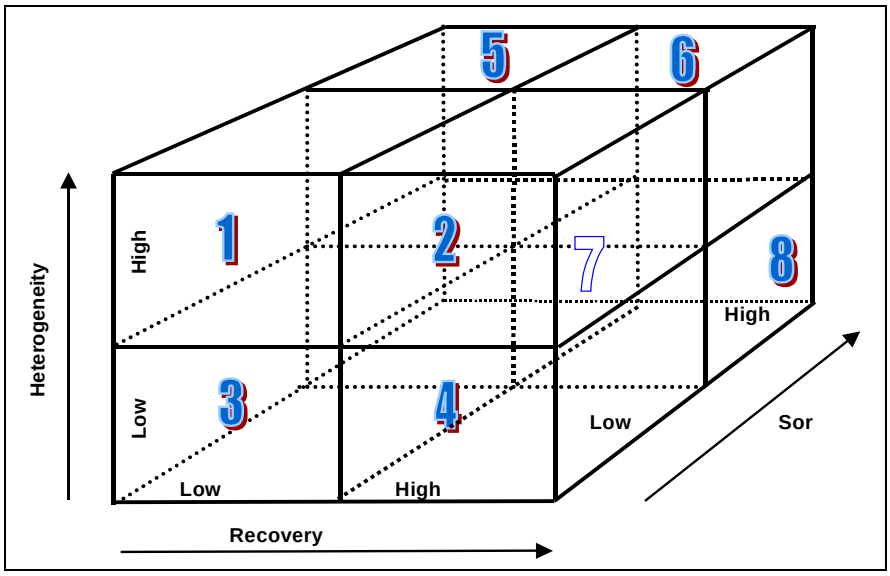

Figure 8.1 – Schematically quantification of reservoir quality

Reservoir-quality*	Sor*		Recovery*		Heterogeneity*		Adjusting-factor
	Low	High	Low	High	Low	High	
1	x		x			x	0,75
2	x			x		x	0,80
3	x		x		x		0,85
4	x			x	x		0,95
5		x	x			x	0,85
6		x		x		x	1,00
7		x	x		x		1,00
8		x		x	x		1,10

Sor*: Water flooded/mainly water flooded reservoir (high), gas or WAG (low)
Recovery*: Recovery (% of STOIIP) without EOR
Heterogeneity*: Faulted/layered and/or high well rate (high), else low

Table 8.1 – Reservoir quality parameters and estimated adjustment factor for EOR calculations

The adjustment factors, f (Sor*, Recovery*, Heterogeneity*) are lumped into the spreadsheet in table 8.4. The factors are weighted to Gullfaks properties where the function f (Sor*, Recovery*, Heterogeneity*)$_{Gullfaks}$ = 1. The Gullfaks recovery has increased from around 4 to about 8 % of STOIIP since the first screening study was completed, and it is likely to expect the same for Ekofisk and Brage if they had gone further with their studies. The adjustment factors are therefore optimised to match a higher recovery from these fields. One could also optimise the adjustment factors in relation to reservoir sizes. But since about 92 % of the STOIIP (candidates of CO_2 EOR) contribution comes from a reservoir (or group of reservoirs) with more than 50 million Sm^3 of oil, and about 77 % from reservoirs with more than 100 million Sm^3 of oil, it is decided not to refine the model according to reservoir sizes. The model may easily be modified, however, to include new or corrected data.

8.2 Estimation

In the spreadsheet model, table 8.4, the result shows a total EOR potential of 279 million Sm^3 before risk analysis and Monte Carlo simulations are run. This is with an average recovery factor of 6 % of STOIIP, and by using the specified adjustment factors. All fields (and reservoirs) that are included in the thesis are listed according to geographical areas. The areas are the southern part of the North Sea, Jotun Balder area, Troll Oseberg area, Tampen area and fields in the Norwegian Sea. The reason for this is to show the potential in the different areas, which may be useful for further investigation and infrastructure studies. Further, the potential is split into mature candidates that can start CO_2 injection within 5 years and candidates that can start in 5 year or later.

The model is simple, but the initial screening, MMP calculations and valuation of the fields and reservoirs involved are based on specific field data. The weakest link in the methodology chain is the expected mean value of the recovery factor, which is totally dependent on the results from the CO_2 studies on Forties (to some degree), Ekofisk, Brage and Gullfaks. However, the recovery factors are considered to be conservative compared to industry experience from existing CO_2 projects worldwide, and the possibility for overestimating is regarded as low. The nature of the recovery factors leads to using a triangle distribution for risk analysis and Monte Carlo simulation. This is mainly because there are only 4 fields that have been studied. If there had been a larger number of inputs, a log normal distribution could have been more convenient. In the spreadsheet model, both sandstone and chalk reservoirs are given a variation in recovery of between 4 and 8 % of STOIIP

Table 8.2 shows the result from the Monte Carlo simulations, while table 8.3 shows the un-risked potential compared to the risked potential. The results from the Monte Carlo simulations are enclosed in appendix A.

Area	**< 5 year**	**> 5 year**	**Total (million Sm3)**
Southern North Sea	10 - 18	78 - 136	93 - 148
Troll Oseberg	9 - 16	10 - 15	21 - 30
Tampen	44 - 66	24 - 42	71 - 103
Norwegian Sea	3 - 5	33 - 50	37 - 54
Sum total	72 - 100	160 - 225	242 - 323

Table 8.2 – CO_2 EOR potential from Monte Carlo Simulations

Estimation	< 5 year	> 5 year	Total (million Sm3)
Un-risked (1)	58 - 117	138 - 277	197 - 393
Partly risked (2)	57 - 114	129 - 258	186 - 372
Risked (3)	72 - 100	160 - 225	242 - 323

1) Screened EOR STOIIP and recovery 4 - 8 %
2) Screened EOR STOIIP with adjusting factors and recovery 4 – 8 %
3) Full Monte Carlo simulation (sum total in table 8.2)

Table 8.3 – Un-risked compared to risked EOR potential

8.3 Conclusions

The results of this thesis indicate that there are great EOR potential from CO_2 injection in mature oil field on the Norwegian Continental Shelf. The potential is estimated to between 242 and 323 millions Sm^3 of additional oil. Compared to a traditional new field development, this corresponds to a 600 million Sm^3 STOIIP field. (Gullfaks size). Development costs and operating costs for implementing CO_2 floods are not included, but considering the large amount of additional oil, such flooding is definitely an alternative to any other EOR techniques.

The result must, however, be regarded as a provisional estimate because of the lack of CO_2 experience on offshore oil fields. The method of calculation is based on a combination of detailed reservoir data and a limited number of CO_2 data, but compared to industry experience, the expected total EOR potential should not be overestimated. The MMP calculations may also be conservative in that it has rejected some candidates. However, the intention was not to give an accurate answer, but to inspire further investigation and research. Finally, the author of this thesis realises that the field owners may not agree with the results, or the interpretation of the data used in this thesis.

An interesting finding from the literature study is that an oilfield that has behaved well under water flooding seems to behave well under CO_2 flooding. Another finding is that (not surprisingly) increased oil production, up to a certain point, is almost linear to the amount of CO_2 injected. This is also seen for the North Sea candidates dealt with in this thesis.

8.4 Spreadsheet model used for Monte Carlo simulations (overleaf)

Oil fields	Reservoirs	STOIIP	Candidates		Correlation factors		< 5 year	> 5 year	
			No = 0 Yes = 1	< 5 year = 1 > 5 year = 0	f (res)	f (rec)	EOR	EOR	
Southern part of the North Sea									
EKOFISK	Ekofisk og Tor	1049.0	1	0	1.00	6.000	0.0	62.9	
ELDFISK	Ekofisk og Tor	428.6	1	0	0.85	6.000	0.0	21.9	
EMBLA	Dev. og Perm.	43.4	0			6.000	0.0	0.0	
GYDA	Gyda Jurassic	63.9	1	1	0.85	6.000	3.3	0.0	
GYDA	Gyda South	14.0	1	1	0.85	6.000	0.7	0.0	
HOD	Hod	14.5	0			6.000	0.0	0.0	
HOD	Tor/Ekofisk	39.8	0			6.000	0.0	0.0	
TAMBAR	Gyda Jurassic	21.9	0			6.000	0.0	0.0	
TOR	Ekofisk og Tor	129.9	0			6.000	0.0	0.0	
ULA	Ula Jurassic	155.0	1	1	1.10	6.000	10.2	0.0	
VALHALL	Hod	114.0	1	0	0.85	6.000	0.0	5.8	
VALHALL	Tor	302.0	1	0	0.85	6.000	0.0	15.4	
Sum Southern part of the North Sea:							**14.2**	**106.0**	**120.3**
Jotun Balder area									
BALDER	Balder	76.8	0			6.000	0.0	0.0	
BALDER	Balder E4	13.8	0			6.000	0.0	0.0	
BALDER	Balder E5	12.9	0			6.000	0.0	0.0	
BALDER	Forseti	25.4	0			6.000	0.0	0.0	
BALDER	Ringhorn Jurassic	33.9	0			6.000	0.0	0.0	
BALDER	Ringhorne "prospecter"	19.9	0			6.000	0.0	0.0	
GLITNE	Glitne, Heimdal Fm.	14.6	0			6.000	0.0	0.0	
JOTUN	Elli	34.8	0			6.000	0.0	0.0	
JOTUN	Elli South	4.1	0			6.000	0.0	0.0	
JOTUN	Tau	18.6	0			6.000	0.0	0.0	
VARG	Varg	20.4	0			6.000	0.0	0.0	
Sum Jotun Balder area:							**0.0**	**0.0**	**0.0**
Troll Oseberg area									
BRAGE	Fensfjord	79.2	1	1	0.80	6.000	3.8	0.0	

BRAGE	Sognefjord	18.3	0			6.000	0.0	0.0	
BRAGE	Statfjord	45.3	1	1	1.00	6.000	2.7	0.0	
OSEBERG	Ness	95.9	0			6.000	0.0	0.0	
OSEBERG	ORELN2	376.8	0			6.000	0.0	0.0	
OSEBERG	Tarbert	87.9	0			6.000	0.0	0.0	
OSEBERG SØR	C	25.1	1	0	0.85	6.000	0.0	1.3	
OSEBERG SØR	G Øst	23.1	1	0	0.85	6.000	0.0	1.2	
OSEBERG SØR	K Vest	13.2	1	0	0.85	6.000	0.0	0.7	
OSEBERG SØR	K Øst	3.3	0			6.000	0.0	0.0	
OSEBERG SØR	Omega Nord	64.0	1	0	0.85	6.000	0.0	3.3	
OSEBERG SØR	Omega Sør	48.0	1	0	1.00	6.000	0.0	2.9	
OSEBERG VEST	Gamma Nord	10.7	0			6.000	0.0	0.0	
OSEBERG ØST	Beta Sadel Nord Ness	1.3	0			6.000	0.0	0.0	
OSEBERG ØST	Beta Sadel Nord Ore	2.0	0			6.000	0.0	0.0	
OSEBERG ØST	Beta Sadel Nord Tarb+Heath	0.4	0			6.000	0.0	0.0	
OSEBERG ØST	Beta Sadel LOSST	0.2	0			6.000	0.0	0.0	
OSEBERG ØST	Beta Sadel Ness	10.0	1	0	0.75	6.000	0.0	0.5	
OSEBERG ØST	Beta Sadel ORE	25.7	1	0	0.75	6.000	0.0	1.2	
OSEBERG ØST	Beta Sadel Tarbert+Heather	2.7	0			6.000	0.0	0.0	
OSEBERG ØST	Beta Sør LOSST	0.3	0			6.000	0.0	0.0	
OSEBERG ØST	Beta Sør Ness	13.3	1	0	0.85	6.000	0.0	0.7	
OSEBERG ØST	Beta Sør ORE	18.5	1	0	0.85	6.000	0.0	0.9	
OSEBERG ØST	Beta Sør Tarbert+Heather	5.4	0			6.000	0.0	0.0	
TROLL	Gassprovinsen	444.0	0			6.000	0.0	0.0	
TROLL	Mellomområdet	19.0	0			6.000	0.0	0.0	
TROLL	Oljeprovinsen	155.0	0			6.000	0.0	0.0	
TROLL	Troll Vest Fensfjord	26.5	0			6.000	0.0	0.0	
VESLEFRIKK	Brent/IDS	106.9	1	1	1.00	6.000	6.4	0.0	
VESLEFRIKK	Statfjord	5.7	0			6.000	0.0	0.0	
Sum Troll Oseberg area:							**12.9**	**12.5**	**25.4**
Tampen area									
GULLFAKS	Brent u/GFVest	441.0	1	1	1.00	6.000	26.5	0.0	
GULLFAKS	Cook	45.0	1	1	1.10	6.000	3.0	0.0	
GULLFAKS	Gullfaks Vest inkl. Shetland	6.9	0	1		6.000	0.0	0.0	

GULLFAKS	Lunde	3.1	0			6.000	0.0	0.0	
GULLFAKS	Statfjord inkl. Krans, ++	92.0	1	1	1.10	6.000	6.1	0.0	
GULLFAKS SØR	GF Sør Brent	39.9	0			6.000	0.0	0.0	
GULLFAKS SØR	GF Sør Statfjord	35.7	0			6.000	0.0	0.0	
GULLFAKS SØR	Gullveig Brent	7.0	0			6.000	0.0	0.0	
GULLFAKS SØR	Rimfaks Brent	23.9	1		0.85	6.000	0.0	1.2	
GULLFAKS SØR	Rimfaks Statfjord	10.8	1		0.85	6.000	0.0	0.6	
SNORRE	Snorre Syd, Statfjord/Lunde	399.0	1	0	1.00	6.000	0.0	23.9	
SNORRE	Snorre B, Statfjord/Lunde	143.0	1	0	0.80	6.000	0.0	6.9	
STATFJORD	Brent	665.0	0			6.000	0.0	0.0	
STATFJORD	Dunlin	18.4	0			6.000	0.0	0.0	
STATFJORD	Statfjord	179.2	0			6.000	0.0	0.0	
STATFJORD NORD	Brent og Munin	77.1	1	1	1.00	6.000	4.6	0.0	
STATFJORD ØST	Brent	59.7	1	1	1.00	6.000	3.6	0.0	
SYGNA	Brent	24.1	1	1	1.00	6.000	1.4	0.0	
TORDIS	Tordis	68.5	1	1	1.00	6.000	4.1	0.0	
TORDIS	Tordis Sør Øst (STUJ)	5.1	0			6.000	0.0	0.0	
TORDIS	Tordis Øst	14.8	1	1	0.80	6.000	0.7	0.0	
TORDIS	Borg	27.7	1	1	1.00	6.000	1.7	0.0	
VIGDIS	Vigdis, Brent	63.3	1	1	0.85	6.000	3.2	0.0	
VISUND	Brent NI	15.0	0			6.000	0.0	0.0	
VISUND	Brent NII	32.7	0			6.000	0.0	0.0	
VISUND	Startfjord/Amund SI	22.7	0			6.000	0.0	0.0	
VISUND	Brent SI	10.3	0			6.000	0.0	0.0	
Sum Tampen area:							**54.9**	**32.6**	**87.4**

The Norwegian Sea									
DRAUGEN	Garn	31.7	1	0	1.00	6.000	0.0	1.9	
DRAUGEN	Rogn	178.2	1	0	1.00	6.000	0.0	10.7	
HEIDRUN	Fangst	155.0	1	0	1.00	6.000	0.0	9.3	
HEIDRUN	Tilje	123.0	1	0	0.85	6.000	0.0	6.3	

HEIDRUN	Åre	162.0	0			6.000	0.0	0.0	
HEIDRUN	Heidrun Nord	8.0	0	0		6.000	0.0	0.0	
NJORD	Ile East/Central	7.5	0	0		6.000	0.0	0.0	
NJORD	Ile North	4.0	0			6.000	0.0	0.0	
NJORD	Tilje East/Central	81.8	1	1	0.75	6.000	3.7	0.0	
NJORD	Tilje North	30.7	0			6.000	0.0	0.0	
NORNE	Norne	157.0	1	0	1.00	6.000	0.0	9.4	
ÅSGARD	Smørbukk	35.5	0			6.000	0.0	0.0	
ÅSGARD	Smørbukk Sør	99.7	1	0	0.75	6.000	0.0	4.5	
Sum the Norwegian Sea:							**3.7**	**42.1**	**45.8**
SUM STOIIP CANDIDATES:		**4915.0**					**85.7**	**193.2**	**278.9**
SUM STOIIP TOTAL:		**7984.0**							

Table 8.4 – Spreadsheet for risk analysis and Monte Carlo simulation

9. ABBREVATIONS AND NOMECLATURE

Abbreviations

STOIIP	=	Stock tank oil initially in place
NCS	=	Norwegian Continental Shelf
SACROC	=	Scurry Area Canyon Reef Operators Committee
SACS	=	Saline Aquifer CO_2 Storage
THERMIE	=	THERMIE is the Demonstration Component of the EU Non-Nuclear Programme JOULE-THERMIE
IEA	=	The International Energy Agency
EOR	=	Enhanced Oil Recovery
FCMMP	=	First contact minimum miscible pressure
MCMMP	=	Multiple contact minimum miscible pressure
MMP	=	Minimum miscible pressure (often used instead of MCMMP)
MME	=	Minimum miscibility enrichment
OP	=	Oil producing well
WI	=	Water injection
GI	=	Gas injection
GOR	=	Gas oil ratio
NGL	=	Natural gas liquid
LPG	=	Liquid petroleum gas
PV	=	Pore volume
EOS	=	Equation of state
4D	=	Four dimensional seismic survey

Nomenclature

T	=	Temperature
Tc	=	Critical temperature
Ttr	=	Triple point temperature
P	=	Pressure
Pc	=	Critical pressure
Ptr	=	Triple point pressure
R	=	Universal gas constant
G	=	Gibbs free energy
ΔG	=	Change in energy
H	=	Enthalpy
S	=	Entropy
ΔH_{fus}	=	Change in enthalpy of the substance that accompany melting (fusion)
ΔV_{fus}	=	Change in volume of the substance that accompany melting
ΔH_{vap}	=	Change in enthalpy of the substance that accompany evaporation
ΔH_{sub}	=	Change in enthalpy of the substance that accompany sublimation
L_1, L_2	=	Liquid mixes
G_1, G_2	=	Gas mixes
t	=	Time
Δt	=	Time step
f	=	Rates of addition of reservoir oil
o	=	Rates of removal of equilibrium oil

v	=	Molar amounts of each component in the gas phase
O	=	Moles of equilibrium oil
V	=	Moles of gas
x	=	Mole fraction in liquid phase
y	=	Mole fraction in vapour phase
z	=	Overall mole fraction
α, β	=	Co-planarity parameters
φ	=	Fugacity coefficient
Sor	=	Residual oil saturation
Sorw	=	Residual oil saturation after water flooding
Sorg	=	Residual oil saturation after gas flooding
f(res)	=	Fixed correlation factors
f(rec)	=	Variable input parameter (recovery factor) to Monte Carlo simulation

10. REFERENCES

1. M. Baviere, Basic Concepts in Enhanced Oil Recovery Processes, published for SCI. Data from US Department of Energy, Target reservoirs for CO_2 miscible flooding. DOE/MC/08341, 17 October 1980.

2. Statoil, "Snøhvit LNG Project PDO support documentation CO_2 deposition", 07.06.2001.

3. Holm," Evaluation of Carbon Dioxide Flooding Process", Journal of Petr. Techn. November 1987. P 245-252.

4. Macintyre, "Design considerations for carbon dioxide injection facilities", Journal of Can Petr. Techn. March-April 1986, P 90-95.

5. Olds, Sage and Lacey, "Partial Volumetric Behaviour of Methane-Carbon Dioxide System, Fundamental Research on Occurrence and Recovery of Petroleum", America Petroleum Institute, 1943.

6. Wiebe and Gady, "Solubility of CO_2 in water", vol 61, February 1939, P 316.

7. Stalkup, "Miscible Displacement", Monograph Series, SPE, 1983.

8. Grigg and Sigan. "Understanding and exploiting four-phase flow in low-temperature CO_2 floods". SPE paper 39790, presented at the SPE Permian Basin Oil & Gas Recovery Conference, Midland, Texas 25 – 27 March 1998.

9. Mizenko, "North Cross Unit CO_2 flood, status report", SPE paper 24210, presented at the 8th SPE/DOE Symposium on EOR, Tulsa 22 – 24 April 1992.

10. McDougal, S.R., Dixit, A.B., and Sorbie, K.S.: "Network Analogous of Wettability at the Pore Scale," *Developments in Petrophysics,* M.A. and P.K. Harvey (eds.), Geological Society Special Publications No. 122, (1997), pp 19-35.

11. John D. Rogers and Reid B. Grigg, "A Literature Analysis of the WAG Injectivity Abnormalities in the CO_2 Process" SPE paper 59329 presented at the 2000 SPE/DOE Improved Oil Recovery Symposium, Tulsa, Oklahoma, 3–5 April 2000.

12. Jackson, D.D., Andrews, G.L., and Claridge, E.L.: "Optimum WAG Ratio vs. Rock Wettability in CO_2 Flooding," SPE paper 4303 presented at the 1985 Annual Technical Conference and Exhibition, Las Vegas, NV, Sept. 22-25.

13. Yuan, Mosley and Hyer. "Mineral scale control in a CO_2 flooded oilfield", SPE paper 65029 presented at the SPE International Symposium on Oilfield Chemistry, Huston 13 – 16 February 2001.

14. Shuler, Freitas and Bowker. " Selection and application of BaSO4 scale inhibitors for a CO_2 flood, Rangely Weber Sand", SPE paper 18973, SPE Petroleum Engineering, August 1991 (page 259)

15. Langston, Hoadley and Young. “Definitive CO_2 flooding response in the SACROC Unit”, SPE paper 17321, presented at the SPE/DOE EOR Symposium, Tulsa 17 – 20 April 1988.

16. Jasek, Frank, Mathis and Smith. “Goldsmith San Andreas Unit CO_2 pilot, design implementation and early performance”, SPE paper 48945, presented at the SPE Annual Tech. Conference and Exhibition”, New Orleans, Louisiana 27 –30 September 1998.

17. Ring, J.N. and Smith, D.J.: "An Overview of the North Ward Estes CO_2 Flood," SPE paper 30729 presented at the 1995 SPE Annual Technical Conference and Exhibition, Dallas, Oct. 22-25.

18. Prieditis J., Wolle, C.R., and Notz, P.K.:"A Laboratory and Field Injectivity Study: CO_2 WAG in the San Andres Formation of West Texas," SPE paper 22653 presented at the 1991 SPE Annual Technical Conference and Exhibition, Dallas, Oct. 6-9.

19. Roper, M.K., *et al.*: “Interpretation of a CO_2 WAG Injectivity Test in the San Andres Formation Using a Compositional Simulator,” SPE paper 24163 presented at the 1992 SPE/DOE Enhanced Oil Recovery Symposium, Tulsa, April 22-24.

20. Christensen, J.R., Stenby, E.H., and Skauge, A.: "Review of WAG Field Experience," SPE paper 39883 presented at the 1998 SPE international Petroleum Conference and Exhibition of Mexico, Villhermosa, March 3-5.

21. Stein, Frey, Walker and Parlani. “Slaughter Estate Unit CO_2 flood”, SPE paper 19375, JPT September 1992 (page 1026)

22. Van Lingen, P.P and Knight, S.: “Evaluation of Capillary Entrapment within Reservoir Flow Units,” SPE paper 38934 presented at the 1997 SPE Annual Technical Conference and Exhibition, San Antonio, Oct. 5-8.

23. Prieditius, J. and Brugman, R.J.: “Effects of Recent Relative Permeability Data on CO_2 Flood Modeling,” SPE paper 26650 presented at the 1993 SPE Annual Technical Conference and Exhibition, Houston, Oct. 3-6.

24. Roper Jr., M.K., Pope, G.A., and Sepehrnoori, K.: "Analysis of Tertiary Injectivity of Carbon Dioxide," SPE paper 23974 presented at the 1992 SPE Permian Basin Oil and Gas Recovery Conference, Midland, 18-20 March.

25. Pizarro, J.O.S., Lake, L.W.: “Understanding Injectivity in Heterogeneous Reservoirs,” paper SPE 39697 presented at the 1998 SPE/DOE Improved Oil Recovery Symposium, Tulsa, April 19-22.

26. Surguchev, L. M., Korbrl, R., Krakstad, O.S.: "Optimum Water Alternate Gas Injection Schemes for Stratified Reservoirs," SPE paper 24646 presented at the 1992 SPE Annual Technical Conference and Exhibition, Washington D.C. Oct. 4-7.

27. Gorrell, S. B.: "Implications of Water-Alternate -Gas Injection Profile Control and Injectivity," SPE paper 20210 presented at the 1990 SPE/DOE Seventh Symposium on Enhanced Oil Recovery, Tulsa, April 22-25.
28. S-H. Chang, L.A. Owusu, S.B. French and F.S. Kovarik; "The Effect of Microscopic heterogeneity on CO_2-Foam Mobility: Part 2—Mechanistic Foam Simulation", SPE paper 20191, prepared for presentation at the SPE/DOE seventh Symposium on Enhanced Oil Recovery held in Tulsa, Oklahoma, April 22-25, 1990.

29. Figure (with small adjustments) after Larry W. Lake, University of Texas and Austin, "Enhanced Oil Recovery", 1989, page 253.

30. Zick, A. A., "A combined condensing/vaporizing mechanism in the displacement of oil by enriched gases", SPE paper 15493, 61st Annual Techn. Conf. and Exhibition of Soc. Petroleum Engineers, Dallas, 27-30-September 1987.

31. Novosad, Z. & Costain, T. G., "Mechanism of miscibility development in hydrocarbon gas-drives, new interpretation." SPE Paper 16717, 62nd Annual Techn. Conf. And Exhibition of Soc. Petroleum Engineers, New Orleans 5-8 October 1986.

32. Slim tube apparatus, source not known

33. F.B Thomas, T. Okazawa, P. Hodgins, X. Zhou, A. Erlian, D.B. Bennion, "Considerations on Solvent Compositions for Hydrocarbon Miscible Flood", SPE paper 35388, Tehn. Symposium on Improved Oil Recovery, SPE/DOE, Tulsa, 21-24 April 1996.

34. Stalkup, F.I. Jr., " Status of Miscible Displacement", SPE paper 9992, International Petroleum Exhibition and Symposium, Beijing, China, 18-26 March 1982

35. Lars Høier and Curtis H. Whitson. SPE paper 49269, Annual Techn. Conf. and Exhibition of Soc. Petroleum Engineers, New Orleans, 27-30 September 1998.

36. Hua Yuan and Russel T. Johns, "Simplified Method for Calculation of Minimum Miscibility Pressure or Enrichment", SPE paper 77381, Annual Techn. Conf. and Exhibition of Soc. Petroleum Engineers, San Antonio, 29 September – 2 October 2002.

37. Russell T. Johns and Hua Yuan, "Quantification of Displacement Mechanisms in Multicomponent Gas floods", SPE paper 77696, Annual Techn. Conf. and Exhibition of Soc. Petroleum Engineers, San Antonio, 29 September – 2 October 2002.

38. Britt R. Gilbert, Burnshire Research Group; Discussion/meeting with NPD and confirmed by Hallvard Nordbø, Enterprise Oil do Brazil (by phone to Petrobraz)

39. Derril J. Stephenson, VIKOR, "Economic Feasibility of Horizontal CO_2 EOR Projects in Alberta," presented at the 2002 Climate Change and Greenhouse Gas (GHG) Technology May 23, 2002

40. Oil & Gas Journal 15 April 2002.

41. Data from Geological Data Services,

http://www.utpb.edu/ceed/GeologicalResources/West_Texas_Geology/Links/west_tx_structure.htm

42. Data from R. F. Lindsay,

http://www.utpb.edu/ceed/GeologicalResources/West_Texas_Geology/Links/west_tx_structure.htm

43. Kinder Morgan, "SACROC Unit Overview", presented at the North Sea CO_2 Workshop, December 6-7, 2001.

44. EPRI, "Enhanced Oil Recovery Scooping Study", Finale Report, October 1999.

45. PanCanadian Energy, "The Weyburn CO2 Flood", Canadian Heavy Oil Association 2001

46. Jazrawi and Stachniak, "International Energy Agency Weyburn CO_2 Monitoring Storage Project", Western Canada 2002 Greenhouse Gas Technology Conference, 24 May, 2002. (Figure source, Encana)

47. http://www.encana.com/index2.shtml (For figure 5.7, click on our project/Weyburn).

48. G. Burrowes (PanCanadian Resources), C. Gilboy (Petroleum Geology Branch, Saskatchewan Energy and Mines), "Investigating Sequestration Potential of Carbonate Rocks during Tertiary Recovery from a Billion Barrel Oil Field, Weyburn, Saskatchewan: the Geoscience Framework (IEA Weyburn CO_2 Monitoring and Storage Project)".
http://www.netl.doe.gov/publications/proceedings/01/carbon_seq/p20.pdf

49. The Weyburn CO_2 Monitoring Project; Request for Funding for the Weyburn CO_2 Monitoring Project Submitted to" Climate Change Central" Government of Alberta Prepared by the Petroleum Technology Research Centre Regina, Saskatchewan January 26, 2000.

50. Charles W. Bloomquist, Keith L. Fuller, Peat, and Michael B. Moranranville, "Miscible Gas Enhanced Oil Recovery Economics and Effects of the Windfall Profit Tax", SPE Paper No 10274, presented at the 56th Annual Fall Technical Conference and Exhibition of the Society of Petroleum Engineers of AlME, held in San Antonio, Texas, October 5-7, 1981.

51. Guntis Moritis, Oil & Gas Journal 14 May 2001, page 68 and 69.

52. Department of Energy Web Site, 4.12.02

53. Data extracted from Oil & Gas Journal 15 April 2002

54. Ruether, Dahowaski and Ramezan, "Prospects for Early Development of Power Plants Employing Carbon Capture", Electric Utilities Environmental Conference, Tucson 22-25 January 2002.

55. Ongoing project at the University of Kansas Energy Research Centre. http://www.kgs.ukans.edu/CO_2/index.html

56. EPRI Technical Report; "Reduction of Greenhouse Gas Emissions through Underground CO_2 Sequestration in Texas Oil and Gas Reservoirs". Final Report, August 1999.

57. W. Thomas Goerold, "Sources of United States Oil Supply", 8 April 2002.

58. http://www.kindermorgan.com/business/co2/finance_flood_detail.cfm

59. Klins, M. A., Carbon Dioxide Flooding, Int. Human Resources Development Corp., Boston, 1984.

60. Stefan Bachu, Alberta Energy and Utilities Board, 4999-98 Avenue Edmonton, AB, T6B 2X3, Canada; " Screening and Ranking of Hydrocarbon Reservoirs for CO_2 Storage in the Alberta Basin, Canada"

61 Tore Torp, Statoil, "Final Technical Report "SACS" – Saline Aquifer CO_2 Storage", February 2000.

62. http://www.iku.sintef.no/projects/IK23430000/

63. SACS Project; http://www.ieagreen.org.uk/sacs2.htm

64. Lindeberg, Zweigel, Bergmo, Ghanderi and Lothe, "Prediction of CO_2 distribution pattern improved by geology and reservoir simulation and verified by time lapse seismic", The Fifth International Conference on Greenhouse Gas Control Technologies, Cairns, Australia, 13-16 August 2000.

65. Dr Andrew Chadwick, the British Geological Survey, and Laura Durnford, Radio Nederland Science Unit. http://www.rnw.nl/science/html/bubble021119.html

66. Espie, Brand, Skinner, Hubbard and Turan, " Obstacles to the storage of CO2 through EOR operations in the North Sea", presented at the Sixth International Conference on Greenhouse Gas Control Technologies, Japan 1-4 October, 2002.

67. Halil Turan, Roger Skinner and Peter Brand (BP, Aberdeen)
SHARP IOR eNewsletter, January 2003, Issue 4.

68. T.B. Jensen, K.J. Harpole, and A. Østhus¸"EOR Screening for Ekofisk", SPE Paper NO 65124, presented at the SPE European Petroleum Conference held in Paris, France, 24–25 October 2000.

69. Holt and Lindeberg, "Thermal Power – Without Greenhouse Gases and With Improved Oil Recovery", Energy Convers. Mgmt., Vol. 33, No. 5-8, pp. 595-602,1992.

70. Paul Hood, Norsk Hydro, “Feasibility Study for CO_2 Injection in the Brage Field”, SPE Drilling, Completion and Reservoir Management Seminar in Bergen 1 April 2003.

71. Hafsteinn Agustsson, Statoil, “Feasibility Study for CO_2 Injection in Statoil Operated Fields”, SPE Drilling, Completion and Reservoir Management Seminar in Bergen 1 April 2003.

72. ECLIPSE FrontSim (Streamline simulator), http://www.sis.slb.com/content/software/simulation/frontsim.asp

73. Yun Wang, SPE, and Franklin M. Orr, Jr. “Calculation of Minimum Miscibility Pressure”. SPE paper 39683, presented the SPE/DOE Improved Oil Recovery Symposium held in Tulsa, Oklahoma, 19-22 April 1998.

74. Jenssen, Michelsen, and Stenby, "Effective Algorithm for Calculation of Minimum Miscibility Pressure", SPE paper 50632, presented at the SPE European Petroleum Conference held in The Hauge, Netherlands, 20-22 October 1998.

75. Phillips, MMP data for Ekofisk (Communication between Phillips and Tom Andersen NPD)

APPENDIX A : RESULTS FROM THE MONTE CARLO SIMULATION

Simulation Results for
Total CO2 EOR potential: Sum total / J98

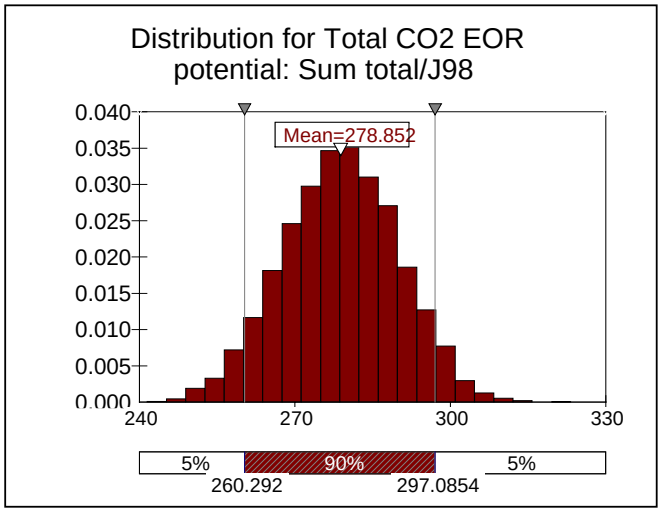

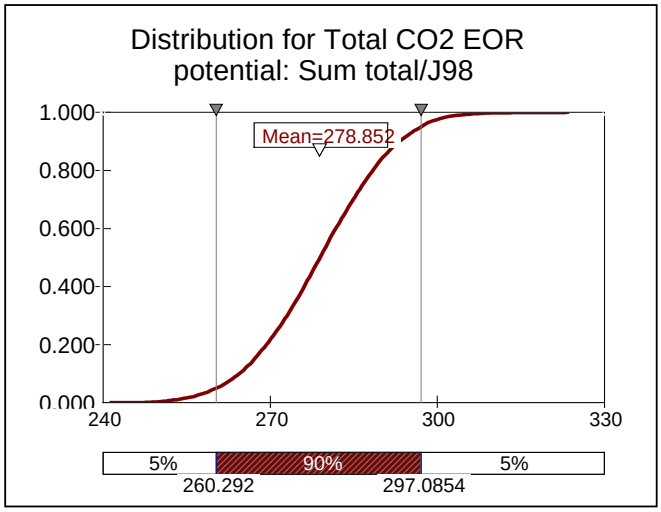

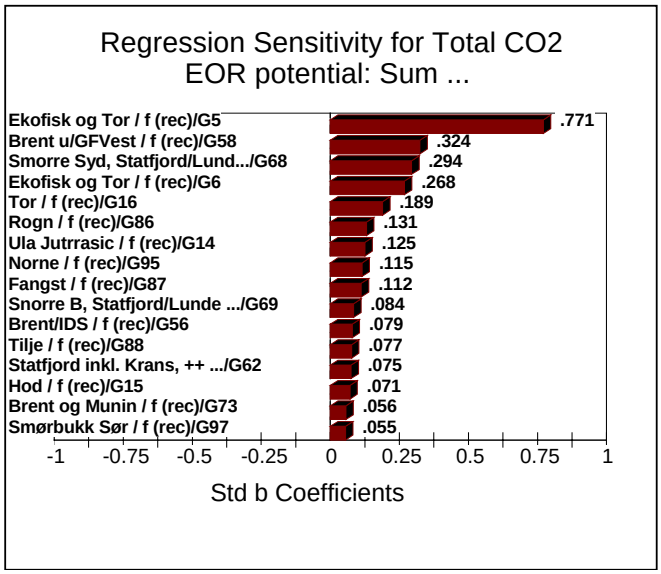

Summary Information	
Workbook Name	put Monte Carlo alle felt.x
Number of Simulations	1
Number of Iterations	10000
Number of Inputs	93
Number of Outputs	1
Sampling Type	Latin Hypercube
Simulation Start Time	07.05.2003 08:58
Simulation Stop Time	07.05.2003 08:59
Simulation Duration	00:00:26
Random Seed	193526971

Summary Statistics			
Statistic	**Value**	**%tile**	**Value**
Minimum	241.5	5 %	260.3
Maximum	323.3	10 %	264.5
Mean	278.9	15 %	267.1
Std Dev	11.1	20 %	269.3
Variance	123.2685271	25 %	271.2
Skewness	-0.028566161	30 %	273.0
Kurtosis	2.834638894	35 %	274.6
Median	278.9	40 %	276.1
Mode	266.5	45 %	277.5
Left X	260.3	50 %	278.9
Left P	5 %	55 %	280.3
Right X	297.1	60 %	281.7
Right P	95 %	65 %	283.4
Diff X	36.8	70 %	284.9
Diff P	90 %	75 %	286.6
#Errors	0	80 %	288.4
Filter Min		85 %	290.5
Filter Max		90 %	293.1
#Filtered	0	95 %	297.1

Sensitivity			
Rank	**Name**	**Regr**	**Corr**
#1	Ekofisk og Tor /	0.771	0.761
#2	Brent u/GFVest	0.324	0.307
#3	Smorre Syd, Sta	0.294	0.262
#4	Ekofisk og Tor /	0.268	0.238
#5	Tor / f (rec) / $G	0.189	0.193
#6	Rogn / f (rec) / $	0.131	0.124
#7	Ula Jutrrasic / f	0.125	0.131
#8	Norne / f (rec) /	0.115	0.116
#9	Fangst / f (rec) /	0.112	0.118
#10	Snorre B, Statfj	0.084	0.115
#11	Brent/IDS / f (re	0.079	0.078
#12	Tilje / f (rec) / $	0.077	0.062
#13	Statfjord inkl. Kr	0.075	0.058
#14	Hod / f (rec) / $	0.071	0.055
#15	Brent og Munin	0.056	0.066
#16	Smørbukk Sør /	0.055	0.052

Simulation Results for
Total CO2 EOR potential: CO2 injection after 5 year / I98

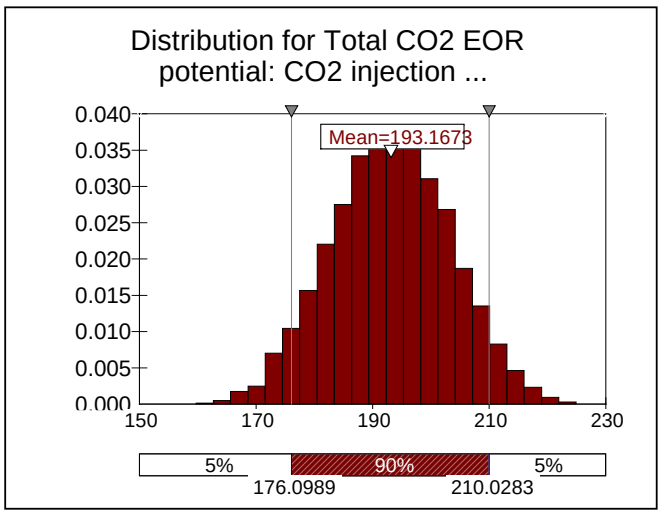

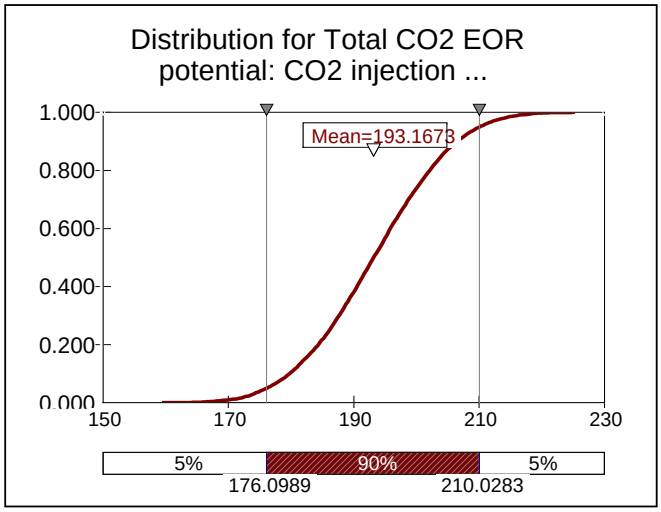

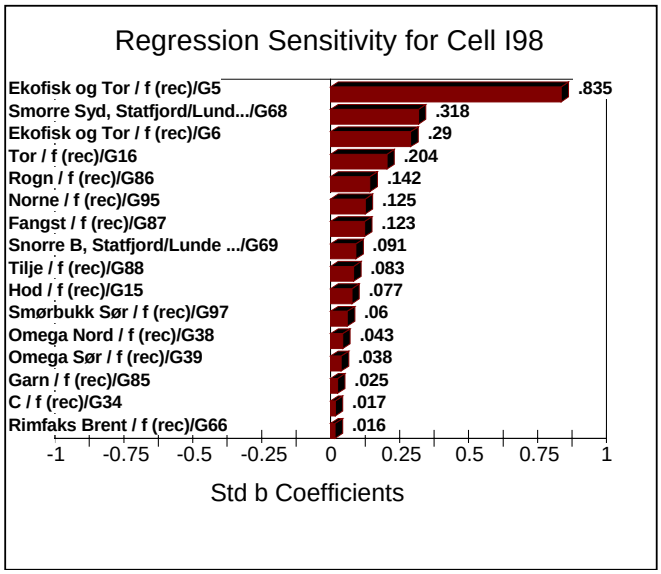

Summary Information	
Workbook Name	put Monte Carlo alle felt.x
Number of Simulations	1
Number of Iterations	10000
Number of Inputs	93
Number of Outputs	1
Sampling Type	Latin Hypercube
Simulation Start Time	07.04.2003 12:37
Simulation Stop Time	07.04.2003 12:37
Simulation Duration	00:00:25
Random Seed	1070136162

Summary Statistics			
Statistic	**Value**	**%tile**	**Value**
Minimum	159.7	5 %	176.1
Maximum	225.0	10 %	179.7
Mean	193.2	15 %	182.2
Std Dev	10.3	20 %	184.3
Variance	105.2962833	25 %	186.2
Skewness	-0.012581339	30 %	187.6
Kurtosis	2.720091868	35 %	189.1
Median	193.2	40 %	190.5
Mode	173.6	45 %	191.8
Left X	176.1	50 %	193.2
Left P	5 %	55 %	194.5
Right X	210.0	60 %	195.8
Right P	95 %	65 %	197.3
Diff X	33.9	70 %	198.7
Diff P	90 %	75 %	200.4
#Errors	0	80 %	202.1
Filter Min		85 %	204.0
Filter Max		90 %	206.6
#Filtered	0	95 %	210.0

Sensitivity			
Rank	**Name**	**Regr**	**Corr**
#1	Ekofisk og Tor /	0.835	0.830
#2	Smorre Syd, Sta	0.318	0.293
#3	Ekofisk og Tor /	0.290	0.280
#4	Tor / f (rec) / $G	0.204	0.200
#5	Rogn / f (rec) / $	0.142	0.140
#6	Norne / f (rec) /	0.125	0.108
#7	Fangst / f (rec) /	0.123	0.121
#8	Snorre B, Statfjo	0.091	0.084
#9	Tilje / f (rec) / $C	0.083	0.059
#10	Hod / f (rec) / $C	0.077	0.072
#11	Smørbukk Sør /	0.060	0.049
#12	Omega Nord / f	0.043	0.057
#13	Omega Sør / f (	0.038	0.021
#14	Garn / f (rec) / $	0.025	0.041
#15	C / f (rec) / G	0.017	0.031
#16	Rimfaks Brent /	0.016	0.030

Simulation Results for
Total CO2 EOR potential: CO2 injection within 5 year / H98

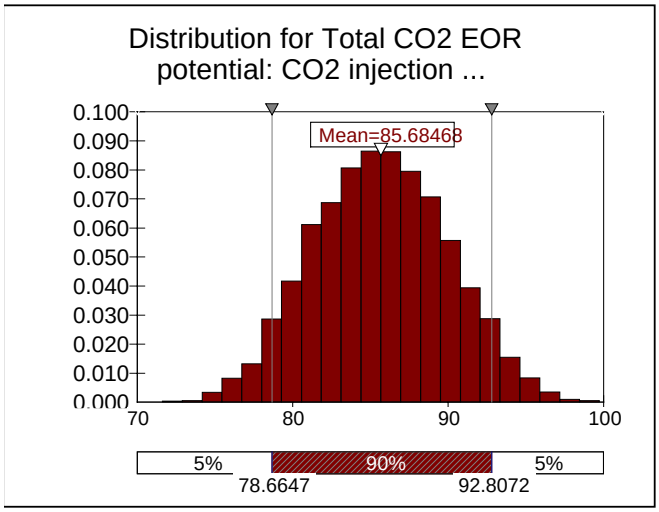

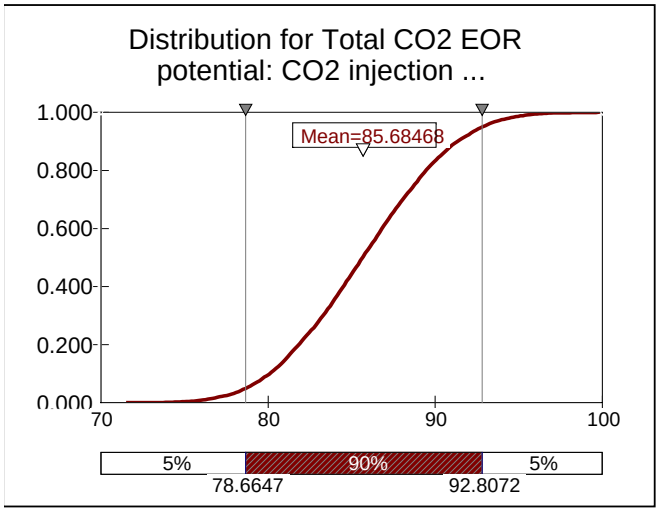

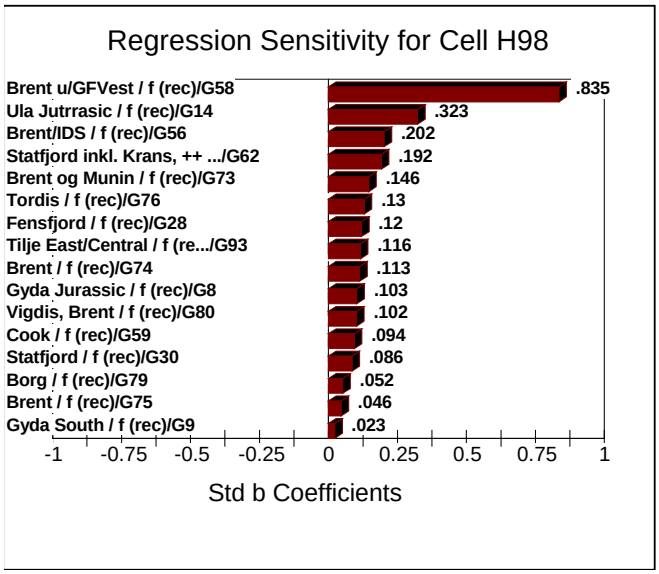

Summary Information	
Workbook Name	put Monte Carlo alle felt.x
Number of Simulations	1
Number of Iterations	10000
Number of Inputs	93
Number of Outputs	1
Sampling Type	Latin Hypercube
Simulation Start Time	07.05.2003 08:54
Simulation Stop Time	07.05.2003 08:54
Simulation Duration	00:00:27
Random Seed	1399412072

Summary Statistics			
Statistic	Value	%tile	Value
Minimum	71.6	5 %	78.7
Maximum	99.8	10 %	80.1
Mean	85.7	15 %	81.1
Std Dev	4.3	20 %	81.8
Variance	18.59731218	25 %	82.6
Skewness	0.032848554	30 %	83.3
Kurtosis	2.650582792	35 %	83.9
Median	85.7	40 %	84.5
Mode	79.3	45 %	85.1
Left X	78.7	50 %	85.7
Left P	5 %	55 %	86.2
Right X	92.8	60 %	86.8
Right P	95 %	65 %	87.4
Diff X	14.1	70 %	88.1
Diff P	90 %	75 %	88.8
#Errors	0	80 %	89.4
Filter Min		85 %	90.3
Filter Max		90 %	91.3
#Filtered	0	95 %	92.8

Sensitivity			
Rank	Name	Regr	Corr
#1	Brent u/GFVest	0.835	0.834
#2	Ula Jutrrasic / f	0.323	0.306
#3	Brent/IDS / f (re	0.202	0.196
#4	Statfjord inkl. Kr	0.192	0.195
#5	Brent og Munin	0.146	0.141
#6	Tordis / f (rec) /	0.130	0.109
#7	Fensfjord / f (rec	0.120	0.118
#8	Tilje East/Centra	0.116	0.110
#9	Brent / f (rec) / $	0.113	0.085
#10	Gyda Jurassic /	0.103	0.095
#11	Vigdis, Brent / f	0.102	0.106
#12	Cook / f (rec) / $	0.094	0.088
#13	Statfjord / f (rec)	0.086	0.075
#14	Borg / f (rec) / $	0.052	0.038
#15	Brent / f (rec) / $	0.046	0.044
#16	Gyda South / f (	0.023	0.047

Simulation Results for Norwegian Sea: Sum total / J18

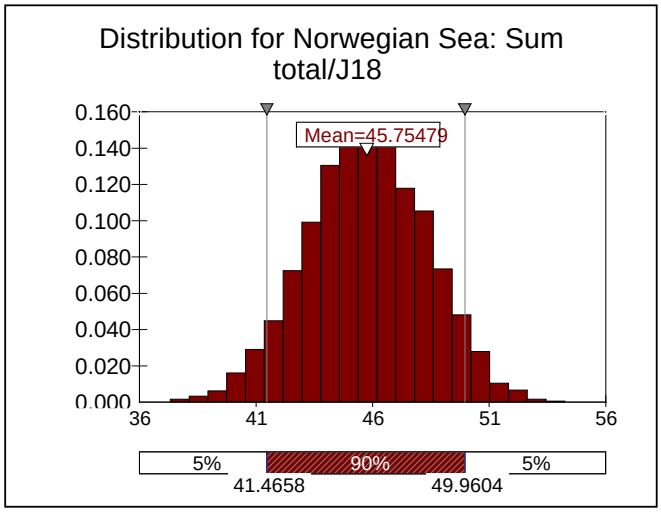

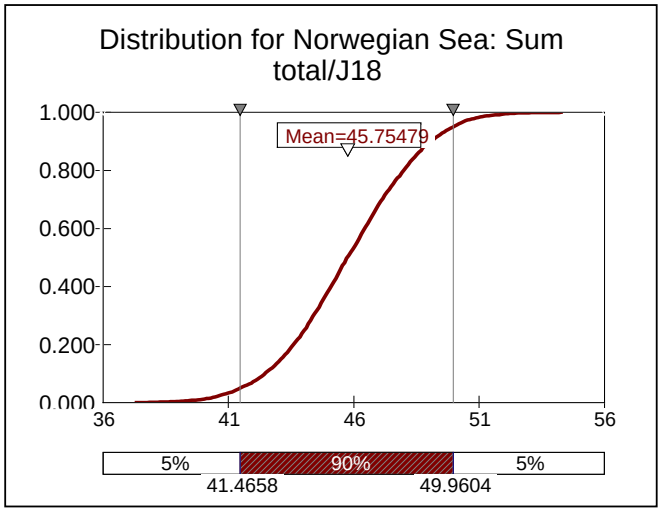

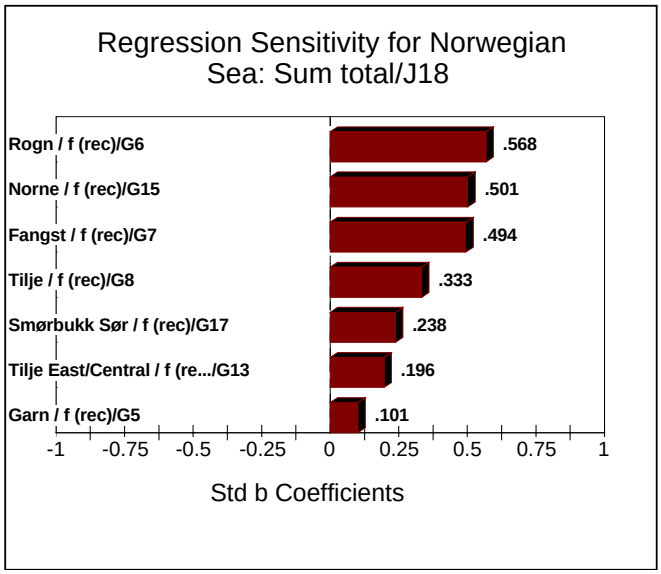

Summary Information	
Workbook Name	t Monte Carlo Norskehave
Number of Simulations	1
Number of Iterations	5000
Number of Inputs	13
Number of Outputs	1
Sampling Type	Latin Hypercube
Simulation Start Time	07.04.2003 12:24
Simulation Stop Time	07.04.2003 12:25
Simulation Duration	00:00:04
Random Seed	516539911

Summary Statistics			
Statistic	Value	%tile	Value
Minimum	37.3	5 %	41.5
Maximum	54.3	10 %	42.4
Mean	45.8	15 %	43.1
Std Dev	2.6	20 %	43.6
Variance	6.560164025	25 %	44.0
Skewness	-0.051612417	30 %	44.4
Kurtosis	2.85669199	35 %	44.7
Median	45.7	40 %	45.1
Mode	43.9	45 %	45.4
Left X	41.5	50 %	45.7
Left P	5 %	55 %	46.1
Right X	50.0	60 %	46.4
Right P	95 %	65 %	46.8
Diff X	8.5	70 %	47.1
Diff P	90 %	75 %	47.5
#Errors	0	80 %	48.0
Filter Min		85 %	48.5
Filter Max		90 %	49.0
#Filtered	0	95 %	50.0

Sensitivity			
Rank	Name	Regr	Corr
#1	Rogn / f (rec) / $	0.568	0.550
#2	Norne / f (rec) /	0.501	0.476
#3	Fangst / f (rec) /	0.494	0.449
#4	Tilje / f (rec) / $0	0.333	0.305
#5	Smørbukk Sør /	0.238	0.229
#6	Tilje East/Centra	0.196	0.188
#7	Garn / f (rec) / $	0.101	0.099
#8	Åre / f (rec) / $G	0.000	0.035
#9	Ile East/Central	0.000	-0.025
#10	Heidrun Nord / f	0.000	-0.001
#11	Smørbukk / f (re	0.000	0.005
#12	Tilje North / f (re	0.000	0.006
#13	Ile North / f (rec)	0.000	0.011
#14			
#15			
#16			

Simulation Results for Norwegian Sea: CO2 injection after 5 year / I18

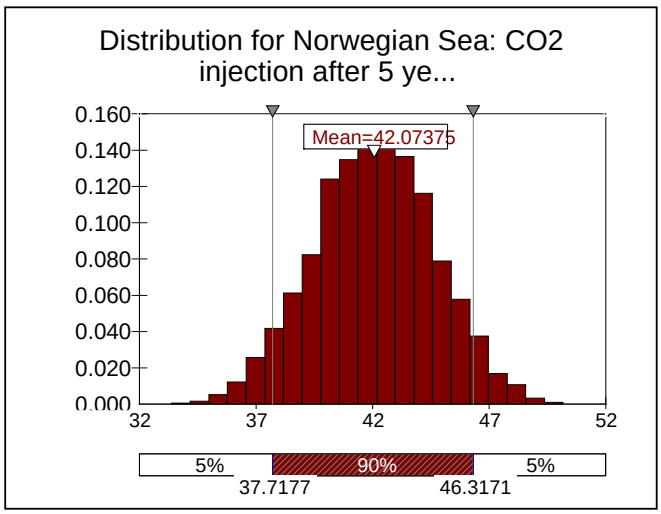

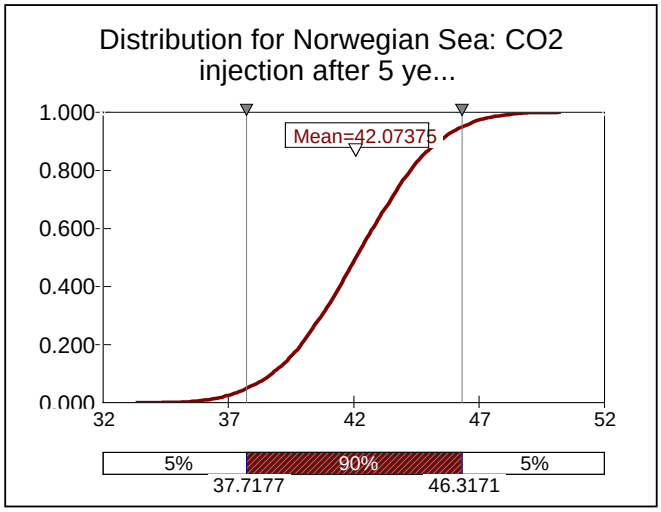

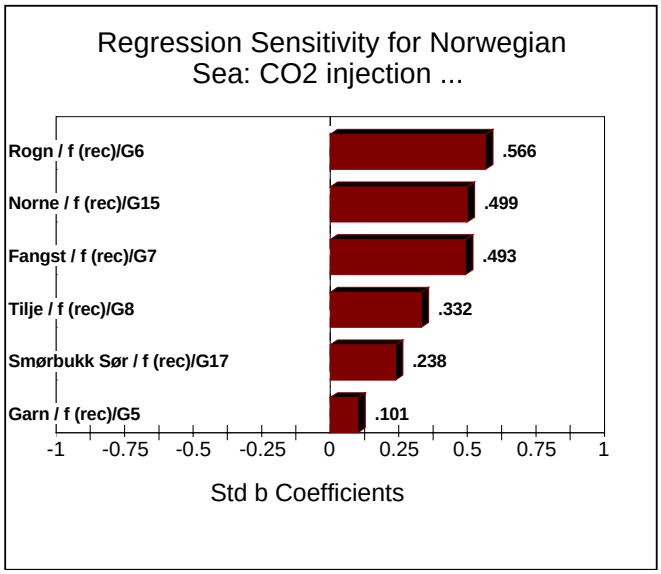

Summary Information	
Workbook Name	t Monte Carlo Norskehave
Number of Simulations	1
Number of Iterations	5000
Number of Inputs	13
Number of Outputs	1
Sampling Type	Latin Hypercube
Simulation Start Time	07.04.2003 12:22
Simulation Stop Time	07.04.2003 12:22
Simulation Duration	00:00:03
Random Seed	2055165268

Summary Statistics			
Statistic	**Value**	**%tile**	**Value**
Minimum	33.4	5 %	37.7
Maximum	50.2	10 %	38.7
Mean	42.1	15 %	39.4
Std Dev	2.6	20 %	39.9
Variance	6.597231847	25 %	40.3
Skewness	-0.035621984	30 %	40.7
Kurtosis	2.809427747	35 %	41.1
Median	42.1	40 %	41.4
Mode	43.5	45 %	41.8
Left X	37.7	50 %	42.1
Left P	5 %	55 %	42.4
Right X	46.3	60 %	42.8
Right P	95 %	65 %	43.1
Diff X	8.6	70 %	43.5
Diff P	90 %	75 %	43.8
#Errors	0	80 %	44.3
Filter Min		85 %	44.7
Filter Max		90 %	45.4
#Filtered	0	95 %	46.3

Sensitivity			
Rank	**Name**	**Regr**	**Corr**
#1	Rogn / f (rec) / $	0.566	0.576
#2	Norne / f (rec) /	0.499	0.476
#3	Fangst / f (rec) /	0.493	0.466
#4	Tilje / f (rec) / $0	0.332	0.335
#5	Smørbukk Sør /	0.238	0.251
#6	Garn / f (rec) / $	0.101	0.103
#7	Tilje North / f (re	0.000	-0.003
#8	Smørbukk / f (re	0.000	0.011
#9	Åre / f (rec) / $G	0.000	-0.004
#10	Heidrun Nord / f	0.000	-0.001
#11	Ile East/Central	0.000	-0.002
#12	Tilje East/Centra	0.000	0.016
#13	Ile North / f (rec)	0.000	-0.016
#14			
#15			
#16			

Simulation Results for
Norwegian Sea: CO2 injection within 5 year / H18

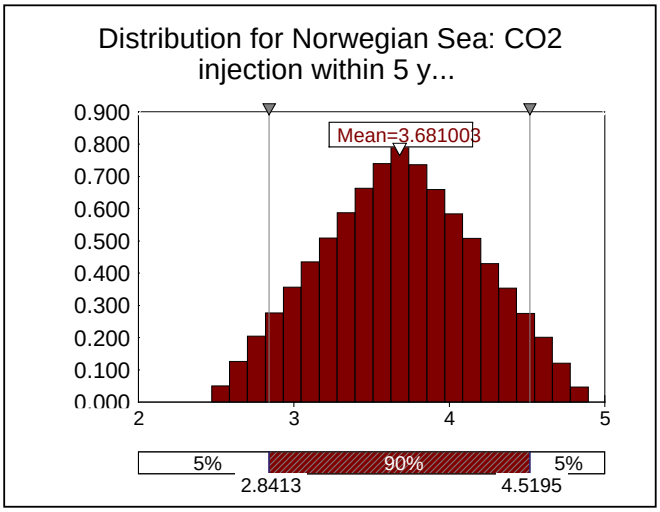

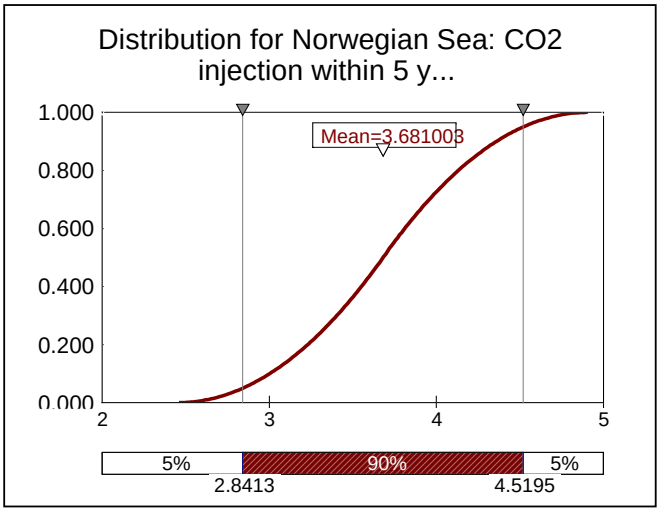

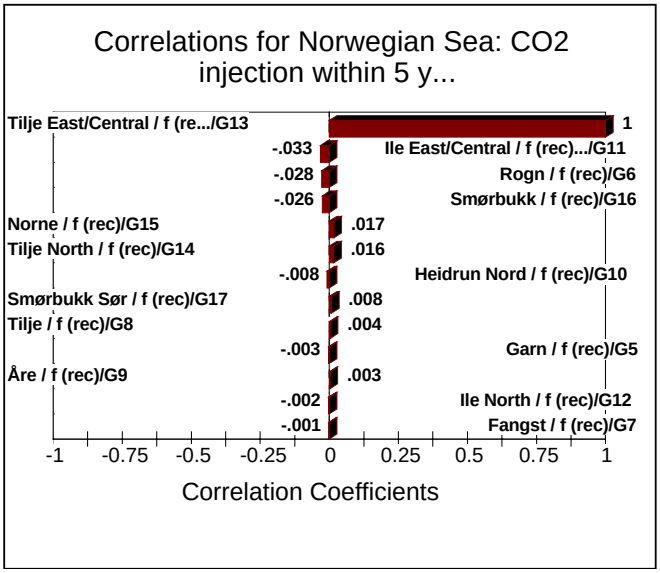

Summary Information	
Workbook Name	t Monte Carlo Norskehave
Number of Simulations	1
Number of Iterations	5000
Number of Inputs	13
Number of Outputs	1
Sampling Type	Latin Hypercube
Simulation Start Time	07.04.2003 11:22
Simulation Stop Time	07.04.2003 11:22
Simulation Duration	00:00:03
Random Seed	2046581132

Summary Statistics			
Statistic	Value	%tile	Value
Minimum	2.5	5 %	2.8
Maximum	4.9	10 %	3.0
Mean	3.7	15 %	3.1
Std Dev	0.5	20 %	3.2
Variance	0.250971955	25 %	3.3
Skewness	3.49464E-05	30 %	3.4
Kurtosis	2.402508467	35 %	3.5
Median	3.7	40 %	3.6
Mode	3.7	45 %	3.6
Left X	2.8	50 %	3.7
Left P	5 %	55 %	3.7
Right X	4.5	60 %	3.8
Right P	95 %	65 %	3.9
Diff X	1.7	70 %	4.0
Diff P	90 %	75 %	4.0
#Errors	0	80 %	4.1
Filter Min		85 %	4.2
Filter Max		90 %	4.4
#Filtered	0	95 %	4.5

Sensitivity			
Rank	Name	Regr	Corr
#1	Tilje East/Centra	1.000	1.000
#2	Tilje / f (rec) / $C	0.000	0.004
#3	Smørbukk / f (re	0.000	-0.026
#4	Heidrun Nord / f	0.000	-0.008
#5	Fangst / f (rec) /	0.000	-0.001
#6	Ile North / f (rec)	0.000	-0.002
#7	Tilje North / f (re	0.000	0.016
#8	Garn / f (rec) / $	0.000	-0.003
#9	Smørbukk Sør /	0.000	0.008
#10	Rogn / f (rec) / $	0.000	-0.028
#11	Åre / f (rec) / $G	0.000	0.003
#12	Ile East/Central	0.000	-0.033
#13	Norne / f (rec) /	0.000	0.017
#14			
#15			
#16			

Simulation Results for Tampen area: SUM total / J32

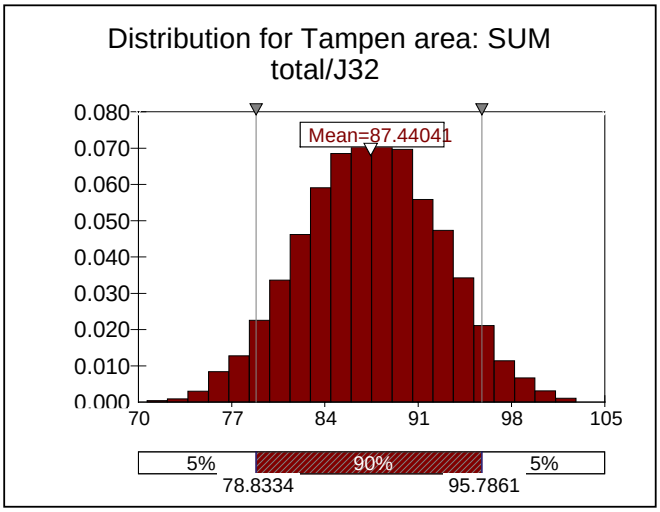

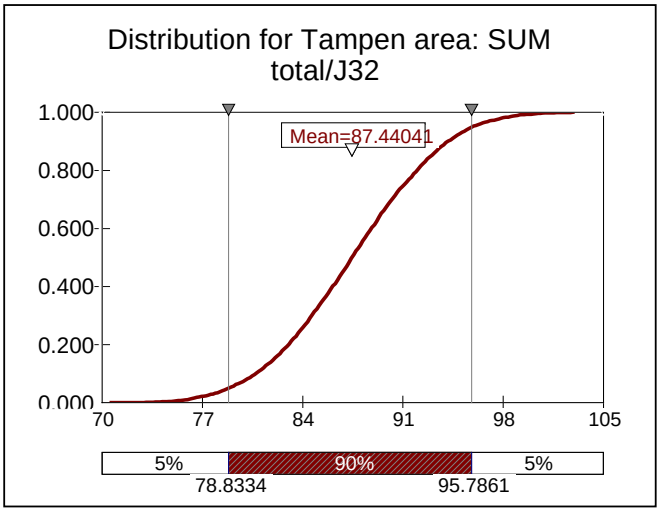

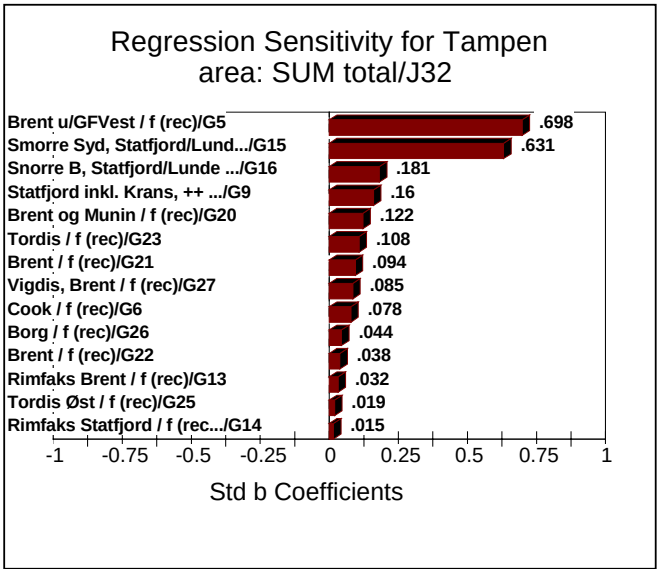

Summary Information	
Workbook Name	ut Monte Carlo Tampen.
Number of Simulations	1
Number of Iterations	5000
Number of Inputs	27
Number of Outputs	1
Sampling Type	Latin Hypercube
Simulation Start Time	07.04.2003 11:13
Simulation Stop Time	07.04.2003 11:13
Simulation Duration	00:00:05
Random Seed	107157192

Summary Statistics			
Statistic	**Value**	**%tile**	**Value**
Minimum	70.7	5 %	78.8
Maximum	102.9	10 %	80.7
Mean	87.4	15 %	82.0
Std Dev	5.2	20 %	83.0
Variance	26.64446297	25 %	83.9
Skewness	-0.015340793	30 %	84.6
Kurtosis	2.71912679	35 %	85.4
Median	87.4	40 %	86.1
Mode	88.7	45 %	86.8
Left X	78.8	50 %	87.4
Left P	5 %	55 %	88.1
Right X	95.8	60 %	88.8
Right P	95 %	65 %	89.5
Diff X	17.0	70 %	90.2
Diff P	90 %	75 %	91.0
#Errors	0	80 %	92.0
Filter Min		85 %	93.0
Filter Max		90 %	94.1
#Filtered	0	95 %	95.8

Sensitivity			
Rank	**Name**	**Regr**	**Corr**
#1	Brent u/GFVest	0.698	0.688
#2	Smorre Syd, Sta	0.631	0.612
#3	Snorre B, Statfjo	0.181	0.187
#4	Statfjord inkl. Kr	0.160	0.131
#5	Brent og Munin	0.122	0.135
#6	Tordis / f (rec) /	0.108	0.117
#7	Brent / f (rec) / $	0.094	0.095
#8	Vigdis, Brent / f	0.085	0.086
#9	Cook / f (rec) / $	0.078	0.069
#10	Borg / f (rec) / $	0.044	0.074
#11	Brent / f (rec) / $	0.038	0.064
#12	Rimfaks Brent /	0.032	0.034
#13	Tordis Øst / f (re	0.019	0.017
#14	Rimfaks Statfjor	0.015	0.011
#15	Startfjord/Amun	0.000	-0.005
#16	Gullveig Brent /	0.000	-0.001

Simulation Results for
Tampen area: CO2 injection after 5 year / I32

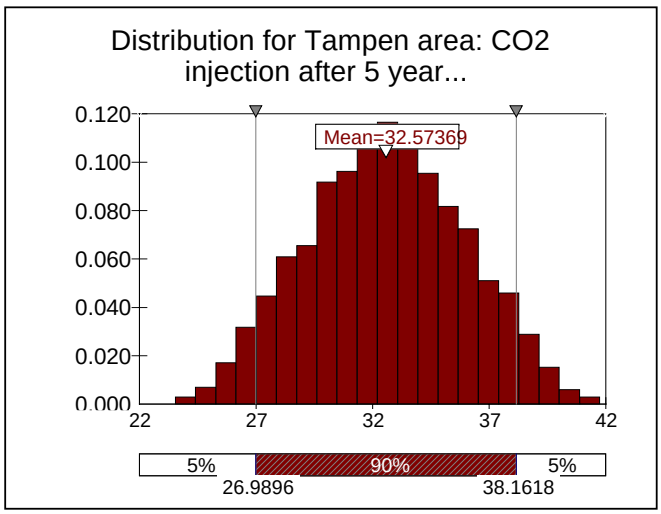

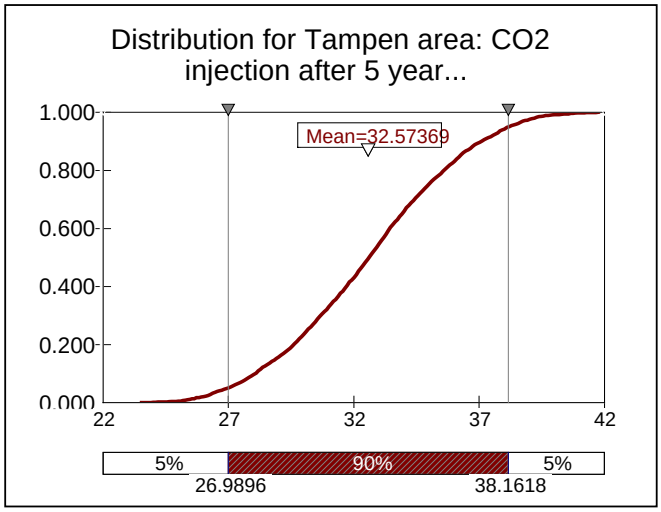

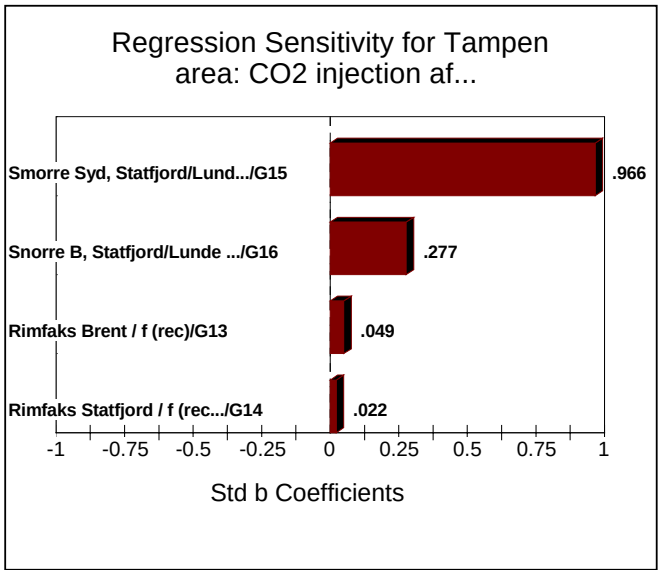

Summary Information	
Workbook Name	ut Monte Carlo Tampen.
Number of Simulations	1
Number of Iterations	5000
Number of Inputs	27
Number of Outputs	1
Sampling Type	Latin Hypercube
Simulation Start Time	07.04.2003 11:11
Simulation Stop Time	07.04.2003 11:11
Simulation Duration	00:00:05
Random Seed	1854066579

Summary Statistics			
Statistic	**Value**	**%tile**	**Value**
Minimum	23.5	5 %	27.0
Maximum	41.7	10 %	28.1
Mean	32.6	15 %	28.9
Std Dev	3.4	20 %	29.6
Variance	11.37961215	25 %	30.2
Skewness	0.003678297	30 %	30.7
Kurtosis	2.500728014	35 %	31.2
Median	32.6	40 %	31.7
Mode	28.8	45 %	32.2
Left X	27.0	50 %	32.6
Left P	5 %	55 %	33.0
Right X	38.2	60 %	33.4
Right P	95 %	65 %	33.9
Diff X	11.2	70 %	34.4
Diff P	90 %	75 %	35.0
#Errors	0	80 %	35.6
Filter Min		85 %	36.2
Filter Max		90 %	37.1
#Filtered	0	95 %	38.2

Sensitivity			
Rank	**Name**	**Regr**	**Corr**
#1	Smorre Syd, Sta	0.966	0.959
#2	Snorre B, Statfjo	0.277	0.236
#3	Rimfaks Brent /	0.049	0.044
#4	Rimfaks Statfjor	0.022	0.022
#5	Brent / f (rec) / $	0.000	0.003
#6	Cook / f (rec) / $	0.000	0.004
#7	Brent og Munin	0.000	0.002
#8	Startfjord/Amun	0.000	0.013
#9	Tordis Sør Øst (	0.000	0.007
#10	Brent / f (rec) / $	0.000	-0.019
#11	GF Sør Statfjord	0.000	-0.005
#12	Lunde / f (rec) /	0.000	0.015
#13	Gullfaks Vest in	0.000	-0.023
#14	Brent NII / f (rec	0.000	-0.008
#15	Statfjord inkl. Kr	0.000	-0.014
#16	Brent NI / f (rec)	0.000	0.024

Simulation Results for
Tampen area: CO2 injection within 5 year / H32

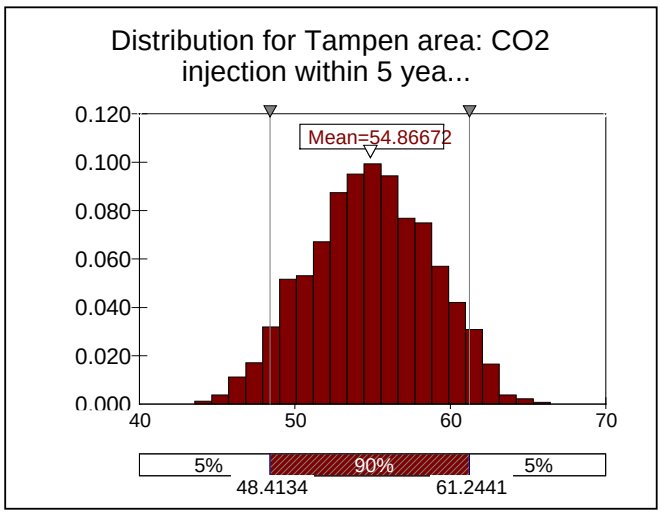

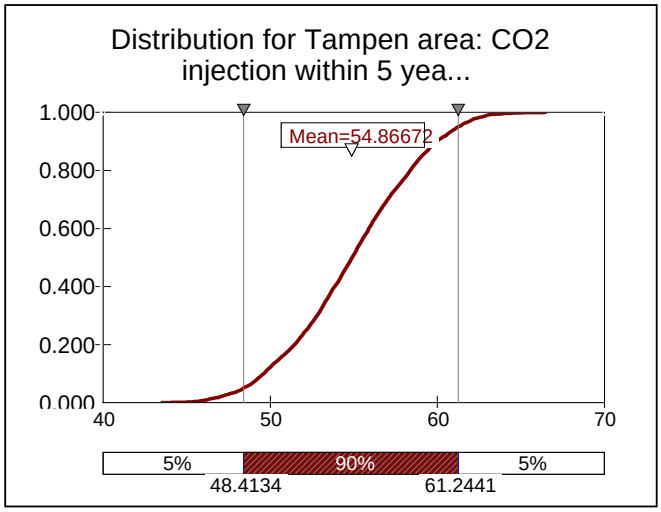

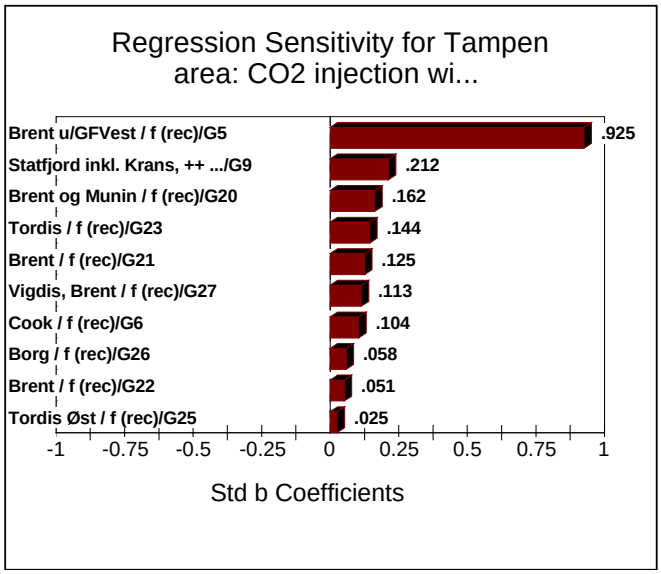

Summary Information	
Workbook Name	ɒut Monte Carlo Tampen.
Number of Simulations	1
Number of Iterations	5000
Number of Inputs	27
Number of Outputs	1
Sampling Type	Latin Hypercube
Simulation Start Time	07.04.2003 11:08
Simulation Stop Time	07.04.2003 11:08
Simulation Duration	00:00:05
Random Seed	1335337573

Summary Statistics			
Statistic	**Value**	**%tile**	**Value**
Minimum	43.6	5 %	48.4
Maximum	66.4	10 %	49.6
Mean	54.9	15 %	50.5
Std Dev	3.9	20 %	51.5
Variance	15.16403399	25 %	52.2
Skewness	-0.050075122	30 %	52.8
Kurtosis	2.543247664	35 %	53.3
Median	54.9	40 %	53.9
Mode	54.5	45 %	54.4
Left X	48.4	50 %	54.9
Left P	5 %	55 %	55.4
Right X	61.2	60 %	55.9
Right P	95 %	65 %	56.4
Diff X	12.8	70 %	57.0
Diff P	90 %	75 %	57.7
#Errors	0	80 %	58.4
Filter Min		85 %	59.1
Filter Max		90 %	60.0
#Filtered	0	95 %	61.2

Sensitivity			
Rank	**Name**	**Regr**	**Corr**
#1	Brent u/GFVest	0.925	0.927
#2	Statfjord inkl. Kr	0.212	0.199
#3	Brent og Munin	0.162	0.169
#4	Tordis / f (rec) /	0.144	0.145
#5	Brent / f (rec) / $	0.125	0.117
#6	Vigdis, Brent / f	0.113	0.126
#7	Cook / f (rec) / $	0.104	0.108
#8	Borg / f (rec) / $	0.058	0.053
#9	Brent / f (rec) / $	0.051	0.030
#10	Tordis Øst / f (re	0.025	0.014
#11	Gullveig Brent /	0.000	0.029
#12	Gullfaks Vest in	0.000	0.005
#13	GF Sør Brent / f	0.000	-0.007
#14	Smorre Syd, Sta	0.000	0.012
#15	Statfjord / f (rec)	0.000	0.003
#16	Snorre B, Statfjo	0.000	-0.017

Simulation Results for Troll Oseberg area: Sum total / J35

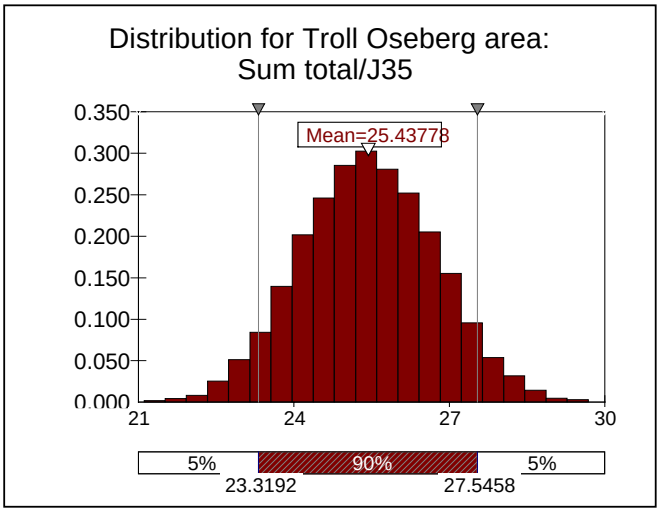

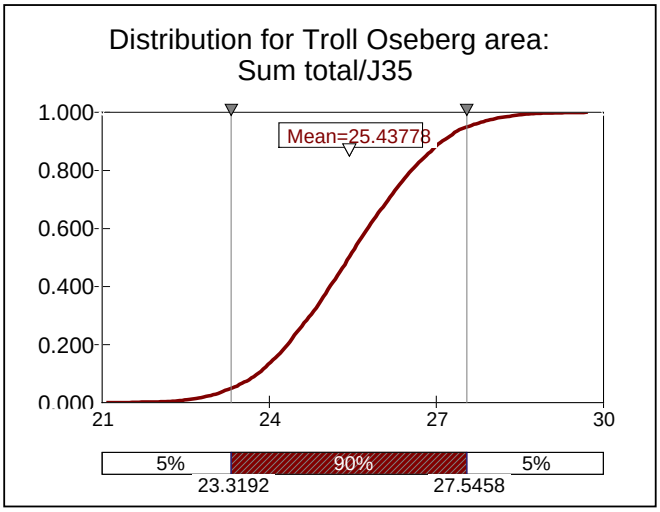

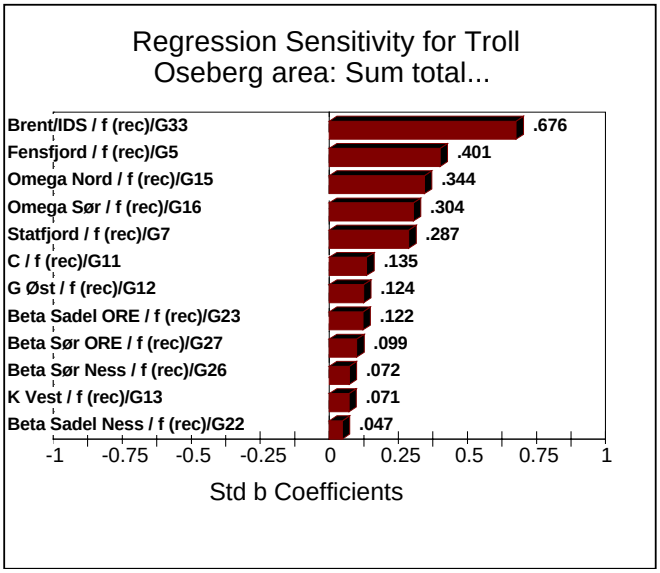

Summary Information	
Workbook Name	Monte Carlo Troll Osebe
Number of Simulations	1
Number of Iterations	5000
Number of Inputs	30
Number of Outputs	1
Sampling Type	Latin Hypercube
Simulation Start Time	07.04.2003 11:02
Simulation Stop Time	07.04.2003 11:02
Simulation Duration	00:00:06
Random Seed	2100978818

Summary Statistics			
Statistic	**Value**	**%tile**	**Value**
Minimum	21.1	5 %	23.3
Maximum	29.7	10 %	23.8
Mean	25.4	15 %	24.1
Std Dev	1.3	20 %	24.3
Variance	1.665756676	25 %	24.5
Skewness	0.026176566	30 %	24.7
Kurtosis	2.838716521	35 %	24.9
Median	25.4	40 %	25.1
Mode	23.8	45 %	25.3
Left X	23.3	50 %	25.4
Left P	5 %	55 %	25.6
Right X	27.5	60 %	25.8
Right P	95 %	65 %	25.9
Diff X	4.2	70 %	26.1
Diff P	90 %	75 %	26.3
#Errors	0	80 %	26.5
Filter Min		85 %	26.8
Filter Max		90 %	27.1
#Filtered	0	95 %	27.5

Sensitivity			
Rank	**Name**	**Regr**	**Corr**
#1	Brent/IDS / f (re	0.676	0.683
#2	Fensfjord / f (rec	0.401	0.400
#3	Omega Nord / f	0.344	0.337
#4	Omega Sør / f (	0.304	0.292
#5	Statfjord / f (rec)	0.287	0.274
#6	C / f (rec) / G	0.135	0.135
#7	G Øst / f (rec) /	0.124	0.117
#8	Beta Sadel ORE	0.122	0.149
#9	Beta Sør ORE /	0.099	0.069
#10	Beta Sør Ness /	0.072	0.093
#11	K Vest / f (rec) /	0.071	0.062
#12	Beta Sadel Nes	0.047	0.039
#13	Troll Vest Fensf	0.000	0.028
#14	Oljeprovinsen /	0.000	-0.015
#15	Statfjord / f (rec)	0.000	0.003
#16	Beta Saddle No	0.000	0.015

Simulation Results for
Troll Oseberg area: CO2 injection after 5 year / I35

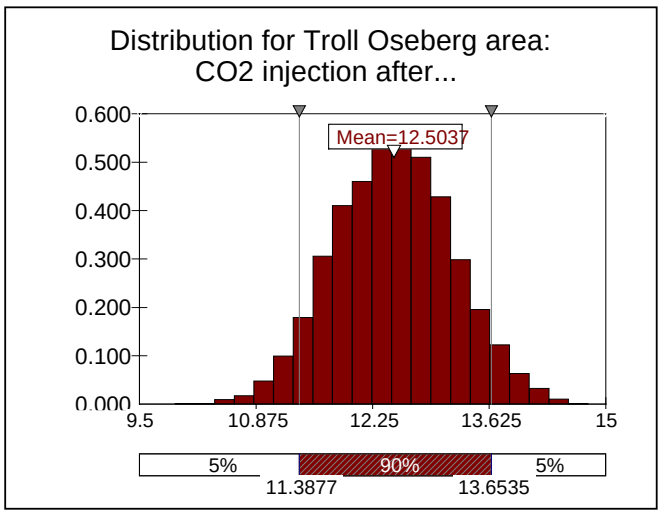

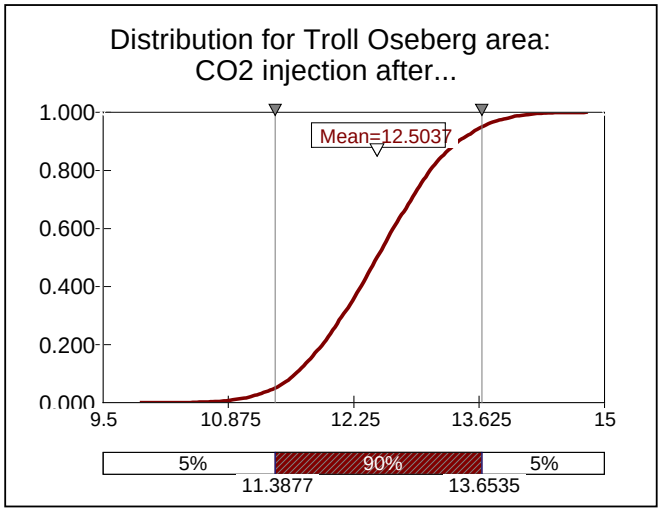

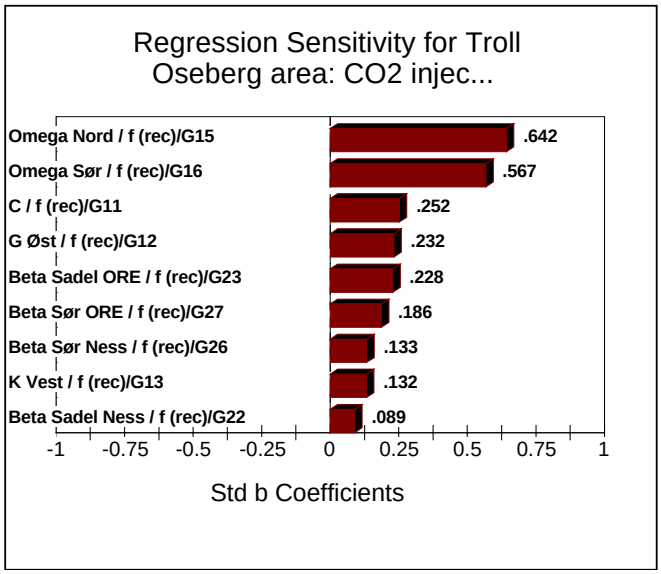

Summary Information	
Workbook Name	Monte Carlo Troll Osebe
Number of Simulations	1
Number of Iterations	5000
Number of Inputs	30
Number of Outputs	1
Sampling Type	Latin Hypercube
Simulation Start Time	07.04.2003 10:59
Simulation Stop Time	07.04.2003 10:59
Simulation Duration	00:00:06
Random Seed	1481974552

Summary Statistics			
Statistic	**Value**	**%tile**	**Value**
Minimum	9.9	5 %	11.4
Maximum	14.8	10 %	11.6
Mean	12.5	15 %	11.8
Std Dev	0.7	20 %	11.9
Variance	0.478282666	25 %	12.0
Skewness	0.008012449	30 %	12.1
Kurtosis	2.817043932	35 %	12.2
Median	12.5	40 %	12.3
Mode	11.9	45 %	12.4
Left X	11.4	50 %	12.5
Left P	5 %	55 %	12.6
Right X	13.7	60 %	12.7
Right P	95 %	65 %	12.8
Diff X	2.3	70 %	12.9
Diff P	90 %	75 %	13.0
#Errors	0	80 %	13.1
Filter Min		85 %	13.2
Filter Max		90 %	13.4
#Filtered	0	95 %	13.7

Sensitivity			
Rank	**Name**	**Regr**	**Corr**
#1	Omega Nord / f	0.642	0.658
#2	Omega Sør / f (	0.567	0.564
#3	C / f (rec) / G	0.252	0.246
#4	G Øst / f (rec) /	0.232	0.232
#5	Beta Sadel ORE	0.228	0.210
#6	Beta Sør ORE /	0.186	0.192
#7	Beta Sør Ness /	0.133	0.112
#8	K Vest / f (rec) /	0.132	0.120
#9	Beta Sadel Nes	0.089	0.072
#10	K Øst / f (rec) /	0.000	-0.007
#11	Oljeprovinsen /	0.000	0.024
#12	Tarbert / f (rec)	0.000	0.015
#13	Brent/IDS / f (re	0.000	0.001
#14	Statfjord / f (rec)	0.000	-0.005
#15	Troll Vest Fensf	0.000	-0.018
#16	Beta Saddle No	0.000	0.020

Simulation Results for
Troll Oseberg area: CO2 injection within 5 year / H35

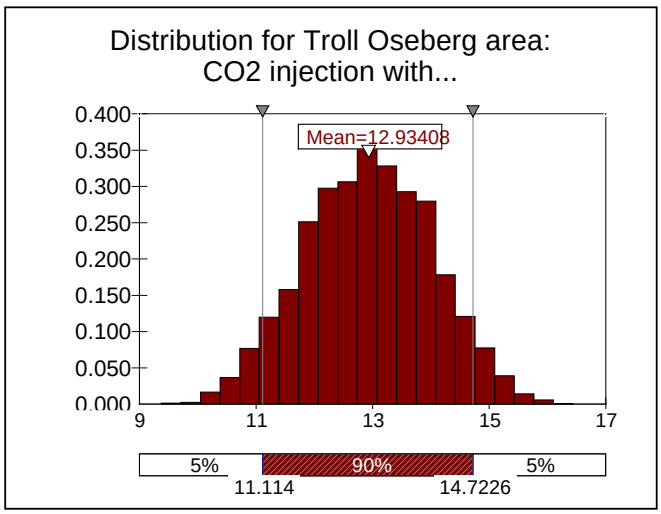

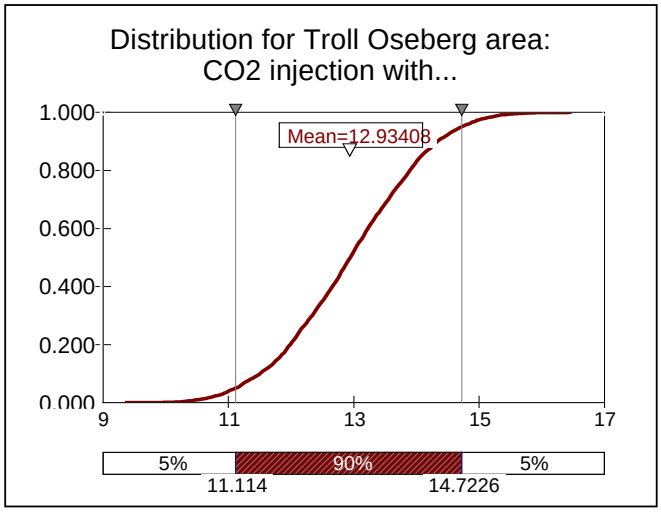

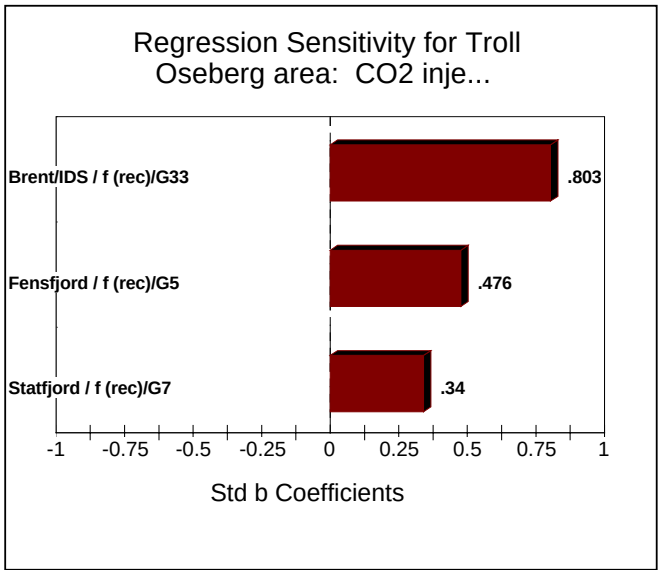

Summary Information	
Workbook Name	Monte Carlo Troll Osebe
Number of Simulations	1
Number of Iterations	5000
Number of Inputs	30
Number of Outputs	1
Sampling Type	Latin Hypercube
Simulation Start Time	07.04.2003 10:56
Simulation Stop Time	07.04.2003 10:56
Simulation Duration	00:00:06
Random Seed	916521405

Summary Statistics			
Statistic	**Value**	**%tile**	**Value**
Minimum	9.4	5 %	11.1
Maximum	16.4	10 %	11.5
Mean	12.9	15 %	11.8
Std Dev	1.1	20 %	12.0
Variance	1.182699701	25 %	12.1
Skewness	-0.023682168	30 %	12.3
Kurtosis	2.641319166	35 %	12.5
Median	12.9	40 %	12.7
Mode	11.9	45 %	12.8
Left X	11.1	50 %	12.9
Left P	5 %	55 %	13.1
Right X	14.7	60 %	13.2
Right P	95 %	65 %	13.4
Diff X	3.6	70 %	13.6
Diff P	90 %	75 %	13.7
#Errors	0	80 %	13.9
Filter Min		85 %	14.1
Filter Max		90 %	14.3
#Filtered	0	95 %	14.7

Sensitivity			
Rank	**Name**	**Regr**	**Corr**
#1	Brent/IDS / f (re	0.803	0.805
#2	Fensfjord / f (rec	0.476	0.474
#3	Statfjord / f (rec)	0.340	0.337
#4	Beta Sør LOSS	0.000	-0.012
#5	Ness / f (rec) / $	0.000	-0.012
#6	Omega Nord / f	0.000	0.001
#7	Beta Sadel Tarb	0.000	-0.003
#8	Beta Sadel LOS	0.000	0.008
#9	Beta Saddle No	0.000	0.005
#10	Beta Sadel ORE	0.000	0.019
#11	C / f (rec) / G	0.000	0.006
#12	Beta Saddle No	0.000	0.014
#13	Omega Sør / f (	0.000	0.001
#14	K Vest / f (rec) /	0.000	0.009
#15	Gamma Nord / f	0.000	-0.008
#16	ORELN2 / f (rec	0.000	-0.007

Simulation Results for
Southern part of the North Sea: Sum total / J17

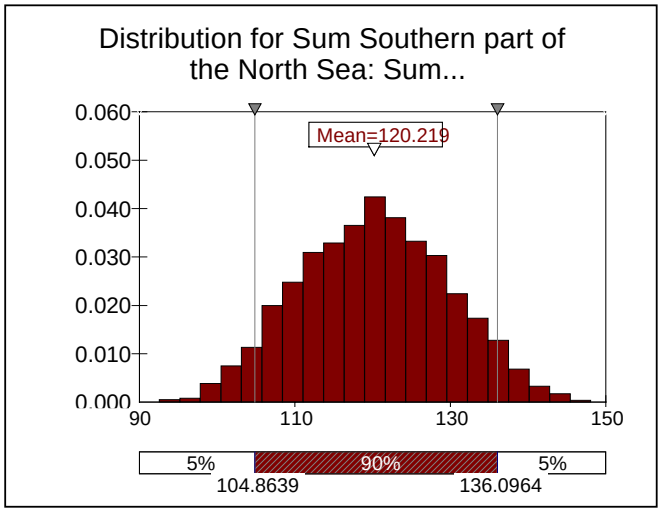

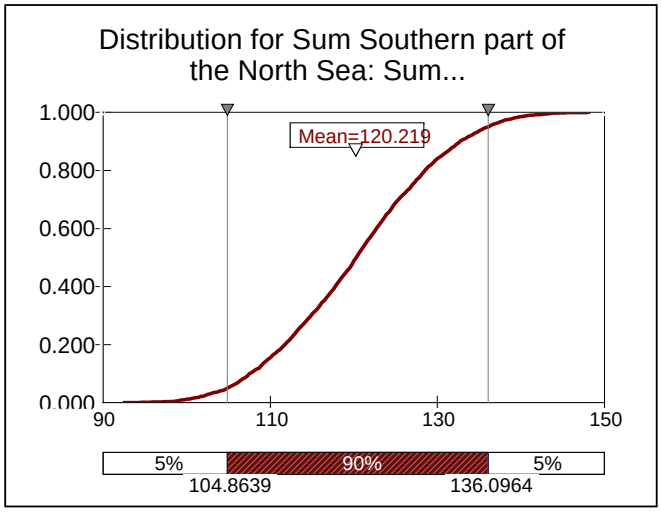

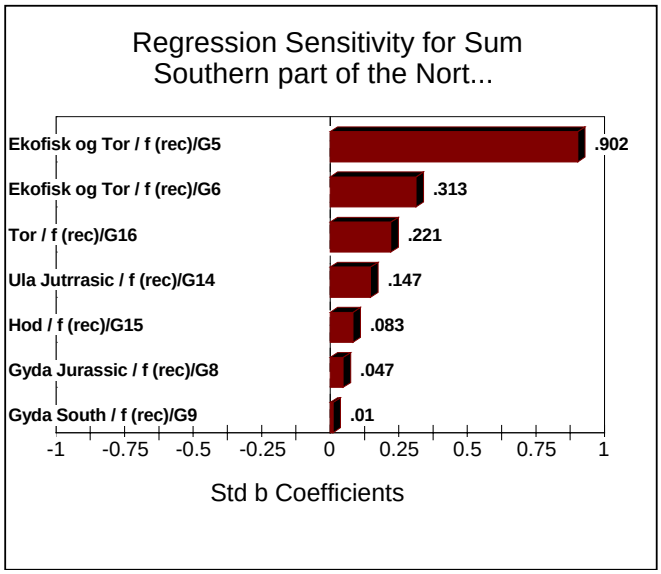

Summary Information	
Workbook Name	Monte Carlo sørlige nords
Number of Simulations	1
Number of Iterations	5000
Number of Inputs	12
Number of Outputs	1
Sampling Type	Latin Hypercube
Simulation Start Time	07.05.2003 08:36
Simulation Stop Time	07.05.2003 08:36
Simulation Duration	00:00:03
Random Seed	1845406161

Summary Statistics			
Statistic	**Value**	**%tile**	**Value**
Minimum	92.6	5 %	104.9
Maximum	148.1	10 %	107.5
Mean	120.2	15 %	109.8
Std Dev	9.5	20 %	111.7
Variance	90.08849765	25 %	113.3
Skewness	0.021018492	30 %	114.9
Kurtosis	2.55875693	35 %	116.3
Median	120.3	40 %	117.8
Mode	119.3	45 %	119.1
Left X	104.9	50 %	120.3
Left P	5 %	55 %	121.5
Right X	136.1	60 %	122.7
Right P	95 %	65 %	123.9
Diff X	31.2	70 %	125.4
Diff P	90 %	75 %	127.0
#Errors	0	80 %	128.5
Filter Min		85 %	130.5
Filter Max		90 %	132.7
#Filtered	0	95 %	136.1

Sensitivity			
Rank	**Name**	**Regr**	**Corr**
#1	Ekofisk og Tor /	0.902	0.902
#2	Ekofisk og Tor /	0.313	0.309
#3	Tor / f (rec) / $G	0.221	0.208
#4	Ula Jutrrasic / f	0.147	0.161
#5	Hod / f (rec) / $C	0.083	0.091
#6	Gyda Jurassic /	0.047	0.047
#7	Gyda South / f (	0.010	0.020
#8	Dev. og Perm. /	0.000	-0.002
#9	Ekofisk og Tor /	0.000	0.001
#10	Hod / f (rec) / $C	0.000	-0.006
#11	Tor/Ekofisk / f (r	0.000	-0.011
#12	Gyda Jurrassic /	0.000	-0.026
#13			
#14			
#15			
#16			

Simulation Results for
Southern part of the North Sea: CO2 injetion after 5 year / I17

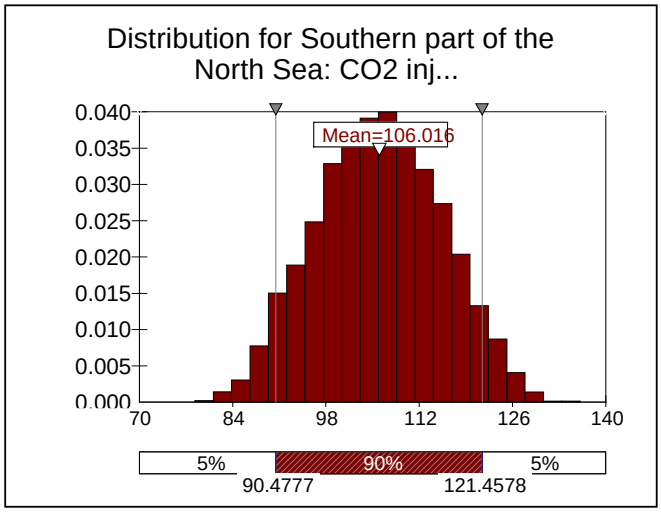

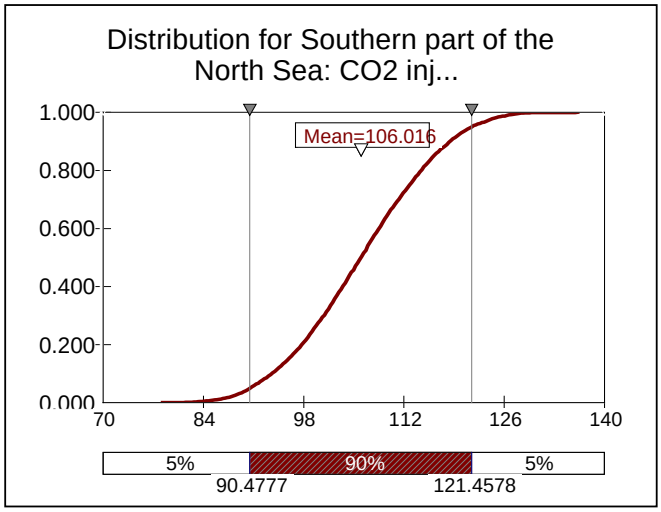

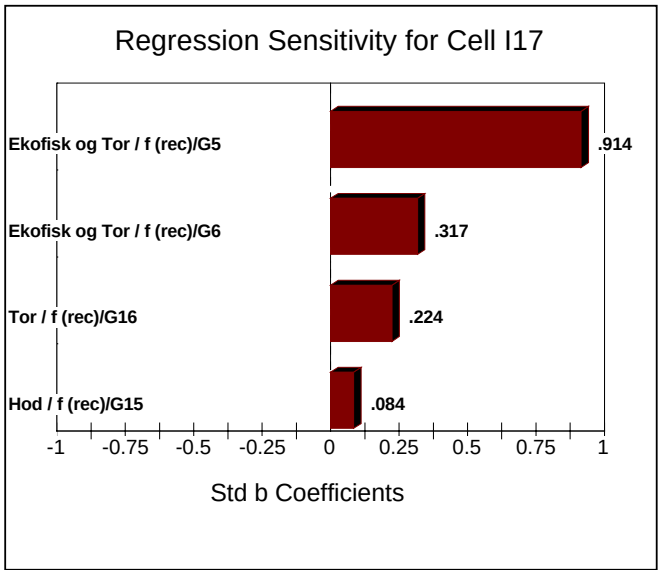

Summary Information	
Workbook Name	Monte Carlo sørlige nords
Number of Simulations	1
Number of Iterations	5000
Number of Inputs	12
Number of Outputs	1
Sampling Type	Latin Hypercube
Simulation Start Time	07.04.2003 10:06
Simulation Stop Time	07.04.2003 10:07
Simulation Duration	00:00:04
Random Seed	936988329

Summary Statistics			
Statistic	**Value**	**%tile**	**Value**
Minimum	78.3	5 %	90.5
Maximum	136.2	10 %	93.5
Mean	106.0	15 %	95.8
Std Dev	9.4	20 %	97.7
Variance	87.84462415	25 %	99.3
Skewness	0.009779209	30 %	100.8
Kurtosis	2.530898318	35 %	102.1
Median	106.0	40 %	103.5
Mode	106.9	45 %	104.7
Left X	90.5	50 %	106.0
Left P	5 %	55 %	107.2
Right X	121.5	60 %	108.5
Right P	95 %	65 %	109.8
Diff X	31.0	70 %	111.3
Diff P	90 %	75 %	112.8
#Errors	0	80 %	114.4
Filter Min		85 %	116.1
Filter Max		90 %	118.4
#Filtered	0	95 %	121.5

Sensitivity			
Rank	**Name**	**Regr**	**Corr**
#1	Ekofisk og Tor /	0.914	0.917
#2	Ekofisk og Tor /	0.317	0.317
#3	Tor / f (rec) / $G	0.224	0.204
#4	Hod / f (rec) / $C	0.084	0.084
#5	Gyda South / f (	0.000	0.018
#6	Dev. og Perm. /	0.000	0.013
#7	Gyda Jurrassic /	0.000	-0.002
#8	Hod / f (rec) / $C	0.000	-0.001
#9	Ula Jutrrasic / f	0.000	0.012
#10	Gyda Jurassic /	0.000	-0.001
#11	Tor/Ekofisk / f (r	0.000	-0.016
#12	Ekofisk og Tor /	0.000	0.006
#13			
#14			
#15			
#16			

Simulation Results for
Southern part of the North Sea: CO2 injection within 5 year / H17

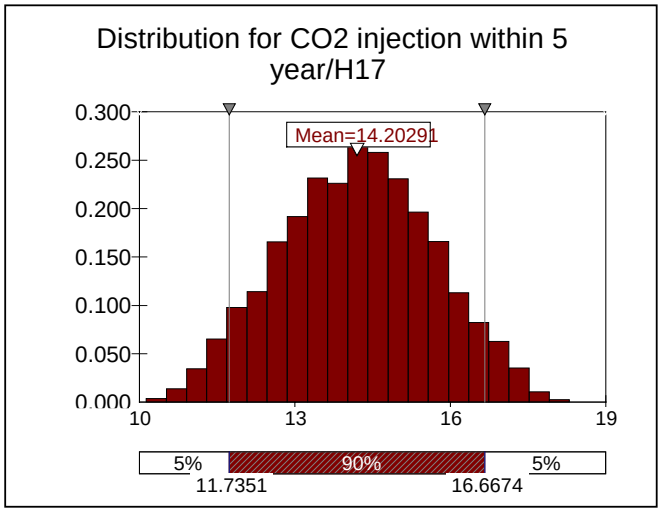

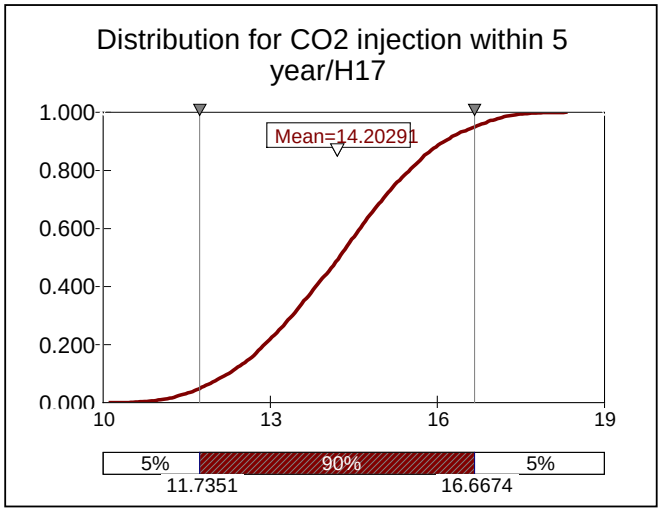

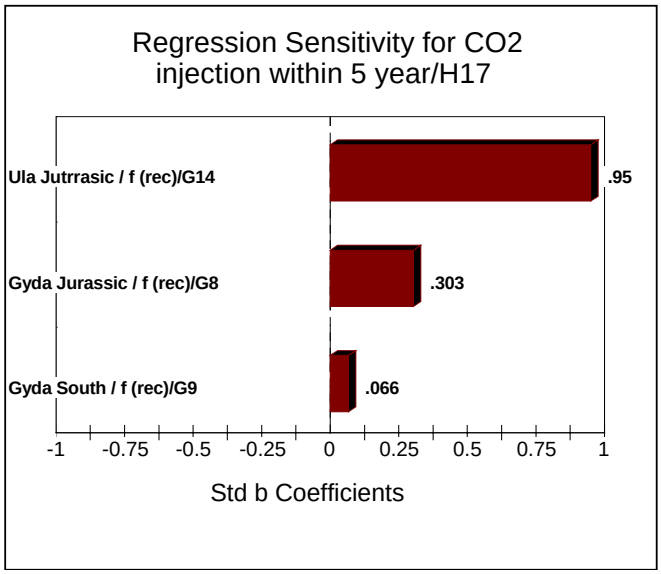

Summary Information	
Workbook Name	Monte Carlo sørlige nords
Number of Simulations	1
Number of Iterations	5000
Number of Inputs	12
Number of Outputs	1
Sampling Type	Latin Hypercube
Simulation Start Time	07.05.2003 08:28
Simulation Stop Time	07.05.2003 08:28
Simulation Duration	00:00:03
Random Seed	164732400

Summary Statistics			
Statistic	**Value**	**%tile**	**Value**
Minimum	10.1	5 %	11.7
Maximum	18.3	10 %	12.2
Mean	14.2	15 %	12.6
Std Dev	1.5	20 %	12.9
Variance	2.145996433	25 %	13.2
Skewness	-0.020386474	30 %	13.4
Kurtosis	2.522307077	35 %	13.6
Median	14.2	40 %	13.8
Mode	14.2	45 %	14.0
Left X	11.7	50 %	14.2
Left P	5 %	55 %	14.4
Right X	16.7	60 %	14.6
Right P	95 %	65 %	14.8
Diff X	4.9	70 %	15.0
Diff P	90 %	75 %	15.2
#Errors	0	80 %	15.5
Filter Min		85 %	15.8
Filter Max		90 %	16.1
#Filtered	0	95 %	16.7

Sensitivity			
Rank	**Name**	**Regr**	**Corr**
#1	Ula Jutrrasic / f	0.950	0.951
#2	Gyda Jurassic /	0.303	0.288
#3	Gyda South / f (	0.066	0.039
#4	Dev. og Perm. /	0.000	-0.014
#5	Hod / f (rec) / $C	0.000	-0.004
#6	Hod / f (rec) / $C	0.000	-0.008
#7	Gyda Jurrassic /	0.000	0.002
#8	Ekofisk og Tor /	0.000	-0.005
#9	Ekofisk og Tor /	0.000	0.004
#10	Ekofisk og Tor /	0.000	-0.008
#11	Tor / f (rec) / $G	0.000	-0.015
#12	Tor/Ekofisk / f (r	0.000	0.004
#13			
#14			
#15			
#16			

APPENDIX B

Confidential enclosure (Not Available)

- Fluid data and compositions used in the MMP simulations
- Oil production, history and prognosis for each of the 36 oilfields